

THE IDENTIFICATION OF A NUCLEOSIDE TRIPHOSPHATE BINDING  
SITE ON EUKARYOTIC RNA-POLYMERASE II

BY

ERWIN FREUND

A DISSERTATION PRESENTED TO THE GRADUATE SCHOOL OF THE  
UNIVERSITY OF FLORIDA IN PARTIAL FULFILLMENT OF THE  
REQUIREMENTS FOR THE DEGREE OF DOCTOR OF PHILOSOPHY

UNIVERSITY OF FLORIDA

1984

To my wife Simha, and my parents Willy and Werner for their  
love, support and patience over the years.

## ACKNOWLEDGEMENTS

I want to express my sincere gratitude to Dr. Peter M. McGuire who always stood by me as an advisor and a friend. I appreciate especially the time he spent and patience he displayed in proofreading my English.

I thank the following members of my graduate committee for their advice: Dr. Richard P. Boyce, Dr. Charles M. Allen, Dr. James F. Preston and Dr. Ben M. Dunn. I extend thanks to all the members of the Department of Biochemistry and Molecular Biology who helped me in my training and for providing excellent word processing facilities. Then, there are those people without whose help this research would not have been completed, first the staff of the labor and delivery room in the Department of Obstetrics and Gynecology, in particular Dr. Kenneth R. Kellner who showed me how to perfuse placentas, and the charge nurse Nelda who was willing to call and inform me that a delivery was about to happen after midnight. Special thanks go to those women who, while enjoying the many blessings of arriving motherhood, were willing to listen, or at least pretend to listen, to my pleas for their placentas. I appreciate the support and encouragement from two graduate students in our lab, Mark Eller and Jan Bradley. Special thanks go to you, Mark Riggensbach, for your part in the purification of placental RNA polymerases and your companionship during the nights while watching the columns. I extend thanks, too, to Dr. Kimon Angelides for allowing me to use his Cary spectrophotometer and Hewlett Packard plotter.

My appreciation goes to Dr. Jim F. Preston for providing me with the radiolabeled alpha-amanitin derivative and for the valuable discussions and to Dr. Michael E. Dahmus (University of California) for providing casein kinase I and performing the kinase blotting experiment. Finally, I am indebted to Dr. Boyd E. Haley (University of Wyoming) and Dr. A. Kemp (University of Amsterdam) for providing me with  $^8\text{N}_3$ -GTP and  $^8\text{N}_3$ -ATP.

## TABLE OF CONTENTS

	PAGE
ACKNOWLEDGEMENTS.....	iii
KEY TO ABBREVIATIONS.....	vii
ABSTRACT.....	ix
 CHAPTER ONE	
INTRODUCTION AND BACKGROUND TO THE TRANSCRIPTION PROCESS.....	1
RNA Polymerase Enzymology.....	1
Prokaryotic RNA Polymerase .....	3
Nuclear Eukaryotic RNA Polymerase.....	5
 CHAPTER TWO	
PURIFICATION OF CALF THYMUS RNA POLYMERASE II.....	12
Introduction.....	12
Materials and Methods.....	13
Results.....	21
Discussion.....	23
 CHAPTER THREE	
PURIFICATION OF HUMAN PLACENTAL RNA POLYMERASE II.....	35
Introduction.....	35
Materials and Methods.....	37
Results.....	41
Discussion.....	45
 CHAPTER FOUR	
PEPTIDE CHARACTERIZATION OF CALF THYMUS AND HUMAN PLACENTAL RNA POLYMERASES.....	57
Introduction.....	57
Materials and Methods.....	58
Results.....	60
Discussion.....	71

CHAPTER FIVE	
ANALYSES OF RNA POLYMERASES II FOR KINASES.....	75
Introduction.....	75
Materials and Methods.....	75
Results.....	77
Discussion.....	84
CHAPTER SIX	
DETECTION OF A NUCLEOSIDE TRIPHOSPHATE BINDING	
SITE IN RNA POLYMERASE II.....	89
Introduction.....	89
Materials and Methods.....	103
Results.....	105
Discussion.....	149
CHAPTER SEVEN	
GENERAL DISCUSSION.....	155
REFERENCES.....	161
BIOGRAPHICAL SKETCH.....	171

## KEY TO ABBREVIATIONS

Act.	activity
ApA	adenylyl (3'-5')adenosine
ara-6-mp	9- $\beta$ -D-arabinofuranosyl-6-mercaptopurine
ATP	adenosine 5'-triphosphate
BME	$\beta$ -mercaptoethanol
bp	base pairs
BPB	bromophenol blue
BSA	bovine serum albumin
C	catalytic subunit of protein kinase
cAMP	adenosine 3',5'cyclic phosphate
CBB-R250	coomassie brilliant blue R-250
Ci	curie
CK I	casein kinase I
cm	centimeter
cpm	counts per minute
CT	calf thymus
CTP	cytosine 5'-triphosphate
1D/2D	one/two dimensional
DATD	N,N'-diallyltartardiamide
DEAE	diethylaminoethyl
°C	degrees centigrade

DeMeABGG	dehydroxymethylamanylazobenzoyl-N-glycylglycine
DNA	deoxyribonucleic acid
DNAP	DNA-dependent DNA polymerase
ds/ss DNA	double/single stranded DNA
DTT	dithiothreitol
EDTA	ethylenediaminetetraacetic acid
g	gravitational force expression
gm	gram
GTP	guanosine 5'-triphosphate
Hepes	N-(2-hydroxyethyl)-piperazine-N'-2-ethanesulfonic acid.
IEF	isoelectric focusing
$k_2$	dissociation rate constant
$k_3$	rate constant for product formation
kD	kilodalton
$K_D$	dissociation constant
kg	kilogram
$K_i$	inhibition constant
$K_M$	Michaelis-Menten constant
M	molar
$\mu\text{Ci}$	microCurie
$\mu\text{g}$	microgram
$\mu\text{l}$	microliter
$\mu\text{M}$	micromolar
$\mu\text{seconds}$	microsecond
mAmp	milliamperes



mg	milligram
ml	milliliter
mm	millimeter
mM	millimolar
mmole	millimole
mRNA	messenger RNA
MW	molecular weight
mWatt	milliWatt
8N <sub>3</sub> -ATP	8-azido-adenosine 5'-triphosphate
8N <sub>3</sub> -GTP	8-azido-guanosine 5'-triphosphate
nM	nanoMolar
nm	nanometer
O.D.	optical density
P	pellet
PAGE	polyacrylamide gel electrophoresis
PBS	phosphate buffered saline
pI	isoelectric point
Pi	inorganic phosphate
PL	placenta
pmole	picomole
PMSF	phenylmethanesulfonyl fluoride
poly[dT]	polydeoxyadenylylic acid
poly[dC]	polydeoxycytidylic acid
psi	pound per square inch
R	regulatory subunit of protein kinase
RNA	ribonucleic acid
RNAP	DNA-dependent RNA polymerase

(d)NTP	(deoxy)ribonucleoside 5'-triphosphate
rpm	revolution per minute
rRNA	ribosomal RNA
SDS	sodium dodecyl sulfate
SN	supernatant
Spec. Act.	specific activity
T <sub>1/2</sub>	half life
TCA	trichloroacetic acid
TIU	trypsin inhibitory units
TLC	thin layer chromatography
Tris-HCl	tris(hydroxymethyl)aminomethane, HCl
tRNA	transfer RNA
UTP	uridine 5'-triphosphate
UV	ultraviolet
v/v	ratio volume over volume
w/v	ratio weight over volume

Abstract of Dissertation Presented to the Graduate School  
of the University of Florida in Partial Fulfillment of the  
Requirements for the Degree of Doctor of Philosophy

THE IDENTIFICATION OF A NUCLEOSIDE TRIPHOSPHATE BINDING SITE  
ON EUKARYOTIC RNA POLYMERASE II

By

Erwin Freund

December, 1984

Chairman: Peter M. McGuire, Ph.D.

Major Department: Biochemistry and Molecular Biology

DNA dependent RNA polymerases use ribonucleoside triphosphates as substrates to synthesize RNA, while using DNA as a template. These are complex enzymes consisting of 5 polypeptides in prokaryotes and 7-15 polypeptides in eukaryotes. The function of each polypeptide during the different phases of transcription is still unclear. In this study the RNA polymerase II enzymes from calf thymus and human placenta were analyzed with respect to the catalytic site.

Both enzymes were purified and characterized with regard to the molecular weight, isoelectric point, and stoichiometry of their peptides. The apparent Michaelis constants for adenosine triphosphate and uridine triphosphate were determined, and the enzymes were analyzed for possible contamination by kinases.

A nucleoside triphosphate binding site was identified using photo-affinity labeling with gamma radiolabeled azido purine ribonucleoside

triphosphates, which upon ultraviolet irradiation yield into a highly reactive group that will covalently attach to nearby sites. Photoaffinity labeling of RNA polymerase II in the absence or presence of template showed one peptide (E) with a molecular weight of 37 kD and an isoelectric point of 5.4 to be the principal target in both enzymes. Ultraviolet irradiation was absolutely necessary for photoaffinity labeling to occur. In addition, no labeling occurred when the probe was prephotolyzed or when the enzyme was inactivated. Furthermore, photoradiolabeling of enzyme could be decreased by preincubation with natural substrates.

To provide evidence that the radiolabeled peptide E forms part of the domain of the catalytic (nucleoside triphosphate binding) site, experiments were performed using unlabeled azido adenosine triphosphate. Although unlabeled analogue was not a substrate for RNA polymerase type II, it inhibited transcription elongation by the enzyme in a competitive manner in the absence of ultraviolet light and photoinactivated the enzyme in the presence of ultraviolet irradiation. As in the case with photoradiolabeling, photoinactivation by azido adenosine triphosphate could be decreased by natural substrates; in both cases purine ribonucleoside triphosphates were more effective than pyrimidine nucleoside triphosphates. Furthermore, photoinactivation showed a saturation effect at about the same concentration as the inhibition constant for azido adenosine triphosphate.

Collectively, these results provide evidence that polypeptide E in these two eukaryotic enzymes is an essential component for activity and suggest that this polypeptide may be part of the purine nucleoside triphosphate binding site for this enzyme.

## CHAPTER ONE INTRODUCTION AND BACKGROUND TO THE TRANSCRIPTION PROCESS

### RNA Polymerase Enzymology

Cellular DNA contains information in the form of genes for thousands of different RNA and protein molecules. Regulation of the expression of these genes is mandatory for proper functioning of the cell. The use of information encoded in the genetic material involves two steps, the synthesis of RNA molecules (transcription), and the use of some RNA molecules as templates for protein synthesis (translation). There are three types of RNA: tRNA, rRNA and mRNA, of which only the last codes for proteins.

Transcription is the production by DNA dependent ribonucleoside triphosphate RNA nucleotidyl transferase (E.C.2.7.7.6); or RNA polymerase, of a complementary single stranded RNA polymer. It catalyzes a template-directed reaction involving ternary complex formation as an intermediate and requires 4 different 5'-NTPs as substrates in an asymmetric process. RNAP binds to a promoter region, upstream of the specific initiation site (5' by definition) on the DNA template, and catalyzes the formation of an RNA strand in the 5'-3' direction using ATP, GTP, UTP, and CTP as substrates. Selection of the specific substrate depends on the formation of Watson-Crick base pairing with the sense strand of the template, and only that DNA strand is transcribed. The RNAP releases the nascent RNA

at the termination site at the 3'-end of the gene. The whole process can be divided into four stages: binding, initiation, elongation, and termination (Krakow et al., 1976). For example, in E. coli transcription starts by a recognition process between the RNAP and DNA, approximately 35 bp upstream of the gene followed by binding of RNAP to the promoter, resulting in the formation of a closed promoter complex at more than 10 bp upstream of the initiating base pair (Gilbert, 1976). Next a localized DNA strand separation occurs, resulting in the formation of an open promoter complex. After binding of the first rNTP, most often a purine ribonucleoside triphosphate and a second NTP, a dinucleoside tetraphosphate is synthesized in the de novo initiation step (Lewis and Burgess, 1980, von Hippel, 1984). Elongation occurs during polymerization and translocation steps. Finally the release of the RNA product takes place during the termination step.

All DNA polymerases, RNA polymerases, and reverse transcriptases follow the same stereochemical course during the polymerization of (d)NTPs (Bartlett and Eckstein, 1982). An inversion takes place in the configuration at the alpha phosphorus atom, indicating a direct nucleophilic attack by the 3'OH group of the growing chain on the alpha phosphorus of the incoming (d)NTP, followed by pyrophosphate displacement, without formation of a covalent intermediate (Knowles, 1980).

The nucleic acid polymerases are metallo enzymes, with  $\text{Zn}^{2+}$  as tightly bound (intrinsic) and  $\text{Mg}^{2+}$  or  $\text{Mn}^{2+}$  as loosely bound (extrinsic) divalent cation, which is most often the case for enzymes that catalyze a displacement at the phosphorus atom (Mildvan and Loeb, 1979). The role of  $\text{Zn}^{2+}$  is still under investigation. Suggestions have been

made that it is involved in template binding and selection of a purine NTP in the initiation step, because  $\text{Zn}^{2+}$  coordinates directly to the base moiety of ATP, both in the presence and absence of template (Chatterji et al., 1984).  $\text{Mg}^{2+}$  and  $\text{Mn}^{2+}$  may facilitate the release of the pyrophosphate (Wu and Tweedy, 1982).

### Prokaryotic RNA Polymerase

Attempts to unravel the reaction mechanism of RNA polymerases started with prokaryotic systems because they contain only one class of RNAP and an almost protein-free template with uninterrupted messages. The ability to isolate large amounts of RNAP from mutant and wildtype E. coli cells and to do reconstitution experiments made it possible to analyze the specific function of RNAP subunits, to resolve the mechanisms of promoter recognition and specific initiation, and to locate and clone the specific genes for all subunits (Yura and Ishihama, 1979, and Glass, 1982).

The prokaryotic RNAP or holoenzyme (454 kD) is composed of a core (380 kD) containing nonspecific catalytic activity in the multimer of  $\alpha$ ,  $\beta$ , and  $\beta'$ , to which the  $\sigma$ -subunit is transiently attached (Chamberlin, 1982). The  $\sigma$ -subunit reduces the affinity of the core for ds-DNA by a factor of 1000, diminishing random interaction and allowing specific and efficient initiation, i.e., interaction of the holoenzyme with a promoter, an AT rich consensus sequence of 7 bases, 10 bases upstream from the initiation site (Chamberlin, 1976).

One way to assign a function to a peptide that occurs in a copurified peptide conglomerate is the use of UV light to crosslink DNA to

RNAP. The product was analyzed by 1D-SDS-PAGE after nuclease treatment. Subunits  $\beta$  and  $\beta'$  were found to be crosslinked to both T7-DNA strands and peptide  $\sigma$  to the nontemplate strand (Park et al., 1980). Subunit  $\alpha$  could not be crosslinked by UV irradiation.

Another way to assign a function to a peptide in RNAP is to cross-link labeled probes which are derivatives of natural substrates. The methodology and results for rNTP affinity labeling are described in the Introduction of Chapter Six.

The application of genetic analysis to E. coli mutants with altered transcription properties resulted in a correlation between the presence of specific peptides in RNAP and their functions (Scaife, 1976, Yura and Ishihama, 1979). The genetic information coding for resistance to the antibiotic rifampicin, which inhibits initiation, was found to be located in the structural gene coding for the  $\beta$  subunit. Temperature sensitive mutants revealed the structural gene locations of the  $\beta$ ,  $\beta'$ , and  $\alpha$  subunits.

A summary of the results obtained with prokaryotic RNAP (Yura and Ishihama, 1979, Chamberlin, 1982, and Wu and Tweedy, 1982) indicates that subunit  $\sigma$  (70.3 kD) directs the core enzyme towards the promoter. Subunits  $\beta$  (150.6 kD) and  $\beta'$  (170 kD) are involved with catalysis. Subunit  $\beta'$  is involved in DNA binding. Subunit  $\alpha$  (dimer of two 36.5 kD polypeptides) is essential to proper functioning of the holoenzyme and to initiate in vitro reconstitution. It is likely that each of the critical steps of transcription involves more than one subunit (Larionov et al., 1979). In addition to the polypeptides necessary for catalytic activity and DNA binding, several transcription factors are known to



impart a certain selectivity during prokaryotic RNAP transcription (Glass, 1982, Greenblat and Li, 1981). These include the  $\sigma$  peptide for specific initiation, the nusA protein (69 kD) and the rho protein (50 kD), which play a role in termination, and the CAP (catabolic activator protein, 45 kD) that, upon binding with cAMP, stimulates initiation at a catabolite repressible promoter. Thus, even in the relatively simple prokaryotic system, a number of polypeptides in addition to those in the core enzyme play a role in critical steps regulating transcription.

#### Nuclear Eukaryotic RNA Polymerase

These enzymes are composed of a much higher number of peptides and occur in three different classes, each containing a number of subclasses (Roeder, 1976, Paule, 1981, Lewis and Burgess, 1982, and Guilfoyle et al. 1983). Reaction conditions can be used to distinguish among the three enzyme classes, i.e., ionic strength, ratio of activity with  $Mn^{2+}$  to that with  $Mg^{2+}$ , and the type of template preferred for optimal activity (Roeder, 1976, Lewis and Burgess, 1982). The earliest classification by Roeder was based on the order of elution from DEAE Sephadex columns, where three peaks of RNAP activity appear with increasing salt concentration. After the discovery that the general chromatographic properties can vary significantly among enzymes from different organisms and that the order of RNAP class elution changes when a DEAE-cellulose column is used, Chambon proposed the use of  $\alpha$ -amanitin inhibition as reference to distinguish the types, because each class of RNAP has a different sensitivity to this toxin. RNAP I, II and III from the higher eukaryotic cells are sensitive to  $\alpha$ -amanitin at greater than 1mM, 1nM

and 0.1 to 0.01 mM respectively (Faulstich, 1980). To correlate each class of RNAP with a specific class of RNA product, experiments were done with isolated mouse nuclei, which were incubated with various  $\alpha$ -amanitin concentrations in the presence of [ $^3$ H]-uridine, followed by autoradiography and RNA analyses. From these and other results the roles of the three RNAPs became clear (Roeder, 1976, Lewis and Burgess, 1982):

RNAP I transcribes reiterated genes, resulting in the precursor 45 S rRNA which matures into 5.8, 18 and 28 S rRNAs. RNAP I is found in nucleoli, and it represents 50-70 % of all nuclear RNAP activity.

RNAP II produces heterogeneous, unstable precursor RNA, which is processed and transported to the cytoplasm as mRNA. RNAP II is found in the nucleoplasm and represents 20-40 % of all nuclear RNA activity.

RNAP III produces 4, 4.5 and 5 S RNA from reiterated genes and some viral sequences. RNAP III activity is found in the nucleoplasm and accounts for 10-15 % of the total nuclear RNAP activity.

There are many similarities (Spindler, 1979) between core E. coli RNAP and purified eukaryotic RNAP II. Neither enzyme initiates efficiently on double stranded DNA. Both enzymes lack transcriptional specificity in vitro and prefer to initiate on any single stranded region of DNA without apparent sequence preference. Both enzymes interact in the presence of specific initiation factors with consensus sequences that occur in the promoter region, the Pribnow box and the Hogness box for prokaryotic and eukaryotic enzymes, respectively. Comparison of their polypeptides shows that they have a complex subunit composition with two large peptides ranging in MW from 120-240 kD and a number of peptides with a MW of less than 100 kD (Paule, 1981).

For prokaryotic RNAP, several factors that control transcription have been isolated (see above). Attempts have been made to identify the proteins of eukaryotic RNAP that are involved in promoter recognition and in catalysis. Unfortunately, no purified peptide complex has ever been isolated from eukaryotic organisms which demonstrated site specific initiation in vitro on defined and deproteinized double stranded templates (Paule, 1981, Coulter and Greenleaf, 1982, and Lewis and Burgess, 1982). Nonrandom interaction was found using a variety of templates, including supercoiled DNA (Tsuda and Suzuki, 1982). When natural chromatin was used, it was shown that RNAP III initiated specifically, but the factor responsible for the specificity could not be isolated from chromatin (Parker et al., 1976). Wu (1978) developed the first soluble cell-free extract with endogenous RNAP III and protein factors to transcribe VA RNA from protein-free adenovirus type 2 DNA. This was followed by similar approaches in the form of cell-free extracts for RNAP II (Weil et al., 1979 and Manley et al., 1980).

These cell extracts have been helpful in studying gene regulation at the transcriptional level in vitro for a number of templates, but have not contributed to a functional understanding of the basic enzymology of eukaryotic RNAP. Several fractions have been used, but how many factors are necessary and their mechanism of action is still unknown (Matsui et al., 1980, Korn, 1982, and Davison et al., 1983). These factors are RNAP class-specific and seem to suppress random initiation, rather than cause specific initiation of transcription. Unfortunately, none of the factors described thus far has been found to be involved in the regulation of gene expression during development in vivo.

It appears that the DNA sequences involved in vivo with promotion of specific transcription are larger than their prokaryotic counterparts and may be related to eukaryotic chromosomal structural organization (Breathnach and Chambon, 1981). Both the Pribnow and the Hogness boxes may help to determine the exact starting site for transcription, whereas more remote DNA segments appear to help to determine the efficiency of transcription (Sassone-Corsi et al., 1984). It should be noted, however, that a Hogness-like box has not been found for RNAP I and III, indicating that the specific transcription by distinct classes of RNAPs can be due to specific recognition sequences, which are characteristic of a specific class of genes. Deletion mutants of DNA have been prepared to detect the location of the control region on the template for the different RNAP classes. RNAP I was found to resemble prokaryotic RNAP most closely, because its control region for proper initiation is near the 5' end (Kohorn and Rae, 1983, and Sommerville, 1984). RNAP II differs more from prokaryotic RNAP because its control region was found further upstream (Jove and Manley, 1984), whereas RNAP III has an intragenic control region (Sakonju et al., 1980, and Bogenhagen et al., 1980).

### RNA Polymerase Structure

The relative complexity of RNAPs I, II, and III is indicated by the number of subunits: 7-10, 12-14, and 10-15, respectively, and the MWs: 450-500 kD, 550-600 kD, and 550-650 kD, respectively (Roeder, 1976, Paule, 1981, Guilfoyle et al., 1983, and Lewis and Burgess, 1982). Immunological studies showed that the large MW subunits of one RNAP

class are unrelated to the large subunits of any other class within one species. Some cross reactivity was detected among the large homologous RNAP subunits from similar RNAP classes obtained from different species (Cleveland et al., 1977, Dahmus, 1983b, Guilfoyle et al., 1983, Guilfoyle, 1984b, and Robbins et al., 1984). This indicates that perhaps some domains on the largest polypeptides were conserved during evolution (Huet et al., 1982).

As far as the the relationship among the low MW subunits from all three RNAPs from eukaryotic species, including plants, is concerned, these can be divided into two categories (Paule, 1981). Some appear to be unique, whereas others are found in two or three RNAP classes, i.e., there seems to be a common core of 3 low MW polypeptides, for example 29, 23 and 19 kD in *Xenopus* (Engelke et al., 1983). This generalization is based on one and two dimensional electrophoretic data and immunological studies (Sentenac et al., 1976, Guilfoyle et al., 1983, Guilfoyle, 1984a, and Robbins et al., 1984).

There are two to three subclasses of each of the mammalian RNAPs. Using graded porosity non-denaturing PAGE, MWs of 570 kD to 600 kD were found for calf thymus RNAP IIa, b, and c (Kedinger et al., 1974). The three subclasses do, however, show identical catalytic properties and sensitivity to  $\alpha$ -amanitin (Roeder, 1976). The transcriptional properties of the subclasses are, however, not similar with respect to specific initiation (Dahmus and Kedinger, 1983a). Most RNAP subclasses differ only in the MW of the largest subunit, which may be due to proteolysis, either in the cell or during purification (Guilfoyle et al, 1984b). Sometimes they differ in charge, which might indicate a

functional modification of the enzymes by phosphorylation (Dahmus et al., 1981a, 1981b, and 1981c and Kranias et al., 1977, 1978a, and 1978b). The physiological function of RNAP subclasses is still unknown.

#### $\alpha$ -Amanitin as Probe for Structure

$\alpha$ -Amanitin is a specific inhibitor of certain eukaryotic RNAPs II (Faulstich, 1980). Inhibition in vitro cannot be relieved by high concentrations of DNA or substrates, but can be alleviated by addition of more enzyme (Cochet-Meilhac and Chambon, 1974 and Faulstich et al., 1981, and Novello et al., 1970). Various preincubation regimes do not affect the inhibition. Inhibition is immediate when  $\alpha$ -amanitin is added at any time during the polymerization process (Lindell et al., 1970). Thus,  $\alpha$ -amanitin inhibited RNA synthesis is not due to binding of  $\alpha$ -amanitin to the template or to hindered RNA product release, but rather to forming a tight complex with the enzyme. Cochet-Meilhac and Chambon (1974) investigated the mechanism of inhibition of RNAP II by  $\alpha$ -amanitin. Their observations put amatoxins in the class of noncompetitive inhibitors. It was concluded indirectly from pyrophosphate exchange experiments that amatoxins most probably block the formation of phosphodiester bonds in the initiation and elongation steps. This cannot be a direct effect, as  $\alpha$ -amanitin does not prevent NTP binding. It was later reported (Vaisius and Wieland, 1982) that the template-directed synthesis of the first phosphodiester bond by calf thymus RNAP II is not inhibited by a high  $\alpha$ -amanitin concentration. However, no subsequent internucleotide bond is formed in the presence of this inhibitor. This suggests that translocation of the nascent RNA and RNAP along the DNA template is the step inhibited by  $\alpha$ -amanitin. Under reaction conditions

which normally favor the elongation of RNA, the transcription process is arrested immediately following the formation of the first phosphodiester bond. Brodner and Wieland (1976) reported the identification of the amatoxin binding subunit of calf thymus RNAP II with an MW of 140 kD. The authors speculated that the subunit which ranges in MW from 135 to 145 kD in RNAP II and III may render these enzymes sensitive to  $\alpha$ -amanitin. The absence of a subunit of a similar size in RNAP I of higher eukaryotic organisms correlates with that hypothesis, as does the presence of a 137 kD subunit in the  $\alpha$ -amanitin sensitive yeast RNAP I (Faustich, 1980).

More recent reports suggest, however, that the largest subunit determines  $\alpha$ -amanitin binding (Greenleaf, 1983, and Ingles et al., 1983). Using a genetic approach, it was found that the 215 kD peptide of Drosophila melanogaster RNAP II contains the site at which mutations to amanitin resistance occur. This does not refute the data of Brodner and Wieland, as the  $\alpha$ -amanitin binding site might be a domain made up by both the 140 and the 215 kD subunits, which would explain why only native RNAP II binds  $\alpha$ -amanitin.

## CHAPTER TWO PURIFICATION OF CALF THYMUS RNA POLYMERASE II

### Introduction

Prokaryotic sources yield large quantities of RNAP, on the order of 500 mg/kg material (Burgess, 1976). In contrast, the yields from eukaryotic sources are 10-100 fold lower, making isolation of pure RNAP II rather costly, especially when cell cultures are used. As an alternative source for mammalian RNAP, the calf thymus is often used because in this immature animal, the thymus is rich in nuclei (Hodo and Blatti, 1977).

This chapter describes the purification of CT RNAP II and the determination of several kinetic parameters of this enzyme. The composition of the enzyme with respect to the MW, stoichiometry, and pIs of the polypeptides is described in Chapter Four. The CT RNAP II was purified from calf thymus according to Hodo and Blatti (1977), because their procedure is used by many other laboratories. Furthermore, the CT RNAP enzyme from this source has been well characterized with respect to polypeptide composition and in vitro transcription properties.

Since this enzyme contains a limited number of polypeptides, it was used as a model enzyme for photoaffinity labeling studies with NTP derivatives. The results were confirmed and extended to human placental RNAP II, whose purification is described in the next chapter.



## Materials and Methods

### Buffers for CT RNAP II Isolation

Buffer A: 10 mM Tris-HCl, 12.5 % (v/v) glycerol, 25 mM KCl, 5 mM  $MgCl_2$  0.06 mM PMSF (Sigma Chemical Company), 0.5 % (v/v) BME, Aprotinin at a concentration of 0.05 Trypsin Inhibitor Units (TIU)/ ml (Sigma Chemical Company), and 0.1 mM EDTA.

Buffer B: 50 mM Tris HCl, 0.1 mM EDTA, 0.5 % (v/v) BME, 0.06 mM PMSF, and 0.05 TIU Aprotinin/ml.

Buffer C: 50 mM Tris-HCl, 10 % (v/v) glycerol, 0.1 mM EDTA, 280 mM ammonium sulfate, 0.5 mM DTT (BIO.RAD Laboratories), and 0.06 mM PMSF.

Buffer D: 50 mM Tris-HCl. 0.1 mM EDTA, 0.5 mM DTT, 25 % (v/v) glycerol, and an amount of ammonium sulfate which was varied as indicated.

The pH of the buffers was adjusted to 7.9 at 20°C. The DTT, PMSF, BME, and Trasylol were added to the buffers just before use.

### Column Resin Preparation

Fine particles were removed from the chromatography resins by decantation. All chromatography resins were warmed to room temperature before degassing by vacuum and cooled to 4°C before the preparation of the columns. After settling of the resins in the columns, extensive equilibration followed, until the ionic strength and the pH of the eluate were equal to that of the equilibration buffers.

DEAE-Sephadex A-25 (Pharmacia Fine Chemicals): The beads were swollen in 5 volumes of distilled water for 6 hours at 23°C. Water regain was 7 ml/gm. HCl was added to the suspension to a final concentration of 0.2 M and left for 20 minutes. This slurry was filtered over a Buchner funnel and washed with distilled water until the pH was 4. The cake was resuspended in 5 volumes of 0.01 M NaOH, left for 20 minutes, filtered, and washed until the pH was 8. The cake was resuspended in buffer containing 145 mM ammonium sulfate and titrated to a final pH of 7.9.

Phosphocellulose, P 11 (Whatmann, Inc): The phosphocellulose was added to 5 volumes of 0.5 M NaOH and left for 20 minutes. The slurry was then filtered through a sintered glass funnel and rinsed with deionized water until a pH of 8 was reached. The cake was resuspended with 5 volumes of 0.5 M HCl and left for 20 minutes, filtered on a sintered glass funnel, and rinsed with deionized water until the pH was 4. The cake was resuspended in 2 volumes of 50 mM Tris-HCl, pH 7.9, containing 0.1 mM EDTA and titrated with 6 M KOH until the pH was 7.9. It was then poured into the column and washed with equilibration buffer D (containing 0.2 mg BSA/ml and 50 mM ammonium sulfate).

DEAE-cellulose, DE-52 (Whatmann, Inc.): The preswollen beads were washed with 5 M NaCl, exposed successively to 0.5 M HCl and 0.5 M NaOH for 20 minutes each, and washed with deionized water until the pH was 8. The cake was resuspended in 3 volumes of buffer D containing 140 mM ammonium sulfate and titrated to the pH of 7.9.

Biogel A-1.5m (BIO.RAD Laboratories): This material comes pre-swollen and was equilibrated with buffer D containing 145 mM ammonium sulfate.

### Polymin P Preparation

Two hundred milliliters of 50 % (v/v) Polymin P (BASF, Wyandotte Corporation) were added to 600 ml of water with continuous and rapid stirring. This basic and viscous solution, with a pH of 12, was neutralized with approximately 38 ml of 12 M HCl until the pH was 7.9 at 4°C. The volume was adjusted to 1 liter and the 10 % solution was filtered through one layer of miracloth, resulting in a clear solution which was stable for 6 months.

### Conductivity Measurements

Conductivity measurements were performed on a conductivity meter (Radiometer, CDM 3) with a flow-through cell. Samples were diluted ten-fold and measured at room temperature. Calibration curves were prepared to measure the ammonium sulfate concentration of the solutions in the absence and presence of 25 % (v/v) glycerol.

### Measurement of Protein Concentration

Protein concentrations were measured as published by Bradford (1976), using BSA as standard. To remove interfering substances, e.g., Polymin P, the aliquot was TCA precipitated and washed in acidic and neutral acetone solutions.

### Assay of RNAP Activity

Activity was assayed (Hodo and Blatti, 1977) in a 100 µl standard reaction mixture containing 100 mM ammonium sulfate, 2 mM  $\text{MnCl}_2$ , 0.6 mM ATP, CTP, GTP, 5 µg denatured calf thymus DNA, and 50 mM TrisHCl, pH 7.9 (22°C). When a substrate limiting assay was used, 0.4 µM (1.25 µCi) of [5,6- $^3\text{H}$ ]-UTP (Amersham International) was added, but when a non-limiting assay was used, 1.25 µCi of radiolabeled UTP was diluted

to 0.06 mM. Enzyme was added last to initiate the reaction. DNA was omitted to test for endogenous template in the RNAP II fraction. The enzyme fraction was heat denatured or the template omitted to obtain background cpm. The incubation was at 37°C for 10 minutes. The reaction was stopped by application of the mixture to a GF/C filter (Whatman) and immersion into 10 % TCA containing 0.02 mM sodium pyrophosphate. The filters were washed 6 times and dried in 95 % ethanol and anhydrous ether. After drying, the filters were immersed in Econofluor (New England Nuclear) and the radioactivity counted in a liquid scintillation counter. One unit of enzyme activity is the amount of enzyme which incorporates 1 nmole of UMP per 10 minutes at 37°C in a [ $^3\text{H}$ ]-UMP incorporation assay under near saturating conditions as described in the legend of figure 4 (Hodo and Blatti, 1977). To follow the incorporation of [ $^3\text{H}$ ]-AMP, 1.25  $\mu\text{Ci}$  of [ $^3\text{H}$ ]-ATP, diluted to a final concentration of 0.1 mM (Amersham International) was used instead of radiolabeled UTP.

$\alpha$ -Amanitin (Boehringer Mannheim) was used to distinguish among the activities of RNAP I, II and III. RNAP I is resistant to 10,000 ng  $\alpha$ -amanitin/100  $\mu\text{l}$ , RNAP II is sensitive to 10 ng  $\alpha$ -amanitin/ 100  $\mu\text{l}$  and RNAP III is resistant to 10 ng  $\alpha$ -amanitin /100  $\mu\text{l}$  but sensitive to 10,000 ng  $\alpha$ -amanitin/100  $\mu\text{l}$ . The use of methanol as solvent for the  $\alpha$ -amanitin solutions lowered the noncompetitive inhibitory activity by the toxin, while the enzyme activity without  $\alpha$ -amanitin was only slightly affected, even at methanol concentrations up to 5 % (v/v). This can be explained by the initial observation by Cochet-Meilhac and Chambon (1974) that organic solvents decrease affinity of the RNAP II for  $\alpha$ -amanitin, indicating hydrophobic interaction between the two. For this

reason the  $\alpha$ -amanitin stock (100  $\mu\text{g/ml}$ ) was diluted in water just before use. The concentration of the toxin was determined from its absorbance at 310 nm. The molar extinction coefficient is 13,500 liter per mole cm.

#### Template for Transcription Assays

Short single strand template was prepared by dissolving 10 mg calf thymus DNA (Sigma Chemical Company) in 10 ml of a solution containing 10 mM Tris-HCl, pH 7.4, 0.1 mM EDTA, and 10 mM NaCl (Kedinger et al., 1972). This solution was sonicated 6 times, in ice, for 30 seconds each, using a Heat Systems Ultrasonics, Inc., instrument, equipped with a macrotip and set at high intensity. The solution was heated in a boiling water bath for 10 minutes, quickly chilled in ice, and stored at  $-80^{\circ}\text{C}$ .

#### Measurement of Radioactivity

The amount of radioisotope was measured by liquid scintillation using a Beckman model LS 8000 instrument, equipped with an external standard. The data are corrected for quenching. The efficiency of  $^3\text{H}$  counting in Econofluor (New England Nuclear) was 24 %.

#### Calf Thymus RNAP Polymerase Purification

Calf thymus was obtained freshly from 13-15 months old Angus bulls from the meat lab at the University of Florida. It consists of two lobes and is located in an area above and behind the sternum where the upper chest and lower neck meet. Immediately after slaughter, the thymus (about one-half pound) was removed, sliced into small pieces, and submerged in ice-water. After several minutes, the pieces that contained mostly fat became hard and were discarded. The other thymus material remained soft and it was submerged in liquid nitrogen and stored at  $-80^{\circ}\text{C}$  until use.

The purification of RNAP II was done according to the procedure of Hodo and Blatti (1977) with some modifications. All steps were done at 4°C and performed directly after one another. All the supernatants were filtered through two layers of cheese cloth to remove lipids.

One kilogram of calf thymus tissue was homogenized in a precooled Waring blender until completely pulverized. Two liters of buffer A were added and the mixture was blended successively for 30 seconds each at low, medium, and high speed. One liter of buffer B was added, followed by 30 seconds of blending at low speed.

The homogenate was centrifuged in a JA-10 rotor for 10 minutes at 8,800 rpm (13,000xg). The first pellet (P1) was discarded. Four microliters of 10 % (v/v) Polymyxin P were added per ml of the first supernatant (SN1). This was stirred for 30 minutes and centrifuged as before. The SN2 was discarded and one liter of buffer C was added to P2 to obtain a final ammonium sulfate concentration of 180 mM. The mixture was blended with a Tissumizer (Tekmar Company) until homogeneous and centrifuged in a JA-10 rotor for 40 minutes as above.

The P3 was discarded and the protein precipitated from SN3 by addition of 0.24 gm/ml ammonium sulfate, yielding a final concentration of 1.82 M or 47 % (w/v). This was stirred for 60 minutes and centrifuged in a Beckman type 19 rotor for 75 minutes at 17,000 rpm (29,000xg). The SN4 was discarded and the P4 was resuspended with the Tissumizer in enough buffer D (800 ml) without ammonium sulfate to lower the ammonium sulfate concentration to 140 mM.

To this was added a 600 ml slurry of DE-52 anion-exchange medium (400 ml bed volume) which had been equilibrated with buffer D containing

140 mM ammonium sulfate. Excess buffer was removed slowly by vacuum filtration through a Buchner funnel, and the slurry was washed with one liter of buffer D containing 140 mM ammonium sulfate to remove RNAP I and III. The slurry was poured into a column and washed with buffer D containing 150 mM ammonium sulfate. The flow-through was collected until no more protein was observed. RNAP II was then eluted stepwise with buffer D containing 500 mM ammonium sulfate. The active fractions were pooled and diluted with buffer D until the ammonium sulfate concentration was 50 mM. BSA was then added to a final concentration of 0.2 mg/ml.

The sample was applied to a 100 ml phosphocellulose column, equilibrated with buffer D containing 50 mM ammonium sulfate and 0.2 mg BSA/ml. The column was washed with the same buffer but without BSA. The RNAP II was eluted with buffer D containing 200 mM ammonium sulfate, and the active fractions were pooled and diluted to a final ammonium sulfate concentration of 145 mM.

This fraction was applied onto a column of previously equilibrated Biogel A-1.5m, overlayed with 2 cm DEAE-Sephadex A-25. Initial concentration of the applied RNAP II took place by adsorption onto the DEAE-A-25 anion exchange beads under low ionic strength. Elution and gel filtration took place during a low salt wash to remove BSA, followed by elution with buffer D containing 600 mM ammonium sulfate.

## Interaction between CT RNAP II and [ $^3\text{H}$ ]-DeMeABGG

### Filter Binding Assay

A filter binding assay allows the measurement of the [ $^3\text{H}$ ]-dehydroxymethylamanitylazobenzoyl-N-glycylglycine (DeMeABGG) interaction with RNAP II. The [ $^3\text{H}$ ]-ABGG (specific activity of 10 Ci/mmol) was a gift from Dr. J.F. Preston (Preston et al., 1981). Nitrocellulose filters were used for RNAP-radiolabeled amanitin binding studies, which were performed as described by Cochet-Meilhac and Chambon, (1974). The binding buffer contained 80 mM Tris-HCl, pH 7.9 (4°C), 0.1 mM EDTA, 0.1 mM DTT, 100 mM ammonium sulfate, 30 % (v/v) glycerol, and 200  $\mu\text{g}$  BSA/ml. The washing buffer was identical except that the glycerol concentration was 15 % (v/v).

### Kinetics of Dissociation

Dissociation kinetics at room temperature were measured to determine the half life of the [ $^3\text{H}$ ]-DeMeABGG-CT RNAP II complex at pH 7.9 and at pH 6. To determine the rate of dissociation, [ $^3\text{H}$ ]-ABGG was mixed with RNAP until equilibrium had been established (Cochet-Meilhac and Chambon, 1974). Then a large excess of unlabeled  $\alpha$ -amanitin was added. Aliquots were taken at various times and the concentration of the CT RNAP II- [ $^3\text{H}$ ]-DeMeABGG complex was measured by filtration. When the excess of unlabeled  $\alpha$ -amanitin is large enough, the reaction should follow first order kinetics (Cochet-Meilhac and Chambon, 1974).



## Results

The results of the calf thymus RNAP II purification are summarized in Table I. After homogenization of the calf thymus tissue, nucleic acids were removed by Polymyxin P precipitation and high salt extraction. Following ammonium sulfate precipitation, RNAP enzymes were adsorbed to and eluted from DE-52 (Figure 1). This fraction was free of endogenous DNA and almost free of RNAP I and III. The RNAP II was further purified by phosphocellulose chromatography (Figure 2), after addition of BSA to stabilize the RNAP II. Final purification took place by gel filtration (Figure 3). RNAP II activity eluted in fractions 48-54. The enzyme was more than 95 % inhibited by 10 ng  $\alpha$ -amanitin/ 100  $\mu$ l. Fractions 10-40 contained a small amount of RNAP II activity, i.e., 15 units. Fractions 58-70 did not contain any RNAP activity. The RNAP II was stable for at least one year at -80°C, but very sensitive to additional thawing and freezing.

The crude homogenate of 1 kg calf thymus contained 90 gm of protein with at least 4050 units of RNAP II (see Table I), i.e., a specific activity of 0.045 units per mg protein. After purification the specific activity was 206 units per mg protein, indicating a purification factor of approximately 4600. Based on similar data, the yield of RNAP II was approximately 31 % (1256 units/4100 units). The calf thymus yields at least 4 units RNAP II per one gram of wet weight tissue (4050 units/1 kg).

After purification of RNAP II, several kinetic parameters were determined using the transcription assays described in the Materials and

Methods section with modifications as described in the figure legends. The apparent  $K_M$  for UTP was 19  $\mu\text{M}$  (Figure 4). The rate constant  $k_3$  of product formation, i.e., [ $^3\text{H}$ ]-uridine monophosphate incorporation, was  $0.44 \text{ second}^{-1}$ , which indicates a turnover number of 1.8 nucleoside monophosphates incorporated per second per CT RNAP II molecule, assuming the total nucleoside monophosphate incorporation equals four times the uridine monophosphate incorporation. The apparent  $K_M$  for ATP was 136  $\mu\text{M}$  (Figure 5). The rate constant  $k_3$  of [ $^3\text{H}$ ]-adenosine monophosphate incorporation was  $0.65 \text{ second}^{-1}$ , which indicates a turnover number of 2.6 nucleoside monophosphates per second per RNAP molecule.

The binding strength between the labeled  $\alpha$ -amanitin derivative [ $^3\text{H}$ ]-ABGG and CT RNAP II was determined based on data from the filter binding assay as described in the Materials and Methods section and in the legend of Figure 6. Equilibrium studies generate binding curves from which the dissociation constant,  $K_D$ , can be derived using a fixed RNAP II concentration and variable concentrations of  $\alpha$ -amanitin labeled derivatives, if the reaction mixture is at equilibrium before filtration. Scatchard plots can be generated from the data, yielding a  $K_D$  and the number of binding sites,  $n$ . The stoichiometric value for  $n$  is 0.92. The slope of the Scatchard plot indicates a  $K_D$  of  $3 \times 10^{-9} \text{ M}$  (Figure 6).

Another indicator of the affinity of the CT RNAP II for [ $^3\text{H}$ ]-DeMe-ABGG is the rate at which the [ $^3\text{H}$ ]-DeMeABGG dissociates from the enzyme. The dissociation rate constant was determined as described in the Materials and Methods section, at pH 6 and 7.9. The pH of 7.9 is the pH at which the enzyme's activity is optimal in in vitro assays. After plotting the data (Figure 7), the dissociation rate constant,

$k_2$ , and the half life of the CT RNAP II- $[^3\text{H}]$ -DeMeABGG complex were calculated: The  $k_2$  was  $6.4 \times 10^{-4}$  second $^{-1}$  and  $1.05 \times 10^{-4}$  second $^{-1}$  at pH 6 and 7.9, respectively. The  $T_{1/2}$  was 18 minutes and 110 minutes at pH 6 and 7.9, respectively.

### Discussion

The results reported here for the purification of CT RNAP II are comparable to those published by Hodo and Blatti (1977) who purified 5.88 mg RNAP II from 1 kg of calf thymus with a specific activity of 160 units per mg protein. The purity was approximately 95 % (see Chapter 4). I could, however, not measure RNAP activity until after the DE-52 chromatography, due to the presence of an endogenous inhibitor(s). For example, the addition of the SN1 to purified CT RNAP II inhibited the transcription rate significantly and could not be reversed by the addition of protease inhibitors (Aprotinin or PMSF) or RNase inhibitors.

The kinetic data derived from transcription studies on CT RNAP II and CT DNA yielded an apparent  $K_M$  of 19  $\mu\text{M}$  for UTP and 136  $\mu\text{M}$  ATP, respectively, in experiments where the concentration of the other three substrates was held at saturating levels.

It should be emphasized that for any RNAP the  $K_M$  as measured is truly apparent, since several factors complicate the assay. For example, the reaction rate is based on measuring the amount of TCA-precipitable  $[^3\text{H}]$ -UMP in product RNA which was present in the assay mixture at one time point and, thus, cannot truly represent the initial velocity. The rate limiting step under saturating conditions is initiation, which is

Table I. Summary of purification results of RNAP II from 1 kg calf thymus.

Purification step	Total Act. units	Volume ml	Protein mg	Spec.Act. units/mg	Units RNAP		
					I	II	III
Resuspended Ammonium sulfate pellet	147	2000	19000	-	13	106	28
DE-52	4050	175	145	28	12	4025	13
Phosphocellulose	2166	165	13.3	163	0	2166	0
Biogel A-1.5m/ DEAE-Seph.A-25	1256	35	6.1	206	0	1256	0

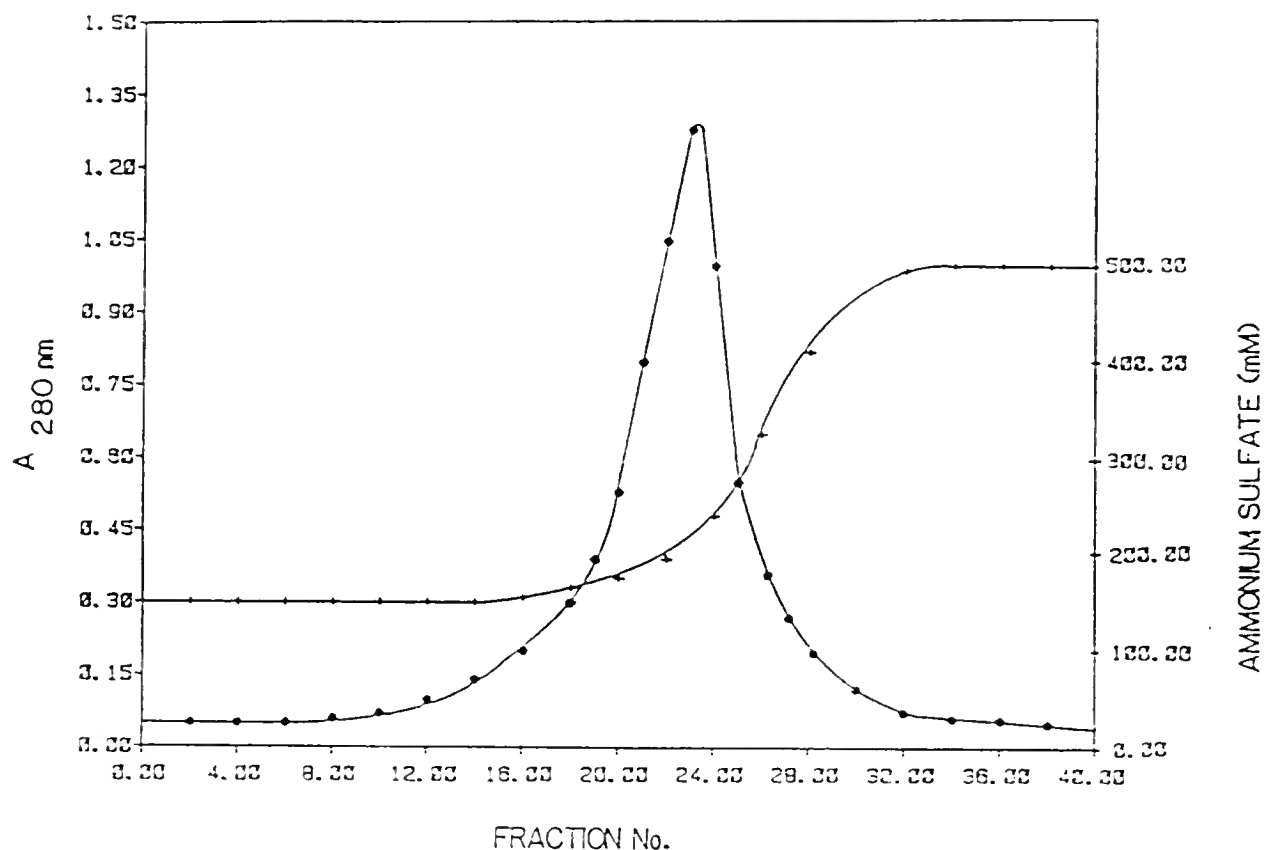


Figure 1. Typical elution profile of CT RNAP II by DE-52 chromatography.

The slurry (1000 ml) was loaded onto a column (5 cm diameter x 55 cm) and washed at a rate of 2.5 ml/hour until the absorbance at 280 nm was less than 0.1. The RNAP II was eluted with buffer D containing 500 mM ammonium sulfate into 10 ml fractions. RNAP II eluted at an ammonium sulfate concentration 150 to 380 mM in a total volume of 180 ml. To stabilize the enzyme, BSA was added to the eluate and to buffer D to a final concentration of 0.2 mg/ml. Indicated are the absorbance at 280 nm (—●—) and the ammonium sulfate concentration (—+—). The elution profile of the material during the 140 mM ammonium sulfate wash has not been included. The ammonium sulfate concentration of the pooled active fractions was 200 mM and contained 145 mg protein.

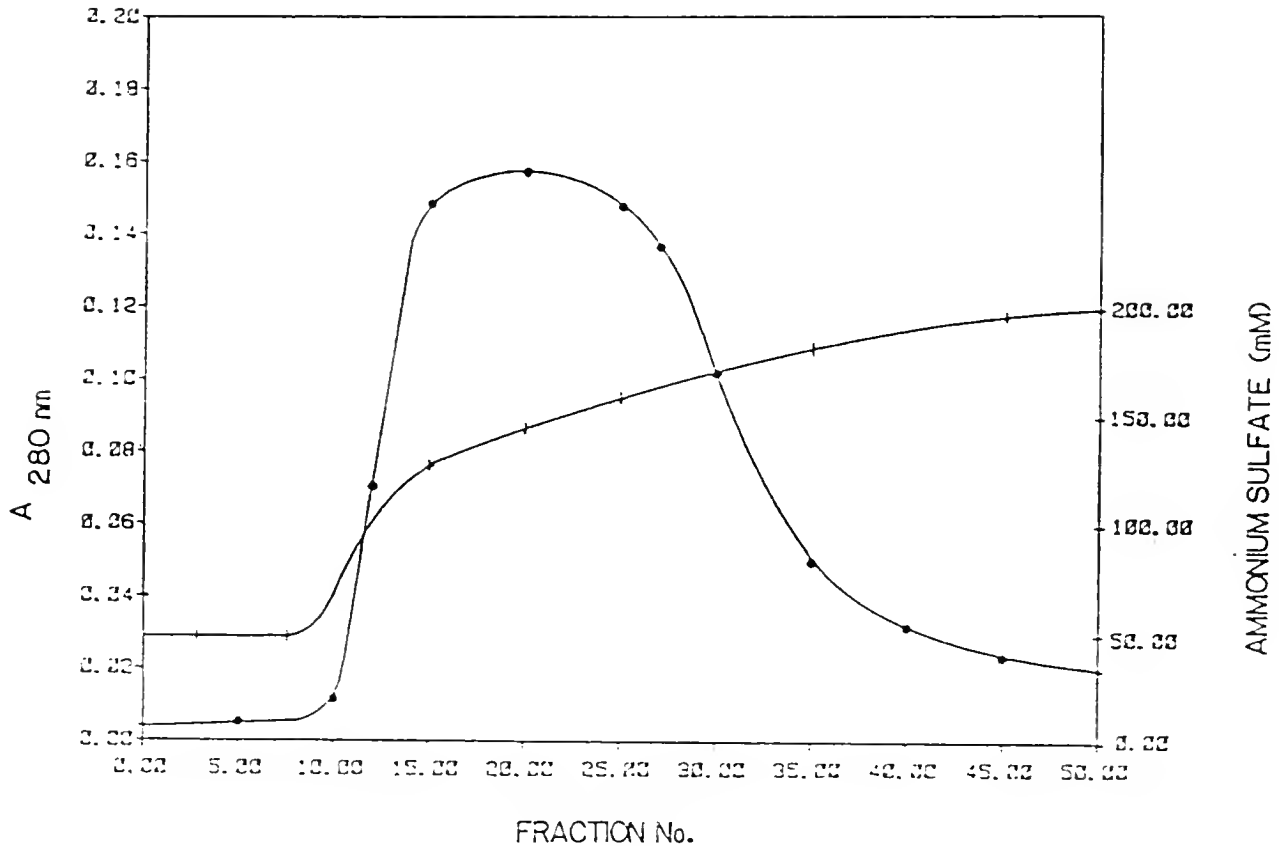


Figure 2. Elution profile of CT RNAP II by phosphocellulose chromatography.

The ammonium sulfate concentration of the DE-52 column active eluate was adjusted to 50 mM in buffer D containing 0.2 mg BSA/ml. The final volume of 700 ml was applied onto a phosphocellulose column (5 cm diameter x 6 cm) at a rate of 2 ml/minute. The column was washed with 250 ml buffer D containing 50 mM ammonium sulfate, but no BSA, until the absorbance at 280 nm was less than 0.1. Indicated are the absorbance at 280 nm (—●—) and the ammonium sulfate concentration (—+—). The RNAP II was eluted with buffer D containing 200 mM ammonium sulfate. RNAP II eluted from the phosphocellulose column between 50 and 180 mM. The ammonium sulfate concentration of the 160 ml pool of active fractions was 130 mM.

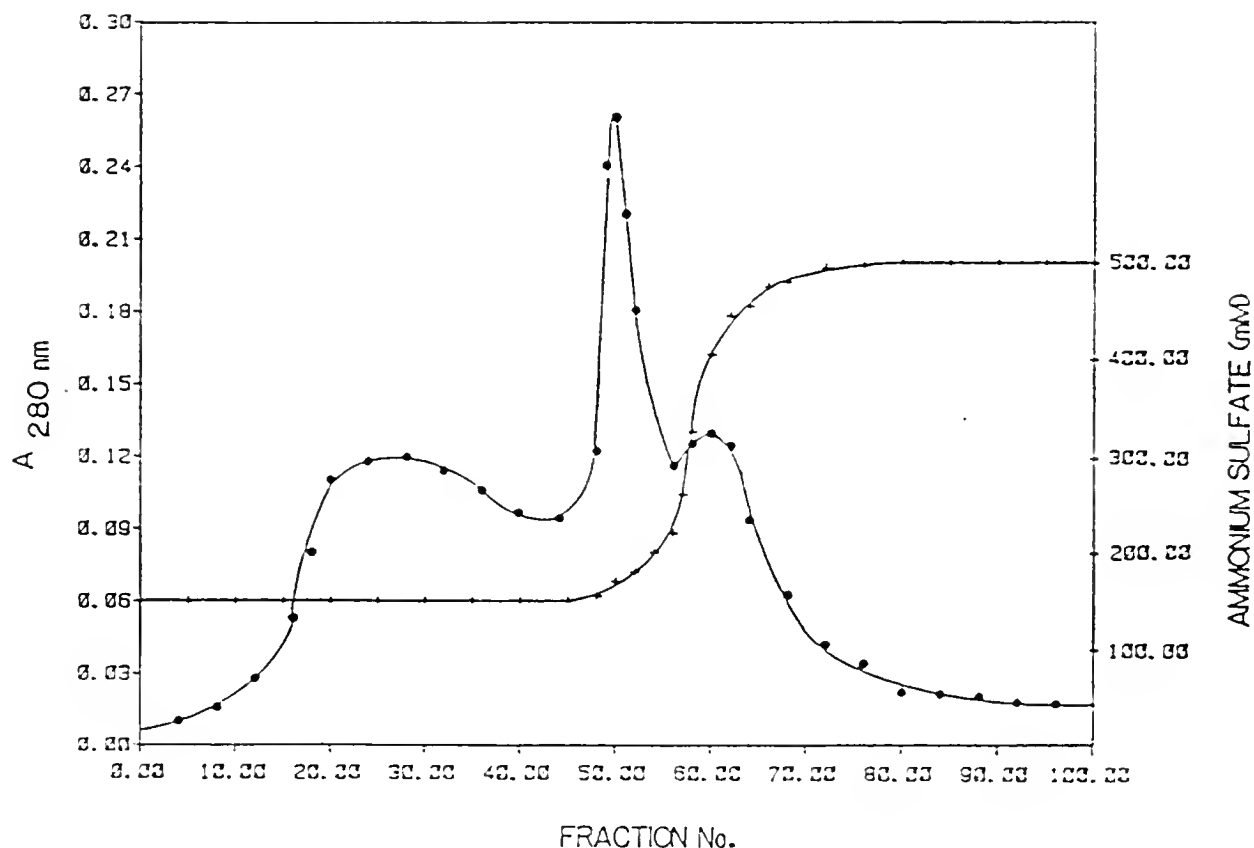


Figure 3. Elution profile of CT RNAP II by Biogel A-1.5m chromatography.

The phosphocellulose column fractions containing enzyme activity were pooled and the ammonium sulfate concentration adjusted to 145 mM. The pooled fractions (160 ml) were applied at a rate of 1 ml/minute onto a column (2 cm diameter x 12 cm) with a 10 cm high Biogel A-1.5m layer which was overlayed with 2 cm DEAE Sephadex A-25. The column was washed with buffer D, until the absorbance at 280 nm was 0.1. The RNAP II was eluted with buffer D containing 600 mM ammonium sulfate. Fractions (5 ml) containing activity were pooled (35 ml), and stored at  $-80^{\circ}\text{C}$ . The final ammonium sulfate concentration was 150 mM. Indicated are the absorbance at 280 nm (●) and the ammonium sulfate concentration (+).

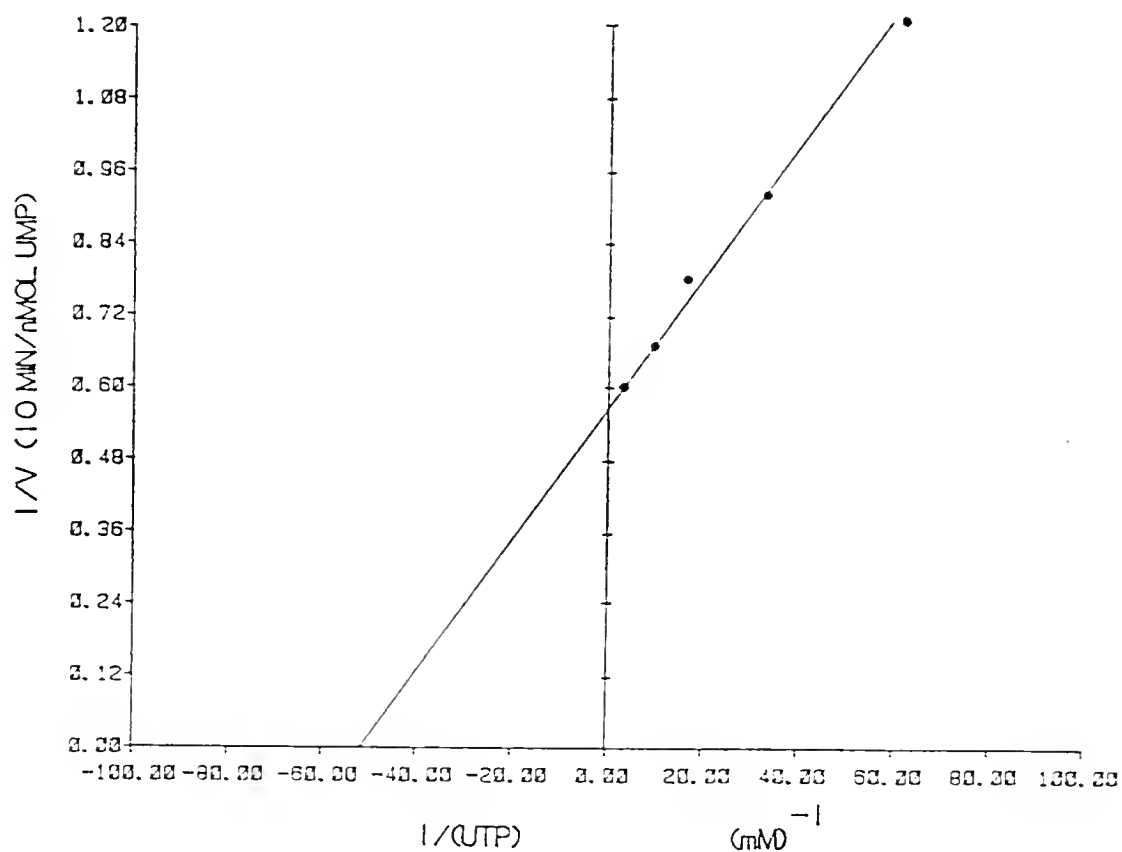


Figure 4. Double reciprocal plot of the velocity versus the UTP concentration.

The composition of the reaction mixture (100  $\mu$ l) containing 6.4 pmoles CT RNAP II was as described in the Materials and Methods section. The 1.25  $\mu$ Ci tritiated UTP was diluted with unlabeled UTP as indicated. The reaction took place at 37°C for 10 minutes.



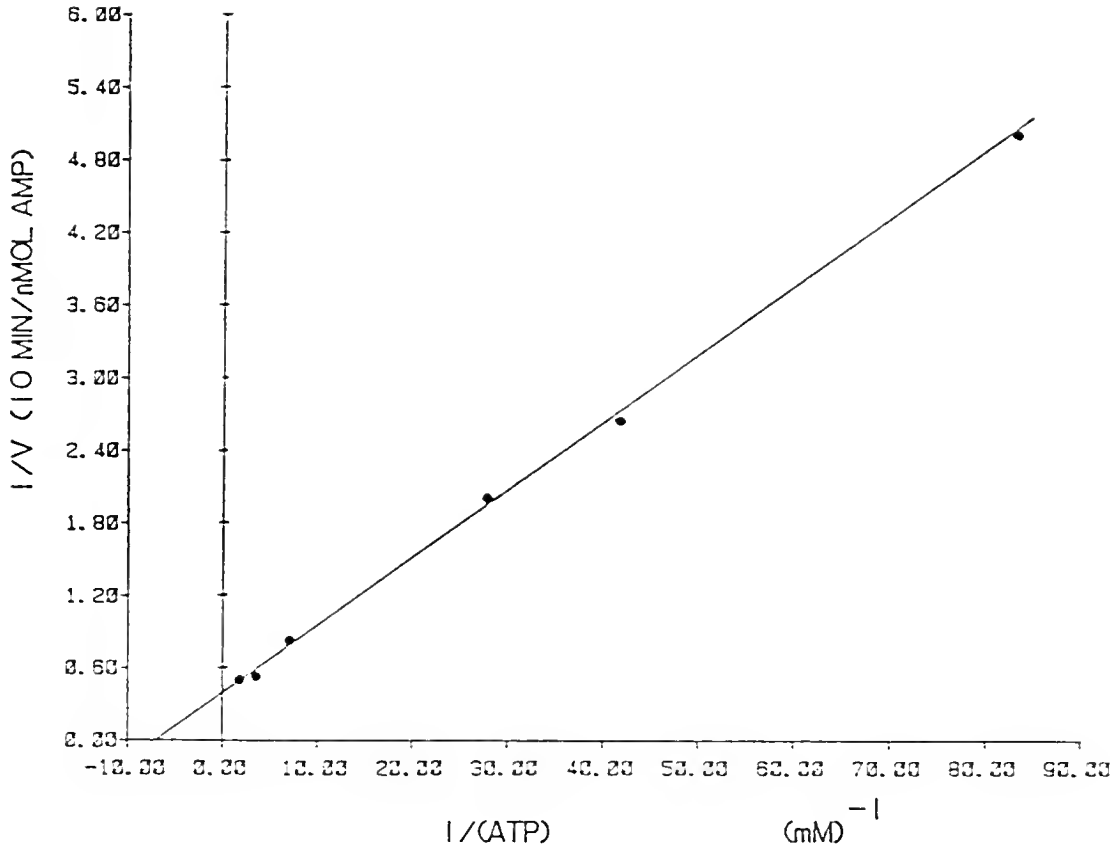


Figure 5. Double reciprocal plot of the velocity versus the ATP concentration.

The composition of the reaction mixture was as described in Figure 4, except that 1.25  $\mu\text{Ci}$  [ $^3\text{H}$ ]-ATP was tritiated instead of UTP (see Materials and Methods). The tritiated ATP was diluted with unlabeled ATP as indicated.

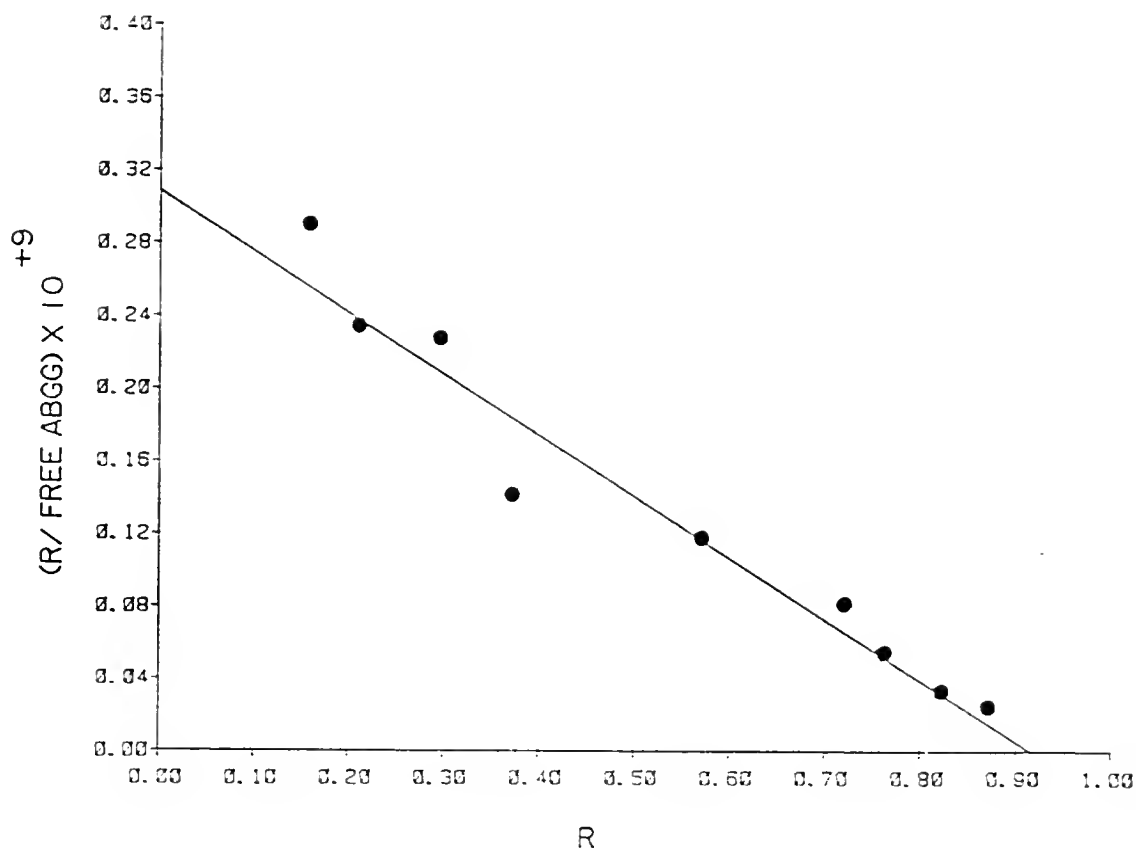


Figure 6. Scatchard analysis of data from filter binding assays measuring interaction between CT RNAP II and the tritiated DeMeABGG.

Mixtures containing 11 pmoles CT RNAP II and 1.12-4.48 nmoles tritiated DeMeABGG were incubated for 12 hours at 4°C in a volume of 0.5 ml of binding buffer. Blank values were obtained by preincubating RNAP with unlabeled  $\alpha$ -amanitin at 240 nM before the addition of labeled amatoxins. The complex was trapped on type HA filters (Millipore) and washed with washing buffer as described in the Materials and Methods section. After drying and counting the filters in Econofluor, the data were plotted according to the Scatchard method.

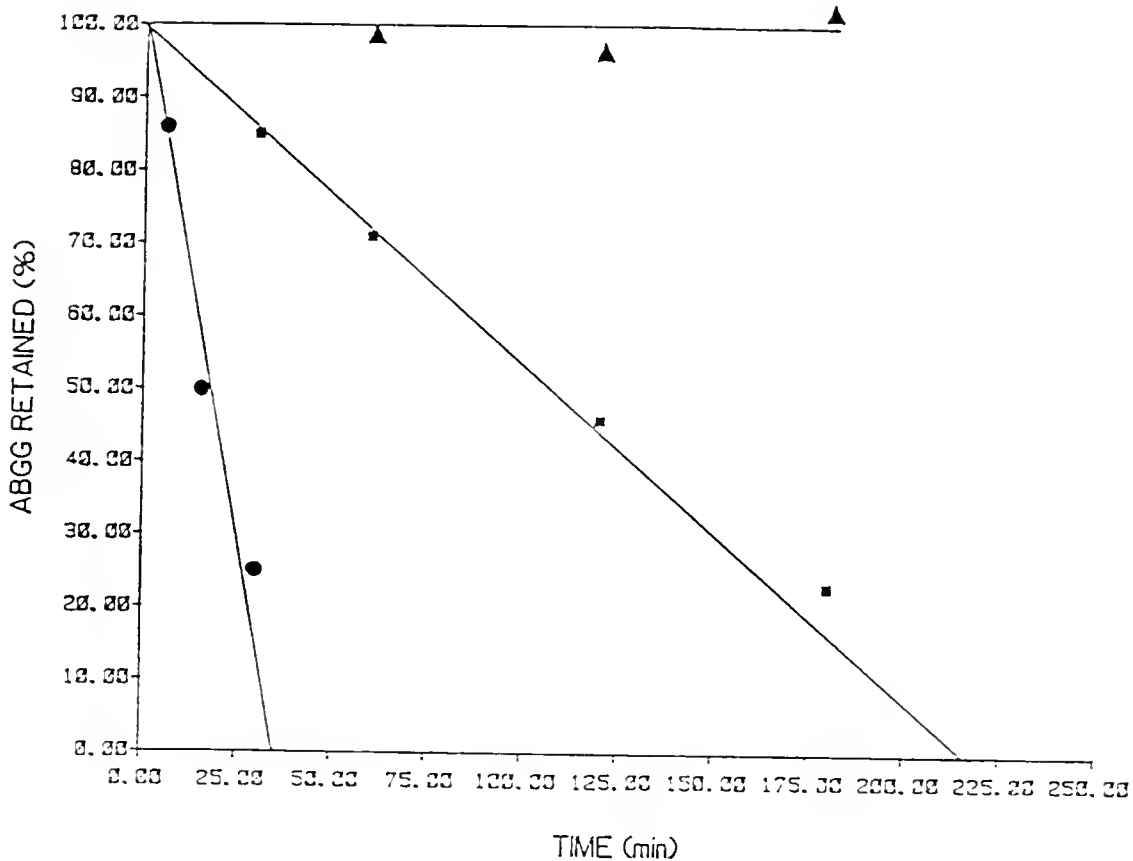


Figure 7. Dissociation curve to measure the half life of the non-covalent complex between CT RNAP II and tritiated-DeMeABGG at pH 6 and 7.9.

Eighteen  $\mu\text{g}$  (32.7 pmoles) of CT RNAP II were mixed with 41.5 pmoles of tritiated DeMeABGG (600 kcpm) in 1 ml binding buffer (as in Figure 6). After incubation at 22 °C for one hour the reaction mixture was divided into two 500  $\mu\text{l}$  fractions. The pH of one was adjusted to 6.0 by adding Hepes-HCl at the zero time point. After removing an aliquot of 100 $\mu\text{l}$  from each fraction for filter binding assays, unlabeled  $\alpha$ -amanitin was added to a final concentration of 40  $\mu\text{M}$ . This is a 1000 fold excess over the labeled ABGG (41.5 nM). Water was added instead of unlabeled  $\alpha$ -amanitin in a control reaction (—▲—). Subsequent aliquots were taken at 5, 15, 30 and 60 minutes for the sample at pH 6 (—●—) and at 30, 60, 120 and 180 minutes for the sample at pH 7.9 (—■—). The CT RNAP II-tritiated-DeMeABGG complex was trapped on type HA filters, washed, dried, and counted in Econofluor.

included here in the average rate of transcription over 10 minutes. Thus, any initial lag of the enzyme activity during initiation, as well as reinitiation after termination during the 10 minute period, will affect the  $K_M$ . In addition, the RNAP enzyme, according to the model described in Chapter Six, has one binding site for UTP, but two binding sites for ATP, which are unlikely to have equal affinities towards ATP. Furthermore, as described for CT RNAP II by Kadisch and Chamberlin (1982), there is the problem of a sequence dependent elongation, which causes the enzyme to "pause." Thus at best the kinetic data reported for any RNAP must be interpreted in the proper perspective.

The turnover number for the CT RNAP II purified here ranges between 1.8 and 2.6 for [ $^3\text{H}$ ]-uridine monophosphate and [ $^3\text{H}$ ]-adenosine monophosphate, respectively. This number is somewhat higher than the turnover number of 0.8 reported previously for CT RNAP II in similar transcription assays using CT DNA as template (Kadesch and Chamberlin, 1982). Although the in vitro turnover rate can be increased several fold by using by preincubating RNAP II with highly efficient templates and by limiting the elongation reaction to 90 seconds (Kadesch and Chamberlin, 1982, Spindler, 1979), all published in vitro results are far below the reported in vivo turnover rate of 50-100 nucleoside monophosphates per second per RNAP molecule (Darnell et al., 1967). This difference between in vitro and in vivo rates might be due to the energy stored in negatively wound template DNA (Pedone and Ballario, 1984) or to undefined chromosomal proteins.

$\alpha$ -Amanitin is a specific inhibitor of eukaryotic RNAP II, and the binding properties of several radiolabeled derivatives to CT RNAP II

have been well described by Cochet-Meilhac and Chambon (1974) and Preston et al. (1981). Using a filter binding assay, two parameters that describe the interaction between [ $^3\text{H}$ ]-ABGG and CT RNAP II were measured at 22°C in the present studies, i.e., the dissociation constant  $K_D$  and the half life of the CT RNAP II-ABGG complex at pH 7.9 and 6. The radiolabeled derivative [ $^3\text{H}$ ]-ABGG did bind to CT RNAP II with a high affinity (a  $K_D$  of  $3 \times 10^{-9}\text{M}$ ), which is comparable to the  $K_D$  of  $6.6 \times 10^{-10}\text{M}$  measured by Cochet-Meilhac and Chambon (1974) with CT RNAP II and O-[ $^3\text{H}$ ]-Methyl-deMethyl- $\gamma$ -amanitin. The value of the  $K_D$  should be equal or close to the inhibition constant  $K_i$  (Cochet-Meilhac and Chambon, 1974), indicating a direct relationship between binding of  $\alpha$ -amanitin to RNAP II and its inhibitory effect on RNA synthesis. The  $K_i$  of ABGG with respect to CT RNAP II is  $6.1 \times 10^{-9}\text{M}$  (Preston et al., 1981), which is near the value for  $K_D$  of  $3 \times 10^{-9}\text{M}$  as shown in figure 6. The inhibitory strength of ABGG is comparable with that of  $\alpha$ -amanitin since the  $K_i$  of the latter compound for CT RNAP II is  $1.8 \times 10^{-9}\text{M}$  (Preston et al., 1981).

The straight line in the Scatchard plot and the value of the stoichiometric constant "n" of 0.92, indicate one amanitin binding site per CT RNAP II molecule, which agrees with the conclusions by Cochet-Meilhac and Chambon (1974) who used CT RNAP II. The value of "n" of 0.92 indicates that the enzyme is at least 90 % pure, which agrees with the results obtained in Chapter Four.

Furthermore the half life for the CT RNAP II-ABGG complex determined here is 110 minutes at pH 7.9, which is consistent with the half life of 81 minutes reported by Cochet-Meilhac and Chambon for CT RNAP II

and O-[<sup>3</sup>H]-Methyl-demethyl- $\gamma$ -amanitin (1974). The dissociation rate experiments show that the RNAP II-ABGG complex dissociates six times faster at pH 6 than at the optimal pH of 7.9. Cochet-Meilhac and Chambon (1974) showed that  $\alpha$ -amanitin binding decreases upon heat denaturation of the CT RNAP II; for example, a treatment of 45°C for 60 minutes reduced amanitin binding six-fold and enzyme activity completely. These data imply that the enzyme has a lower affinity for the inhibitor under conditions which are less than optimal with respect to transcription rate. The data shown in Figure 7 indicate that this holds not only at a higher temperature but also at an acidic pH.

## CHAPTER THREE PURIFICATION OF RNAP II FROM HUMAN PLACENTA.

### Introduction

The placenta has become an attractive tissue for scientific study because it undergoes rapid differentiation, growth, and aging. Furthermore, with regard to humans, it is the only non-transformed material readily available. At present not much is known about the control of gene expression in the cytotrophoblast and syncytiotrophoblast, the two tissues of the trophoblast of the human placenta.

In humans, the placenta is engaged in the synthesis of large amounts of protein hormones. For example, chorionic gonadotropin (HCG) and placental lactogen (HPL) are synthesized by the syncytiotrophoblast in early and late gestation, respectively (Lau et al., 1980 and Munro, 1979). Although the peak of placental synthetic activity occurs in the first half of pregnancy (Sybalski and Trembly, 1967), during its maximal growth rate (Munro et al., 1979), when its total protein synthesis surpasses that of any other organ including the liver (Whipple et al., 1955), the term placenta is also very active in mRNA and protein synthesis. The total amount of RNA per placenta increases until term (Hayashi, 1977), and experiments with full term placental tissue preparations have demonstrated that this tissue still responds to steroid hormones (Sarkar and Mukherjee, 1977).

The human placenta has at term an average total weight of approximately 500 gm. After removal of the umbilical cord and amniochorionic membranes, the wet weight of the placenta is about 350 gm. The majority of this material (cotyledons) consists of connective and fibrous tissue, septa, and blood in the arterio-capillary-venous system (Munro, 1979, see also Figure 8). The cotyledons, which are used for RNAP II extraction, consist of groups of chorionic villi, which are bathed in maternal blood in the intervillous space. With the increase in gestational age, the ratio of syncytiotrophoblast cells over cytotrophoblast cells increases, such that at term, only a very few cytotrophoblast cells are left (Moore, 1977). That part of the trophoblast that is still actively synthesizing and secreting hormones accounts for only 13 % of the placental mass (Laga et al., 1973).

The first work on partially purified human placenta RNAP II (PL RNAP II) came from the Max-Planck Institute (Mertelsmann and Matthaei, 1968, Mertelsmann, 1969, Voigt et al., 1970, and Kaufmann and Voigt, 1973). They purified RNAP II by DEAE-cellulose chromatography and characterized the RNAP II with respect to optimal ionic strength, pH, template, and metal requirements, and to its sensitivity to several toxins and steroids in in vitro experiments. Later the RNAP II activity and template availability in placentas from normal patients at 18 weeks and at full term were reported (Kusamran et al., 1980, and Lau et al., 1980). Term placenta was found to contain slightly more RNAP II activity per cell than at midterm. More recently, Surzycki's group studied the location of binding sites for human PL RNAP II on adenovirus type 2 DNA by electron microscopy, as well as several properties of transcription



in vitro (Witney et al., 1980, and Seidman et al., 1980). Since to date, these authors have published neither the RNAP II purification procedure nor results on the characterization of its polypeptides, this enzyme was isolated from this tissue and purified here beyond an ionexchange chromatography step. RNAP II was purified from human placenta, in order to compare the photoaffinity labeling results (see Chapter Six) between the RNAP II from calf thymus and placenta.

### Materials and Methods

#### Buffers for the isolation of PL RNAP II

The pH of all solutions was 7.9 at 4°C. Aprotinin, PMSF, and thiols were added just before use.

Buffer I :250 mM Tris-HCl, 0.25 mM EDTA, 10 % glycerol, 2 mM  $MgCl_2$ , 80 mM ammonium sulfate, 6 mM BME, 0.06 mM PMSF, 0.05 TIU/ml Aprotinin, and 2 mM monothioglycerol.

Buffer II :100 mM Tris-HCl, 0.1 mM EDTA, 10 % glycerol, 300 mM ammonium sulfate, 1 mM DTT, 0.06 mM PMSF, and 1 mM monothioglycerol.

Buffer III :100 mM Tris-HCl, 0.1 mM EDTA, 25 % glycerol, 25% ethylene glycol, 1 mM DTT, 0.06 mM PMSF.

Buffer IV :100 mM Tris-HCl, 0.1 mM EDTA, 25 % glycerol, 25 % ethylene glycol, 2 mM BME, 0.06 mM PMSF, and 80 mM ammonium sulfate.

Buffer V :100 mM Tris-HCl, 0.1 mM EDTA, 25 % glycerol, 100 mM ammonium sulfate, 2 mM BME, 25 % ethylene glycol.

Buffer VI :100 mM Tris-HCl, 0.1 mM EDTA, 25 % glycerol, 25 % ethylene glycol, 2 mM DTT, 270 mM ammonium sulfate.

Buffer VII :50 mM Tris-HCl, 0.1 mM EDTA, 25 % glycerol, 0.5 mM DTT, and ammonium sulfate as indicated.

Buffer PBS :150 mM NaCl, 15 mM citrate, and 10 mM phosphate, pH 7.4.

### Tissue preparation and storage

Human placentas were obtained from healthy mothers within 20 minutes after parturition, placed on ice, and immediately perfused with ice cold phosphate buffered saline containing 15 mM citrate to prevent blood clotting. Perfusion was continued through the umbilical vein until the return flow from the arteries became clear (about 300 ml). After the chorionic plate and umbilical cord were removed, the remaining tissue of 10-30 cotyledons was washed in PBS, cut into pieces, frozen in liquid nitrogen and stored at -80°C until use. All steps in the purification were performed at 4°C unless noted otherwise.

### Purification of Placental RNAP II

The column resin materials, calf thymus DNA template, and Polymin P solution were prepared as described in Chapter 2, as were the measurements of protein and ammonium sulfate concentrations and of RNAP II activity.

A typical protocol for PL RNAP II purification is presented below. Approximately 350 gm of frozen placenta was pulverized to a fine powder in a precooled, commercial Waring blender, by 3 full speed bursts of 25 seconds each. Buffer I (1350 ml) was added to the blender and stirred 3 times for one minute each, at low speed. NP-40 (BDH Chemicals) was then added to the mixture to a final concentration of 1 % (v/v) followed by

low speed blending for 5 minutes. Since the temperature of the placental homogenate increased during blending, the blender decanter was immersed into ice water for 5 minutes, to decrease the temperature to 18°C, after which low speed blending was resumed for 5 minutes. The mixture was decanted and inert antifoam emulsion (Sigma Chemical Company) was sprayed onto the mixture, and its temperature increased to 37°C by incubation in a 50°C waterbath while continuously stirring. Once 37°C was attained, the homogenate was transferred to a 37°C water bath and incubated for an additional 30 minutes. The placental homogenate, with a volume of about 1.5 liters, was again cooled to 18°C in an ice water bath. DNA was partially removed after filtration of the homogenate through one layer of cheese cloth. The filtrate was centrifuged in a Beckman JA-14 rotor at 10,000 rpm (9,700xg) for 20 minutes, resulting in the first supernatant (SN1).

To precipitate RNAP and nucleic acids, a solution of 10 % (v/v) Polymin P was slowly added to SN1 to a final concentration of 0.17 % (v/v) and stirred rapidly for 15 minutes. The resulting solution was centrifuged for 15 minutes in a JA-14 rotor at 11,600 rpm (13,100xg). The SN2 was discarded and the P2 was resuspended in 380 ml of Buffer II with the Tissumizer at 30 % power for 15 minutes. The P2 resuspension was centrifuged in a Beckman type 19 rotor at 17,000 rpm (28,800xg) for 90 minutes, resulting in the SN3.

To concentrate this fraction, solid ammonium sulfate was added to the SN3, during rapid stirring, over a 30 minute period to a final concentration of 2.2 M (0.23 gm/ml SN3). Following an additional 30 minutes of stirring, the suspension was centrifuged in a Beckman type 19

rotor at 17,000 rpm (28,800xg) for 90 minutes. The P4 was resuspended in sufficient buffer III (500 ml) to lower the ammonium sulfate concentration to 80 mM. The Tissumizer was used at 40 % power for 10 minutes and the remaining particles were removed by slow vacuum filtration through a 30  $\mu$ m nylon filter.

The P4 fraction was mixed for 30 minutes with 160 ml DEAE-Sephadex A-25, pre-equilibrated with buffer IV. The slurry was washed with 550 ml of buffer IV for 30 minutes over a Buchner funnel while applying a slight vacuum. The cake was then resuspended in the same buffer to a total volume of 600 ml, poured into a column, and washed with buffer V until no more protein eluted. RNAP II activity eluted from the column after applying buffer VI.

The pooled active fractions were diluted with buffer VII, until the ammonium sulfate concentration was 50 mM. BSA was added to a final concentration of 0.2 mg/ml. The sample was applied to a 60 ml phosphocellulose column, pre-equilibrated with buffer VII, containing 50 mM ammonium sulfate and 0.2 mg BSA/ml. The column was washed with the same buffer without BSA. The RNAP II activity was eluted with buffer D containing 200 mM ammonium sulfate, and the active fractions were pooled.

The ammonium sulfate concentration of the pooled fractions was adjusted to 125 mM, and the fraction was applied onto a column containing Biogel A-1.5m, overlayed with DEAE-Sephadex A-25 which had been equilibrated with buffer VII containing 125 mM ammonium sulfate. The column was washed with the same buffer to remove BSA and with buffer VII containing 550 mM ammonium sulfate to elute all RNAP II activity.

## Results

The results of the human placental RNAP II purification are summarized in Table II. The procedure is very much like the one used in the purification of calf thymus RNAP II (see Chapter Two), except for the incubation of the crude homogenate at 37°C in the presence of the non-ionic detergent NP-40 and the use of DEAE-Sephadex instead of DE-52 in the first column.

Following ammonium sulfate precipitation, the RNAP enzymes were adsorbed to and eluted from a column of DEAE-Sephadex (Figure 9). The eluted fraction was free from endogenous DNA and almost free of RNAP I and III. Further purification followed using phosphocellulose (Figure 10) and Biogel A-1.5m chromatography (Figure 11). Three peaks appeared during elution from the last column. One peak (not included in the elution profile of Figure 10) contained no RNAP II activity. This was followed by the first broad peak shown in Figure 11, containing RNAP II in fractions 3 through 18, which eluted during the 125 mM ammonium sulfate wash. The fractions were pooled and concentrated by salt precipitation using a saturated (at 4°C) ammonium sulfate solution which was added slowly to give a final concentration of 2.25 M or 55 % (w/v). Following 60 minutes stirring at 4°C, the precipitate was pelleted by centrifugation in a Ti-65 rotor at 55,000 rpm (192,900xg) for 3 hours. The pellet with 4 mg RNAP II was resuspended in 4.4 ml buffer VII without ammonium sulfate. This fraction, which had a final ammonium sulfate concentration of 130 mM and a specific activity of 169 units RNAP II activity per mg protein (see Table II), was divided into 100 µl aliquots and stored at -80°C until use.

The second peak in Figure 11 appeared in fractions 24 through 27, after application of the high ionic strength buffer. This peak also contained RNAP II activity, but with a lower specific activity (97 units per mg protein, see Table II) than the previous peak. The pooled fractions were stored in 100  $\mu$ l aliquots at  $-80^{\circ}\text{C}$ .

The two peaks shown in Figure 11 represent a recovery of approximately 90 % of the units of RNAP II activity applied to the Biogel/Sephadex column. Thus, it was not surprising that when the column was washed extensively with high salt buffer until the ammonium sulfate concentration reached 550 mM in the eluate, no further elution of proteins was detected.

The crude homogenate of 350 gm placenta contained 28 gm of protein with at least 1177 units of RNAP II (see Table II), i.e., a specific activity of 0.042 units of RNAP II activity per mg protein, which is comparable to the specific activity of 0.045 units of RNAP II activity per mg protein in the crude homogenate of the calf thymus. After purification of the PL RNAP II, the specific activity was 169 units per mg protein, indicating a purification factor of approximately 4000. Based on similar data, the yield of RNAP II was approximately 56 % (678 units / 1177 units). The human placenta (based on 500 gm) thus contains at least 2.3 units of RNAP II per gram tissue (1177 units RNAP II / 500 gm) as compared to 4.1 units of RNAP II activity per gram of calf thymus tissue.

The requirements for optimal activity of PL RNAP II were determined with respect to template preference, ionic strength, and metal requirement. For these analyses, the limiting assay with undiluted [ $^3\text{H}$ ]-UTP

was used as described for the calf thymus RNAP II in the Materials and Methods section of Chapter Two.

With regard to template, several different structures of calf thymus DNA, as well as intact adenovirus type 2 DNA, were used at a concentration of 5  $\mu\text{g}$  per 100  $\mu\text{l}$ . The enzyme preferred short single stranded CT DNA (100 % activity), prepared as described in the Materials and Methods section of Chapter Two. When the CT DNA used was sonicated, but not heated, i.e., short double stranded DNA, the activity was reduced to 40 %. With heated native CT DNA or heated placental DNA (purified according to Marmur, 1961), i.e., long single stranded DNA, only 22 % or 24 % activity remained, respectively. The addition of double stranded adenovirus type 2 DNA yielded only 15 % of the maximal activity.

The reaction mixture was titrated with increasing amounts of single stranded short CT DNA to determine the saturation level. The reaction rate was linear up to a DNA concentration of 1  $\mu\text{g}/100 \mu\text{l}$  and remained optimal through 30  $\mu\text{g}/100 \mu\text{l}$  before leveling off. PL RNAP II activity was absolutely dependent on the addition of template.

A concentration of 100-140 mM ammonium sulfate produced maximal RNAP II activity, whereas at 0 and 400 mM only 4 % of activity remained. When 100 mM ammonium sulfate was substituted by 100 mM KCl only 74 % of the activity remained. Ammonium sulfate could be replaced by 100 mM ammonium chloride or 120 mM ammonium acetate without loss of activity. Thus, it appears that the sulfate ion is not important for optimal activity.

The PL RNAP II preferred Mn over Mg, because when added to an assay at their respective optimal concentrations of 3 mM and 6 mM, the activity ratio was 6.

With regard to the use of buffers at 50 mM and pH of 7.9, Tris-Acetate, Hepes-NaOH and Tris-glycine could all substitute for Tris-HCl without loss of activity.

Several agents (at pH 7.9) were tested for their ability to inhibit PL RNAP II. After adding 100 mM phosphate, 1 mM pyrophosphate, or 1 mM pyridoxal 5' phosphate, only 56 %, 50 %, and 59 % of the activity remained, respectively. Heparin (5  $\mu$ g) or Rose Bengal (1 mM) or CBB-R250 (1  $\mu$ g) inhibited the enzyme completely. The enzyme is rather resistant to thiols, since 45 mM BME did not inhibit activity at all, whereas with 20 mM DTT, 83 % of the activity remained.

The non-ionic detergent NP-40 and the antifoam emulsion used during the enzyme purification inhibited enzyme activity only at concentrations greater than 0.2 % (v/v) and 5 % (v/v), respectively. The protease inhibitors Aprotinin and PMSF did not inhibit transcription at the concentrations used during the enzyme purification.

The assay was run at 4 different temperatures. When the activity at 37°C is set at 100 %, the activities at 4°, 25°, and 42°C were 7 %, 70 %, and 88 %, respectively.

Finally, it was noted that the addition of BSA or glycerol to the assay did not enhance the enzyme activity.

Several kinetic parameters of the purified PL RNAP II (from peak one, see Figure 11) were determined under the conditions used for similar experiments on CT RNAP II (Chapter Two), but with modifications as described in the figure legends. The apparent  $K_M$  for UTP was 45  $\mu$ M (Figure 12). The rate constant  $k_3$  for product formation was 0.3 second<sup>-1</sup>, which indicates a turnover number of 1.2 uridine monophosphates incorporated per second per enzyme. The apparent  $K_M$  for ATP



was 62  $\mu\text{M}$  (Figure 13) and the rate constant  $k_3$  was  $0.14 \text{ second}^{-1}$ , which indicates a turnover number of 0.6 adenosine monophosphates per second per enzyme.

### Discussion

A protocol to obtain mg quantities of PL RNAP II has been described here. A number of variations of this protocol were attempted prior to establishing these methods as routine. For example, at first, nuclei were isolated from the placenta in an attempt to obtain a fraction of RNAP with a relatively high specific activity. An extract from intact nuclei was prepared by homogenization in an isotonic buffer, followed by centrifugation in a sucrose step gradient and lysis in 120 mM ammonium sulfate at  $37^\circ\text{C}$  (Kaufman and Voigt, 1973). However, not only was the yield of nuclei relatively low ( $55 \times 10^6$  nuclei per gram tissue), but the yield of RNAP II was far below that obtained here with whole cells.

The use of NP-40 increased the release of RNAP II from the placental tissue (Surzycki, personal communication), which was aided by the incubation at  $37^\circ\text{C}$  (Sugden and Keller, 1973). At a Polymin P concentration of 0.17 % (v/v), no more than 350 gm placenta could be used per procedure because the Polymin P pellet would no longer be firm, resulting in loss of enzyme during this step.

At first, the P2, containing the nucleic acid-protein-Polymin P complex, was washed with 1 liter of buffer II (containing 75 mM ammonium sulfate) before the RNAP II was removed from the pellet by a high salt

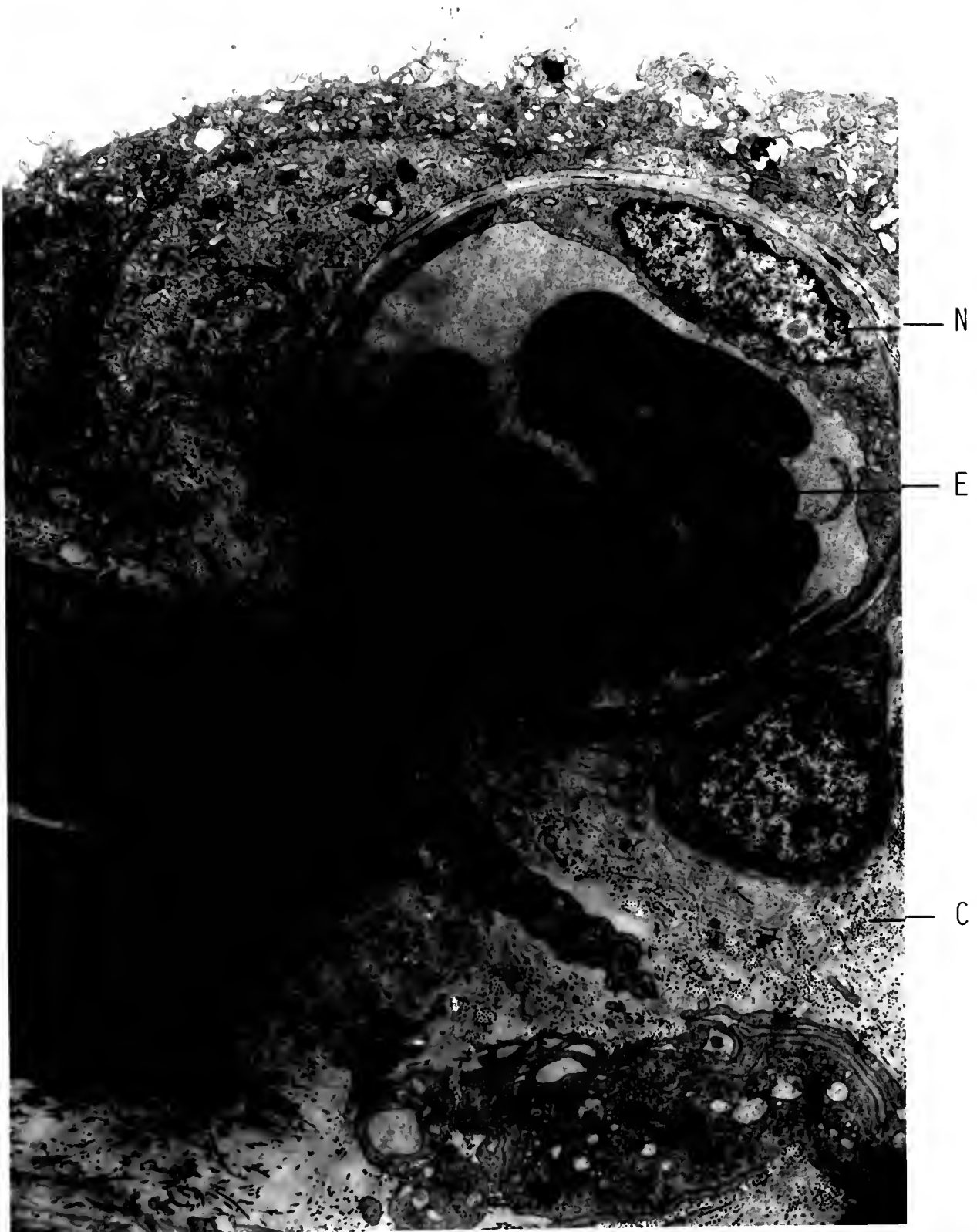
Table II. Summary of purification results of RNAP II from 350 gm human placenta.

Purification step	Total Act. units	Volume ml	Protein mg	Spec.Act. units/mg	Units RNAP		
					I	II	III
Resuspended Ammonium sulfate pellet	962	500	1600	0.6	234	529	199
DEAE-Seph.A-25	1224	105	120	10.2	11	1177	36
Phosphocellulose	937	75	36	26	0	937	0
Biogel A-1.5m/DEAE-Seph.A-25							
First peak	678	4.4	4	169	0	678	0
Second peak	165	10	1.7	97	0	165	0

Figure 8. Electron micrograph of human term placental tissue used for the isolation of PL RNAP II. (Magnification of 7100)

Several 1 mm<sup>3</sup> pieces of the cotyledon tissue were prefixed for 1 hour in 2.5 % gluteraldehyde and 0.1 M cacodylate, pH 7.3, and washed for 12 hours with 3 changes in 0.1 M cacodylate (Hayat, 1981) Fixation took place for 1 hour in 1 % osmium tetroxide in the same buffer and was followed by three washes with buffer alone. The dehydration was performed stepwise in 25 %, 50 % and 75 % ethanol for 10 minutes each. Staining was for 2 hours in 75 % ethanol with 2 % uranyl acetate. Dehydration was continued in 75 % ethanol and twice in 100 % ethanol for 10 minutes each, followed by incubation twice in 100 % acetone for 15 and 30 minutes. Embedding took place in three stages using epoxy plastic dissolved in acetone: 30 % for 1 hour, 70 % for 12 hours and 100 % plastic for 8 hours (Spurr, 1969). After thin sectioning and staining (sodium borate and toluidine blue), several samples were selected using a microscope. Ultrathin (less than 0.08  $\mu$ m thick) sections were obtained with a LKB Ultratome III instrument and placed on HCl/ethanol cleaned 300 mesh copper grids. Final staining took place 1 % uranyl acetate for 15 minutes and 4 % lead citrate for 10 minutes. After drying the samples were photographed using a Hitachi II E transmission electron microscope.

The electron micrograph shows erythrocytes (E) and a nucleus (N) of the endothelial cell forming the inner wall of a capillary vessel, which constitutes a major part of placental tissue. The numerous black dots are cross sections of collagen fibers (C) which are present in great numbers.



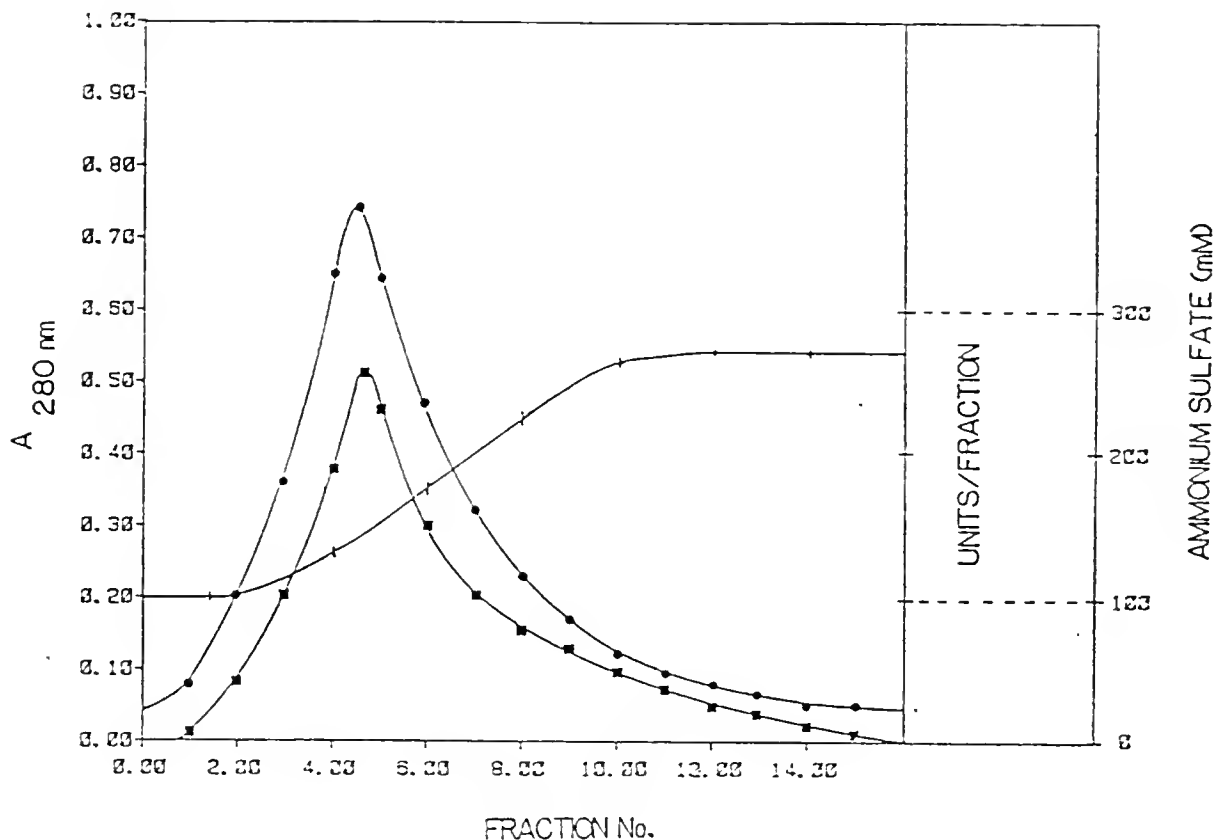


Figure 9. Elution profile of PL RNAP II after DEAE-Sephadex A-25 batch adsorption and chromatography.

After elution of excess buffer and settling of the DEAE-Sephadex, the bed height in the column (5 cm diameter x 55 cm) was 8.1 cm. It was then washed at a flow rate of 2 ml/minute with buffer V until the absorbance at 280 nm was less than 0.05 absorption units (not shown in Figure). When buffer VI was applied to the column more protein (●) eluted at an ammonium sulfate concentration between 110-250 mM (+). The eluate was collected in 10.5 ml fractions and assayed for RNAP activity (■). Fractions 3 through 12 were sensitive to 10 ng  $\alpha$ -amanitin per 100  $\mu$ l and were pooled.

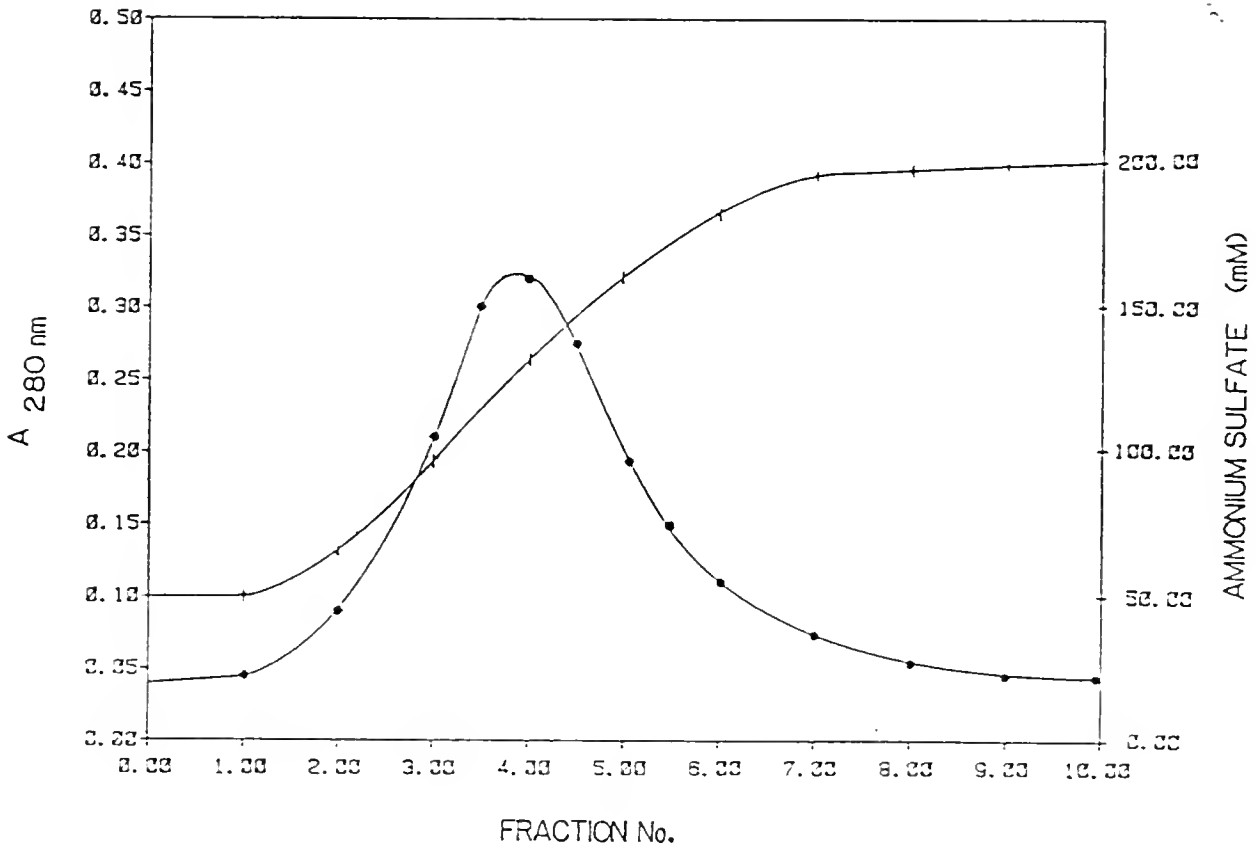


Figure 10. Elution profile of PL RNAP II from the phosphocellulose column.

The phosphocellulose column (5 cm diameter x 5 cm) was pre-equilibrated with buffer VII containing 50 mM ammonium sulfate and 0.2 mg BSA/ml. After application of the pooled DEAE-Sephadex fractions, the phosphocellulose column was washed with the same buffer (without BSA) at a flow rate of 2 ml/minute until no more protein eluted (●). The RNAP II activity eluted in fractions 3 through 7 (10 ml each), after application of buffer VII containing 200 mM ammonium sulfate (+).

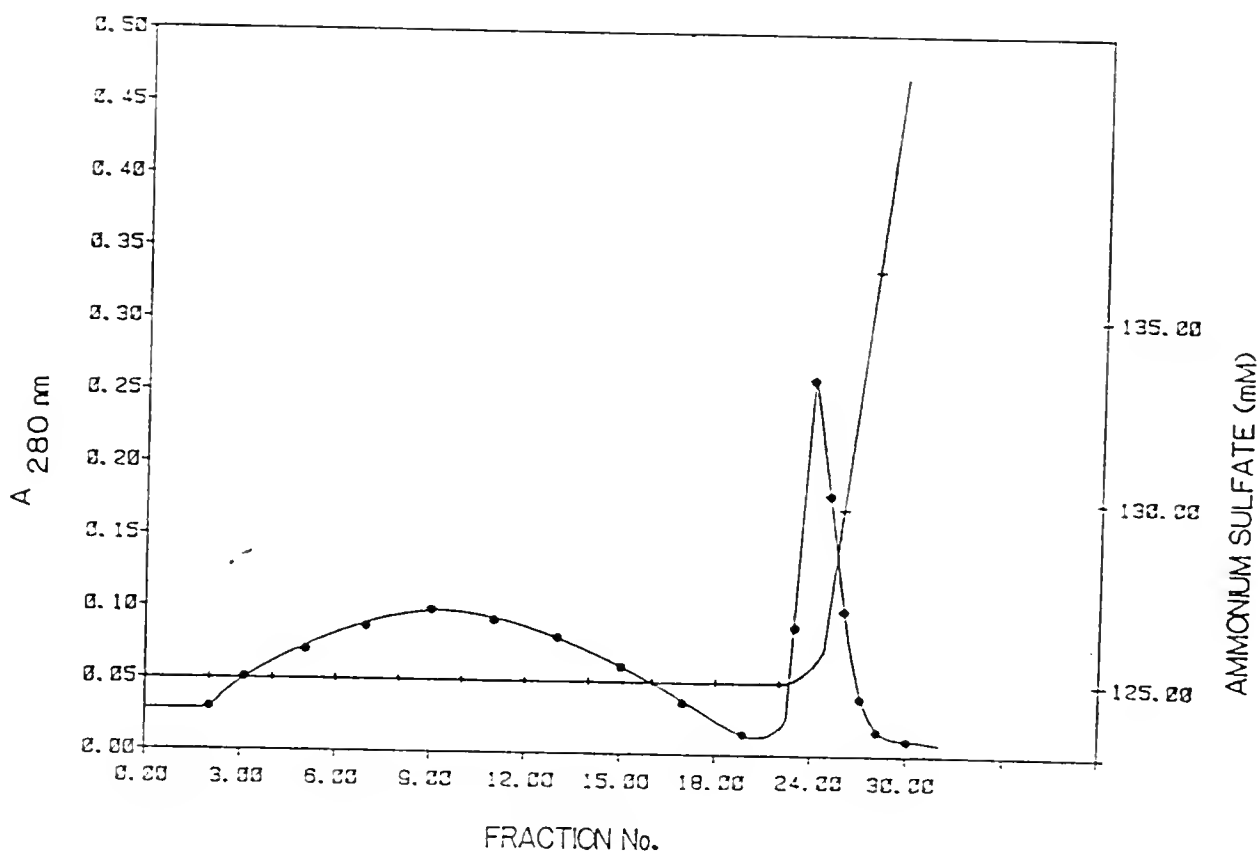


Figure 11. Elution profile of PL RNAP II from the Biogel A-1.5m column.

A column (2 cm diameter x 10 cm) containing Biogel A-1.5m, equilibrated with buffer VII containing 125 mM ammonium sulfate, was overlaid with 1.8 cm of DEAE-Sephadex A-25. After loading of the sample, concentration of the applied RNAP II took place by adsorption onto the DEAE Sephadex A-25 anion exchange beads under low ionic strength (125 mM ammonium sulfate). The column was washed at a flow rate of 1 ml/minute to remove BSA (not shown). This was followed by elution with buffer VII containing 550 mM ammonium sulfate (+). The fraction size was 5 ml for the first 18 fractions and 2.5 ml thereafter. Fractions 3 through 18 (peak one) and 24 through 27 (peak two) were pooled separately and the RNAP activity measured. The protein concentration was measured by the absorbance at 280 nm (●).

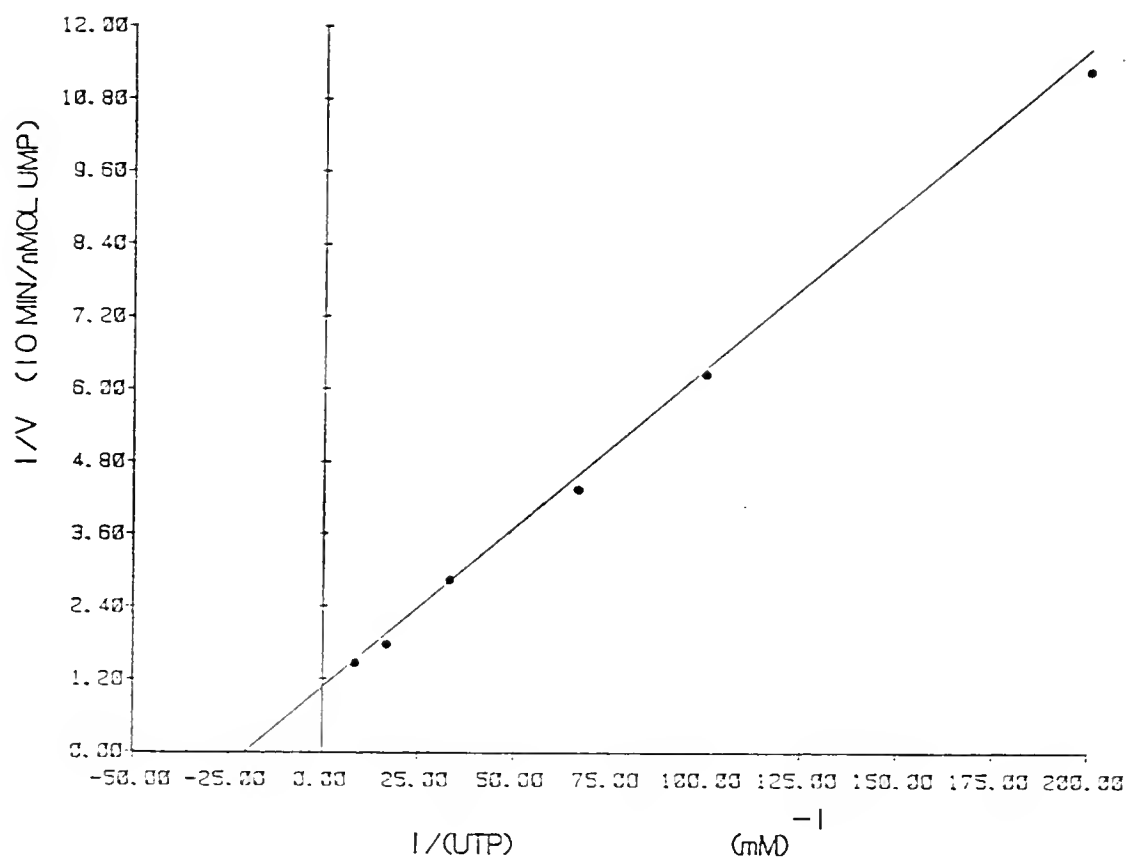


Figure 12. Double reciprocal plot of the velocity versus the UTP concentration.

The reaction mixture of 100  $\mu\text{l}$  contained 5 pmoles PL RNAP II, and the reaction assay composition was as described in the legend of Figure 4 in Chapter Two. The 1.25  $\mu\text{Ci}$  tritiated UTP was diluted with unlabeled UTP as indicated. The reaction took place at 37°C for 10 minutes.



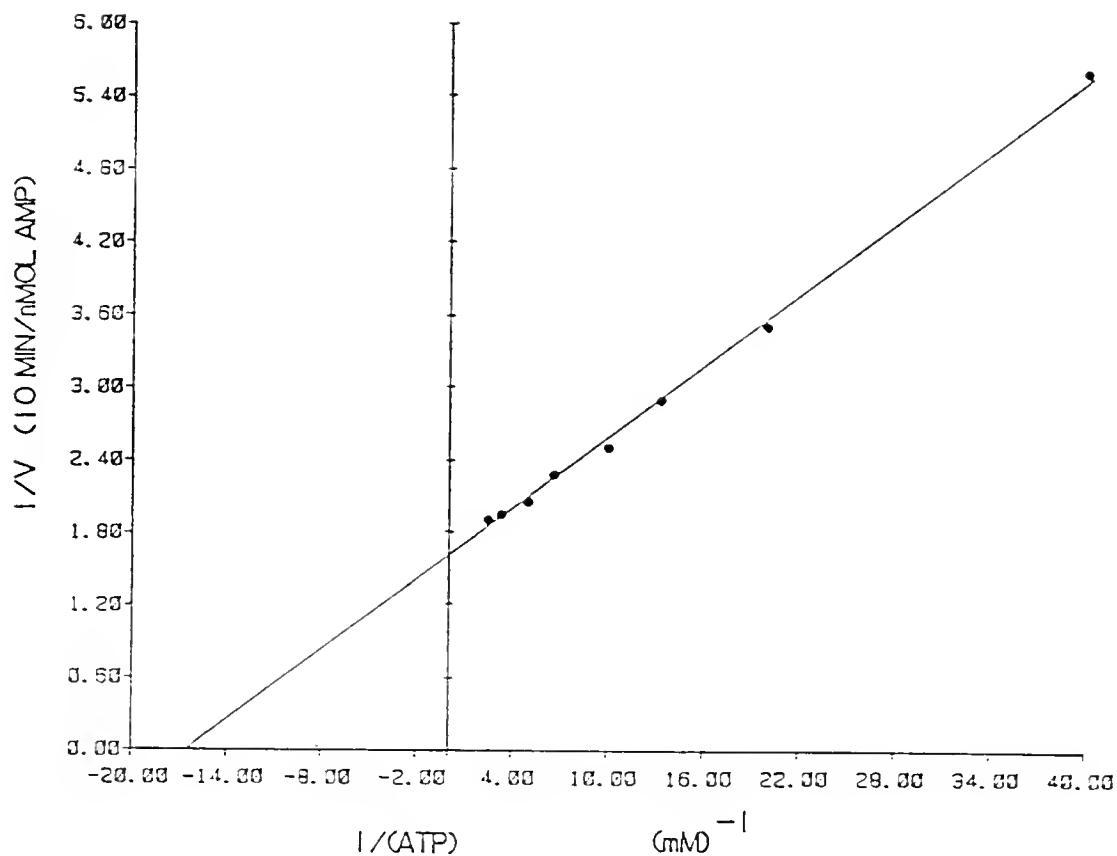


Figure 13. Double reciprocal plot of the velocity versus the ATP concentration.

The composition of the reaction mixture was as described in Figure 12, (except that 6.9 pmoles PL RNAP II were added), and the incorporation of tritiated AMP was determined. The 1  $\mu$ Ci of tritiated ATP per reaction was diluted with unlabeled ATP as indicated.

extraction. However, this step resulted in a large loss of proteins. Therefore, this washing step was omitted prior to elution of RNAP from the pellet with buffer II.

In the first purification schemes, the redissolved ammonium sulfate pellet P4 of 500 ml was applied to a DEAE-Sephadex A-25 column (5 cm diameter x 55 cm), but this proved to be very time consuming due to the large sample volume. An attempt was made to concentrate the sample first, using an Amicon hollow fiber (H1 P30-43) ultrafiltration system at 10°C, employing the CH4 concentrator. However, at a pressure of 25 psi and a recirculation rate of 0.6-1.8 liters of resuspended P4 per minute, the concentration rate was only 4 ml per minute due to the high viscosity of the sample at this temperature. For these reasons a batch adsorption method was ultimately chosen here because it was so successful in the case of CT RNAP II purification.

The final gel filtration step depends not only on the fractionation characteristics of the Biogel A-1.5m (10-1,500 kD), but also on the RNAP II binding to the top layer of DEAE-Sephadex under the ionic strength conditions used. When CT RNAP II was purified, a very small amount of the enzyme appeared before application of the high salt buffer, but in the case of the PL RNAP II purification, the majority of enzyme activity eluted before the high salt step (peak one, see Figure 11). There was no difference in  $\alpha$ -amanitin sensitivity of the two peaks, but there was a difference in peptide composition and stoichiometry (Chapter 4) and in specific activity (Table II). The binding of the enzyme depends on its net surface charge, which is the result of the configuration and aggregation of the several peptides that co-purified up to the gel filtration column.

A different peptide composition with respect to stoichiometry can result in a different surface charge, causing a different elution pattern from the anionic exchange beads.

Each gm of placenta contained 2.4 units of RNAP II, which is less than the content in the calf thymus (at least 4.1 units per gm tissue). Since, however, only 13 % of the placental mass is involved in the synthesis and secretion of peptide hormones, the RNAP II content in trophoblast tissue is probably significantly higher than in calf thymus tissue.

The requirements of PL RNAP II activity and preference for denatured template over native DNA and Mn over Mg correspond with those of CT RNAP II and, for that matter, with all nuclear RNAP II enzymes isolated thus far from mammals (Roeder, 1976, p.287). The data reported here then confirm and extend the earlier findings by Voigt et al. (1970) and Kaufmann and Voigt (1973) who purified PL RNAP II by DEAE-cellulose chromatography. It is clear that even the partially purified enzyme has lost the ability to use a double stranded template efficiently. Maybe it has lost a DNA unwinding peptide, equivalent to the  $\sigma$  subunit in E.coli RNAP, during the purification. Surzycki observed a complete loss of activity on adenovirus type 2 DNA when PL RNAP II was purified beyond DEAE chromatography (Surzycki, personal communication).

Pyridoxal 5'phosphate was shown to be an inhibitor of PL RNAP II, which is in agreement with reports on other prokaryotic and eukaryotic RNAPs. The inhibition is due to the formation of a Schiff's base with an amino group of a lysine, presumably present in the active site (Chapter Six). Rose Bengal was also an inhibitor of PL RNAP II activity, which

corresponds to studies on E. coli RNAP by Wu and Wu (1973), who classified the Rose Bengal as an elongation inhibitor. Srivastava and Modak (1982), who reported Rose Bengal inhibition of viral reverse transcriptase, suggested that the translocation step during elongation was inhibited and that a hydrophobic domain of the enzyme is in a region involved with template binding. Finally, heparin also inhibited PL RNAP II activity. Heparin is a polyanion that competes with DNA for a template binding site on the RNAP (Zillig, et al., 1976). It is clear that there are many similarities with respect to inhibitor action among the various enzymes which polymerize a polymer from DNA or RNA.

The apparent  $K_M$  for UTP and ATP on denatured CT DNA template were determined for PL RNAP II. Upon comparison of these results with those obtained with CT RNAP II, the  $K_M$  for the pyrimidine nucleotide UTP is again lower than the  $K_M$  for the purine nucleotide ATP. The turnover numbers are comparable for UTP but lower for PL RNAP II when the AMP incorporation was followed. With respect to a general interpretation of kinetic parameter values derived from the complex transcription kinetics, the same problems as described for CT RNAP II apply to the PL RNAP II results. Assays that were developed to counter some of these problems are described in Chapter Six.

CHAPTER FOUR  
PEPTIDE CHARACTERIZATION OF CALF THYMUS AND HUMAN  
PLACENTAL RNA POLYMERASES

Introduction

CT RNAP II consists of three subclasses: "O", "A", and "B". This nomenclature is based on the observation that the polypeptide compositions of the three subclasses are identical, with the exception of the largest polypeptides, which occur either as 240 kD ("O"), or 210-214 kD ("A"), or 180 kD ("B") (Hodo and Blatti, 1977 and Kedinger et al., 1974). Protease peptide mapping indicated that these three polypeptides are structurally related to each other and perhaps share the common parent protein "O", from which the polypeptides "A" and "B" are derived after in vivo and/or in vitro proteolysis (Cleveland et al., 1977, and Dahmus and Kedinger, 1983).

The MWs, isoelectric points, and stoichiometries of CT RNAP II B according to Hodo and Blatti (1977) and Benson et al. (1978) are listed in the first three columns of Table III. All the polypeptides are acidic, with the exception of the two largest polypeptides, which are alkaline.

In contrast to CT RNAP II, the polypeptide composition of purified PL RNAP II has not been published. The only available data describe the composition of PL RNAP II after purification through a single column (DEAE Sephacel, Surzycki, personal communication), followed by 1D-SDS-PAGE. A total of 17 to 24 polypeptides were found with MWs ranging from 21.5 to 255 kD.

The purposes of this chapter are to compare the properties of the CT RNAP II purified here with those reported previously and to describe the characteristics of PL RNAP II which was purified similarly to CT RNAP II.

### Materials and Methods

#### One dimensional SDS-PAGE

One dimensional-SDS-PAGE was performed on a Hoefer apparatus (model 600) with a 1.5 mm thick 5 % stacking gel and a 12.5 % separation gel (Laemmli, 1970). Prior to electrophoresis, samples were treated for 5 minutes in a 95°C waterbath in equilibration buffer (1 % SDS, 0.5 % BME in 60 mM Tris-HCl, pH 6.9) containing 10 % glycerol and 0.001 % BPB as marker, or in the same buffer with 50 % BME as described by Hodo and Blatti (1977). Following electrophoresis, the gels were fixed and stained with CBB-R250 or with silver stain (Wray et al., 1981). The MWs were based on a calibration curve derived from the electrophoretic mobilities of low and high MW marker proteins (Sigma Chemical Company) and of BSA that was cross-linked with dimethylsuberimide as described by Davis and Stark (1970).

#### Two dimensional IEF-SDS-PAGE

The purified RNAP II was subjected to 2D-IEF-SDS-PAGE according to the procedure of O'Farrell (1975). The first dimension consisted of IEF in glass tubes (0.35 cm diameter x 14 cm) in the presence of 9.5 M urea, 1 % NP-40 (BDH Chemicals Ltd), using 4.25 % polyacrylamide (Bio.Rad) gels crosslinked with 0.75 % DATD (Bio.Rad). The ampholines (LKB), at a concentration of 2 % (w/v), generated a pH gradient from 3.5-10. After IEF the gels were agitated for 10 minutes in equilibration buffer and subsequently glass tubes (0.35 cm diameter x 14 cm) in the presence of 9.5 M urea, 1 %

NP-40 (BDH Chemicals Ltd), using 4.25 % polyacrylamide (Bio.Rad) gels crosslinked with 0.75 % DATD (Bio.Rad). The ampholines (LKB), at a concentration of 2 % (w/v), generated a pH gradient from 3.5-10. After IEF the gels were agitated for 10 minutes in equilibration buffer and subsequently sealed with 1 % agarose on the 5 % stacker gel of the second dimension, which was as described for 1D-SDS-PAGE. The pH profile obtained during IEF was determined by slicing a gel worm in 0.5 cm sections and incubating them overnight in 1 ml of degassed water containing 20 mM KCl, followed by pH measurement.

#### Non-denaturing PAGE

Non-denaturing 4 % gels (0.6 cm diameter x 6 cm) were prepared (Maizel, 1971) and pre-electrophoresed in the presence of 0.01 % thioglycolic acid, which neutralizes excess ammonium persulfate, in the cathode buffer (25 mM Tris-glycine, pH 8.0) for 1 hour at 4 mA/tube. Prior to electrophoresis the cathode buffer was replaced with fresh 25 mM Tris-glycine, pH 8.0.

Alternatively, non-denaturing gradient PAGE was used, which allows the estimation of the MW of intact proteins. A 1.5 mm thick gradient gel with the polyacrylamide concentration ranging from 4 % to 30 % was prepared as described in the PAGE manual by Pharmacia Fine Chemicals (1980). The gel was pre-electrophoresed at 70 volt for 20 minutes and the sample proteins run into the gel at the same voltage at 4°C. Electrophoresis continued at 150 volts until a total of 2400 volthours had been applied. Under these conditions the BPB marker and lysozyme (14.3 kD) did not run off the gel.

### Preparative Gel Electrophoresis

To isolate the individual polypeptides from RNAP II, preparative electrophoresis was performed at room temperature using the Laemmli gel system in a model 1100 PG electrophoresis instrument (BRL). Briefly, a tube (1 cm diameter) was filled with a 5.2 cm high layer of running gel (8 % polyacrylamide), which was overlaid with a 1 cm stacking gel (6 % polyacrylamide). The proteins eluting from the bottom of the gel were fractionated in the Tris-glycine buffer and their identities determined by 1D-SDS-PAGE.

### Results

The results of the CT RNAP II and PL RNAP II purifications are listed in Tables I and II, in Chapters Two and Three, respectively. The peptide compositions of the extracts and fractions at various stages during the purification were studied by 1D-SDS-PAGE (see Figure 14 for CT RNAP II and Figure 15 for PL RNAP II).

One polypeptide (radiolabeled, see Chapter Six) with a MW of 37 kD (peptide E) was purified from PL RNAP II by preparative gel electrophoresis as described in the Materials and Methods section. The BPB dye eluted at a volume of 44-46 ml Tris-glycine buffer; radiolabeled peptide E eluted at a volume of 54 to 57 ml, as confirmed by 1-D-SDS-PAGE (Figure 15).

To calculate the stoichiometries of the polypeptides present within the purified CT RNAP II, the amount of CBB-R250 dye bound per polypeptide was measured by scanning a lane with stained CT RNAP II at 590 nm (Figure 16). Silverstain intensities were not used for scanning because its



staining with proline-rich and carbohydrate modified proteins is less efficient. The stoichiometric ratios are listed in Table III and are relative to the amount of dye bound per protein mass of polypeptide "B", which was set arbitrarily at one. Because only very small amounts of polypeptide "O" and "A" were present in the preparation of purified CT RNAP II, their stoichiometric ratios are not listed in Table III. The experiment was repeated with PL RNAP II (Figure 17) and the results are listed in Table III.

Purified CT RNAP II was analyzed by non-denaturing PAGE to check its purity, see Figure 18. It was estimated, from a 590 nm scan of the stained gel, that 95 % of all protein migrated as a homogeneous protein under the conditions used. This was further investigated using non-denaturing gradient PAGE as described in the Materials and Methods section. The CT RNAP II appeared as a single major protein with an apparent MW of 675 kD, which was estimated from a calibration curve based on high MW markers.

To check the purity of PL RNAP II and its total MW, the enzyme was analyzed by non-denaturing gradient PAGE. Two major bands appeared, with apparent molecular weights of 520 and 550 kD (Figure 19).

The pIs of the polypeptides of CT RNAP II and PL RNAP II were measured by 2D-IEF-SDS-PAGE. The gels are shown in Figures 20 and 21. The results are summarized in Table III, and for comparison the data published by Hodo and Blatti (1977) and Benson et al. (1978) are included.



Figure 14. SDS-polypeptide analysis of CT RNAP II during purification.

Aliquots of several fractions obtained during purification of CT RNAP II were analyzed by 1D-SDS-PAGE and silver stained as described in the Materials and Methods section. Lane 1: 2  $\mu$ g of the resuspended ammonium sulfate-precipitated protein. Lane 2: 2  $\mu$ g of the DEAE-column eluate that contained RNAP II activity. Lane 3: 2  $\mu$ g of the phosphocellulose column eluate that contained RNAP II activity. Lane 4: 4  $\mu$ g of the Biogel column eluate that contained RNAP II activity. The MWs of several protein markers are indicated: BSA trimer, 198 kD; BSA dimer, 132 kD, BSA, 66 kD; Pepsin, 35 kD; and Trypsin, 24.5 kD; and cytochrome C, 13.1 kD.

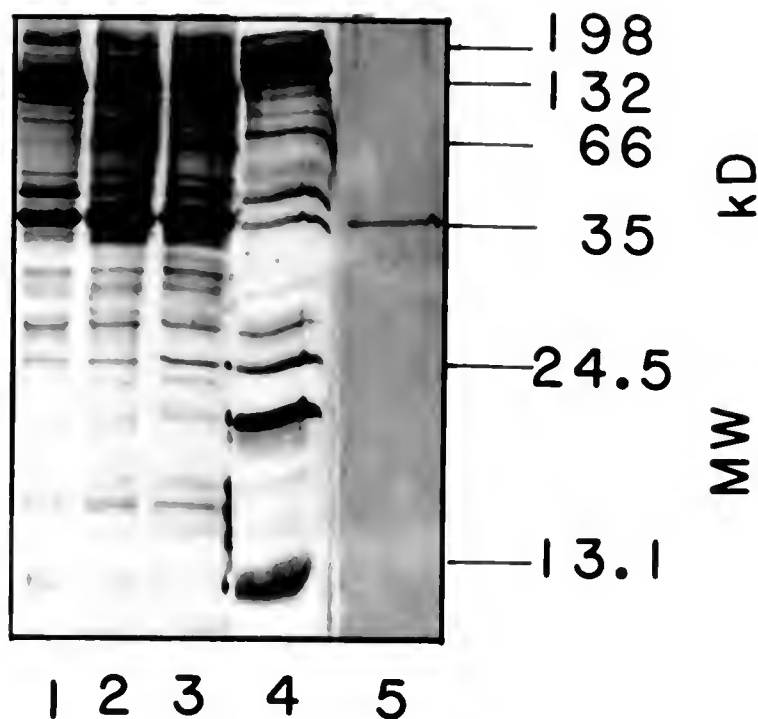


Figure 15. SDS-polypeptide analysis of PL RNAP II during purification.

Aliquots of several fractions obtained during purification of CT RNAP II were analyzed by 1D-SDS-PAGE and silver stained as described in the Materials and Methods section. Lane 1: 4  $\mu$ g of the DEAE-column eluate that contained RNAP II activity. Lane 2: 4  $\mu$ g of the phosphocellulose-column eluate that contained RNAP II activity. Lane 3: 5  $\mu$ g of the Biogel column, peak two. Lane 4: 8.5  $\mu$ g of the Biogel column, peak one before ammonium sulfate precipitation. Lane 5: 170  $\mu$ g PL RNAP II containing 1 % SDS and 5 % BME were run at 130 volts (5 mA) in a preparative electrophoresis instrument. Materials eluting from the running gel were collected in Tris-glycine buffer at a rate of 6 ml/hr, and fractions containing radio-labeled polypeptide E were pooled and their identity confirmed by 1D-SDS-PAGE.



Figure 16. Polypeptide structure of CT RNAP II.

Sixteen  $\mu\text{g}$  of CT RNAP II were analyzed by 1D-SDS-PAGE (panel B), stained with CBB-R250, and scanned at 590 nm (panel A). The polypeptides shown on the absorbance scan and gel pattern are identified by their alphabetical nomenclature.

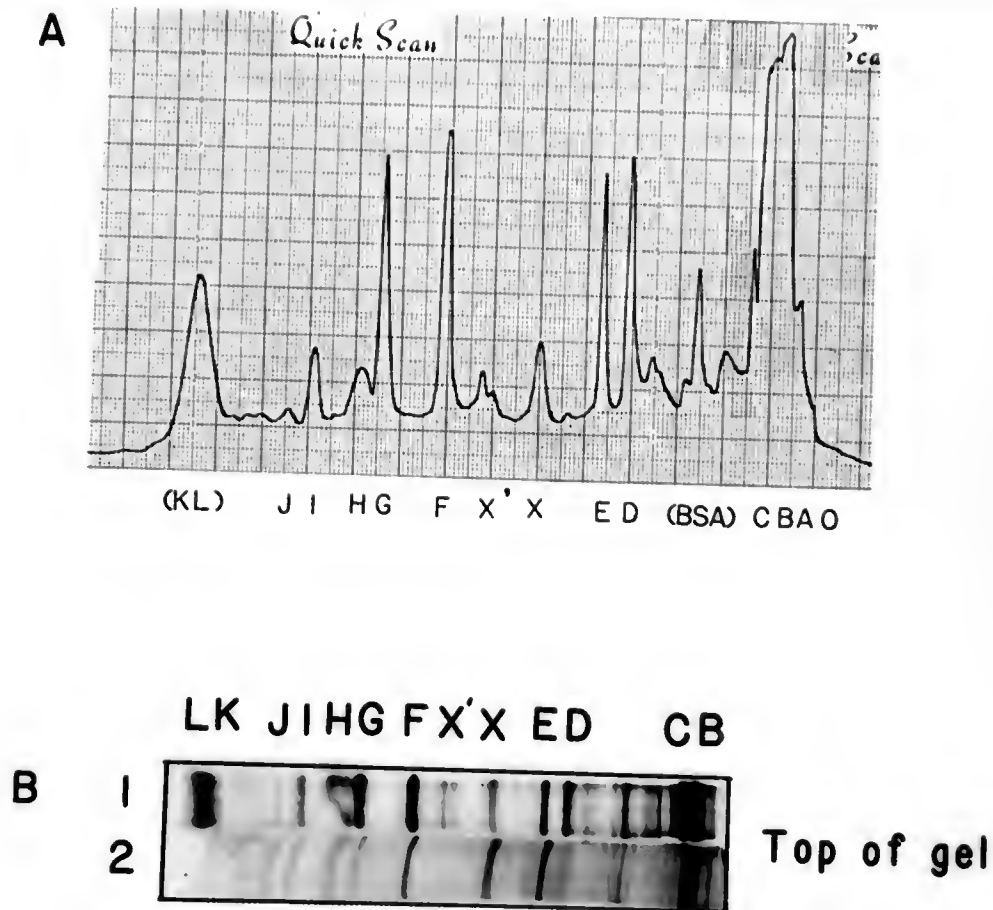


Figure 17. Polypeptide structure of PL RNAP II.

Eighteen  $\mu$ g of PL RNAP II (peak one after ammonium sulfate precipitation) were analyzed by 1D-SDS-PAGE (panel B, lane 1), stained with CBB-R250, and scanned at 590 nm (panel A). The polypeptides shown on the absorbance profile and gel pattern are identified by their alphabetical nomenclature. Lane 2 in panel B shows the polypeptide composition of CT RNAP II (4  $\mu$ g) for comparison with the structure of PL RNAP II.

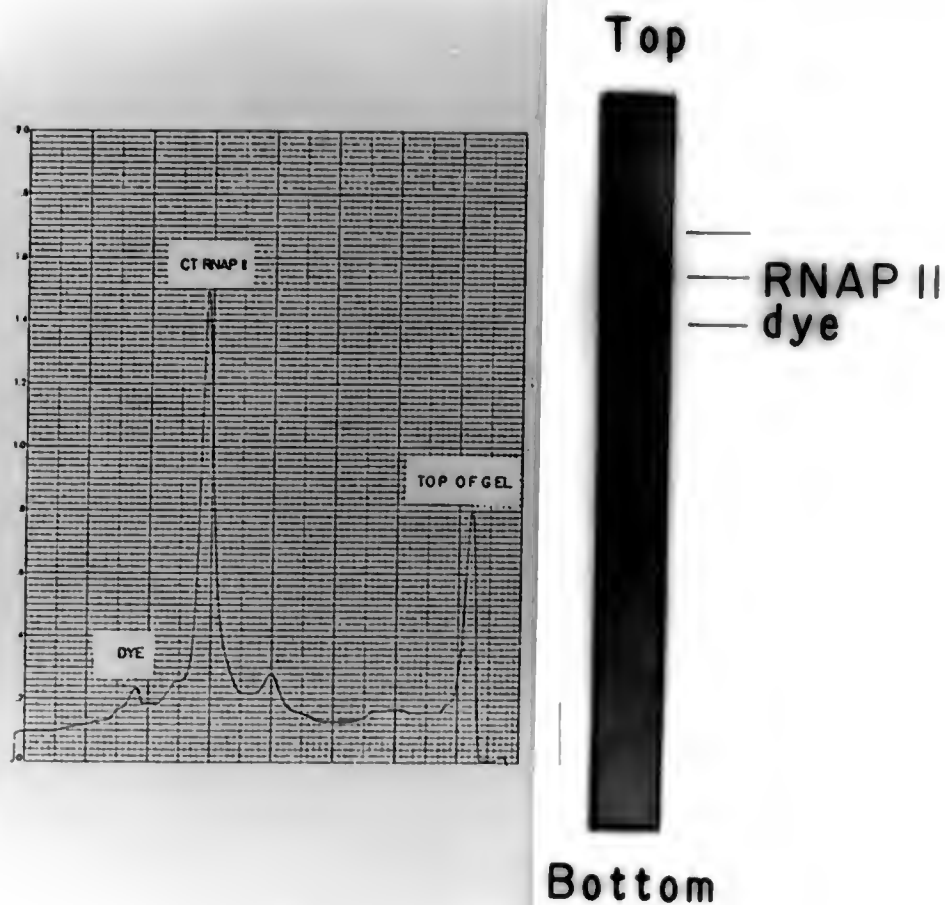


Figure 18. Non-denaturing PAGE of CT RNAP II.

CT RNAP II (5.6  $\mu$ g) was analyzed under non-denaturing conditions by PAGE for 1 hour at 4°C at 0.5 mWatt per gel tube. After staining with CBB-R250, the gel tube was scanned at 590 nm.

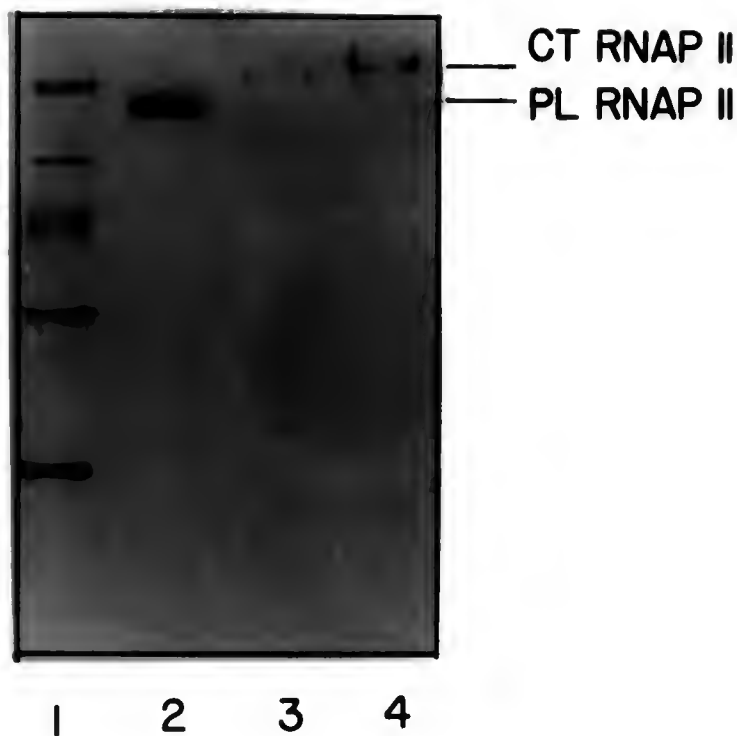


Figure 19. Non-denaturing gradient PAGE of RNAP II.

CT RNAP II and PL RNAP II were analyzed by non-denaturing gradient PAGE (4 % - 30 %) and run at 4°C for 2400 volt hours. Lane 1: Marker proteins: thyroglobulin (669 kD), ferritin (440 kD), catalase (232 kD), lactate dehydrogenase (140 kD), and BSA (66 kD). Lane 2: 6.7  $\mu$ g PL RNAP II (peak one from the Biogel column). Lane 3: 3.6  $\mu$ g of CT RNAP II. Lane 4: 5.4  $\mu$ g of CT RNAP II.

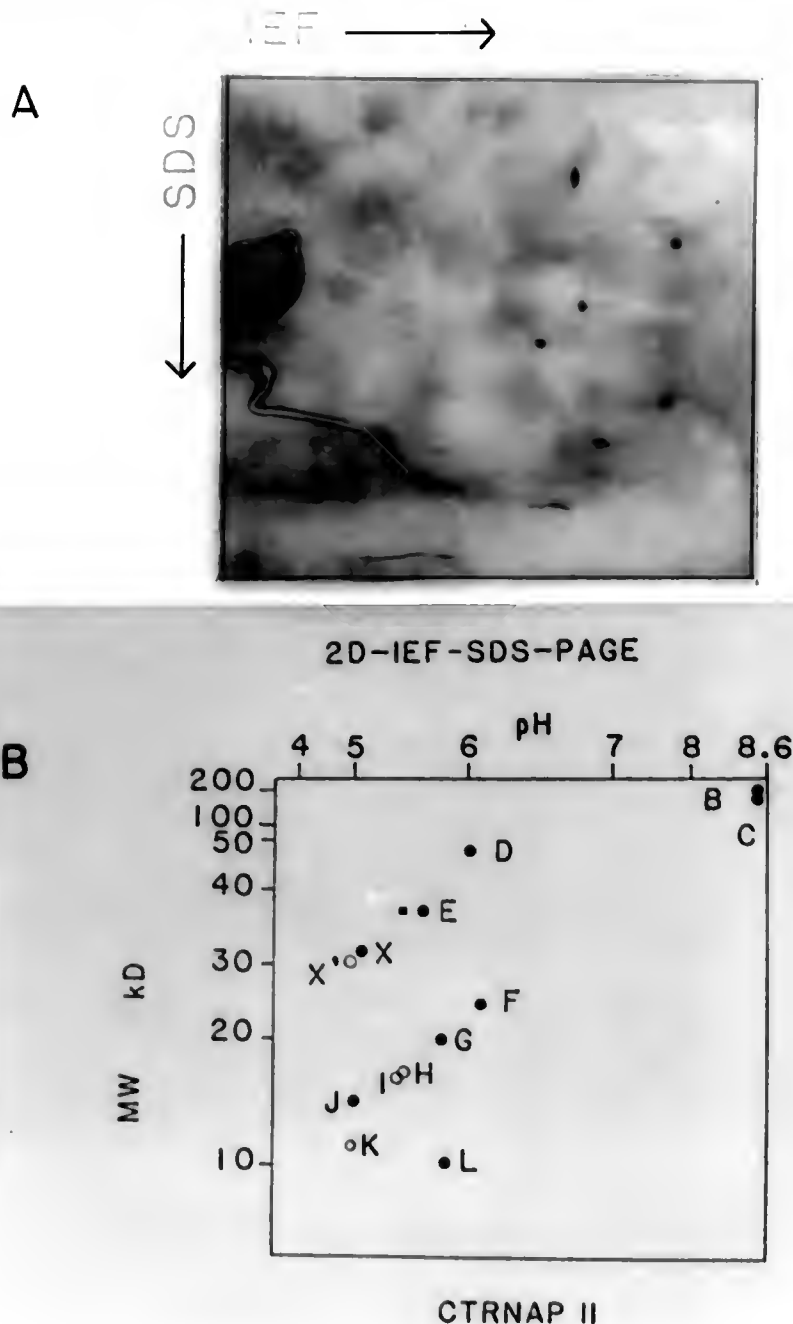


Figure 20. Polypeptide analysis of CT RNAP II.

CT RNAP II (17  $\mu$ g) was analyzed by 2D-IEF-SDS-PAGE and silver stained as described in the Materials and Methods section. Panel A is a picture of the gel. Panel B shows a drawing of the polypeptide pattern including the nomenclature, MWs, and the pIs. The solid dots represent the major polypeptides, whereas the minor polypeptides are shown as open dots. The black square indicates the shift of peptide E after photoaffinity labeling of CT RNAP II with azido-purine NTPs (Chapter Six).



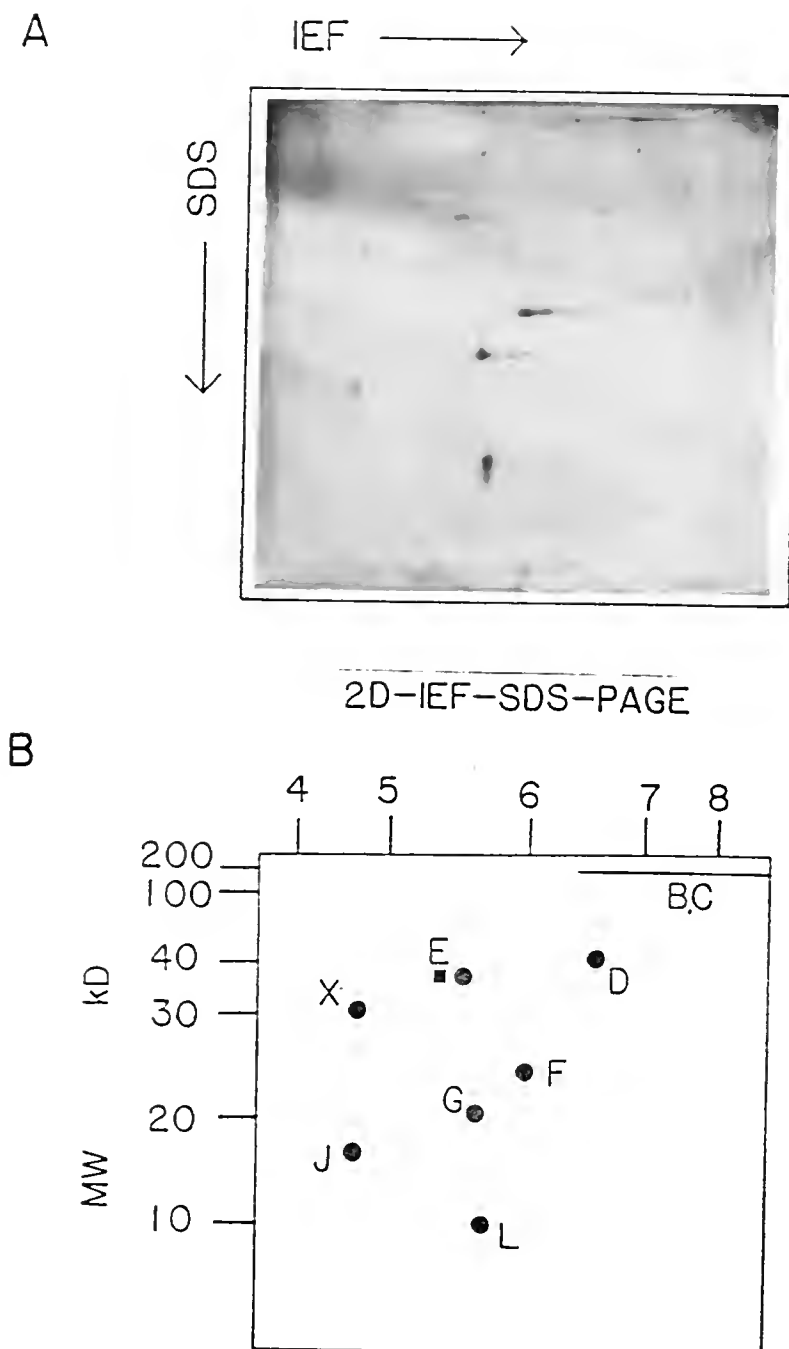


Figure 21. Polypeptide analysis of PL RNAP II.

PL RNAP II (17  $\mu$ g) was analyzed by 2D-IEF-SDS-PAGE and silver stained as described in the Materials and Methods section. Panel A is a picture of the gel. Panel B shows a drawing of the polypeptide pattern including the nomenclature, MWs, and the pIs. The solid dots represent the major polypeptides, whereas the minor polypeptides are shown as open dots. The black square indicates the shift of peptide E after photoaffinity labeling of PL RNAP II with azido-purine NTPs (Chapter Six).

TABLE III. MWs, pIs, and stoichiometries of RNAP II peptides.

Pep- tide	CT RNAP II <sup>a</sup>			CT RNAP II <sup>b</sup>			PL RNAP II		
	MW <sup>c</sup>	pI <sup>c</sup>	St <sup>d</sup>	MW	pI	St	MW	pI	St
B	180	7-8.8	1.0	180	>8.5	1.0	180	f	1.0
C	145	7-8.8	1.0	143	>8.5	1.0	143	f	1.0
D	45	5.0	0.5	43	6.0	0.4	43	6.6	1.4
E	37	5.0	1.24	36	5.4	1.5	36	5.4	1.3
F	25	6.1-6.4	1.67	25	6.1	1.6	25	6.1	2.9
G	20	5.9	0.99	20	5.8	1.2	20	5.5	3.0
H	18.5	4.4	0.72	18	5.5	0.7	18	n.d.	1.3
I	16	5.0	1.87	17.5	5.4	0.3	17	n.d.	1.2
J	15	-	1.78	15.1	5.0	2.3	15	4.6	1.0
K	13	5.3	-	12.3	5.0	0.6	9-11	n.d.	4.0
L	11.5	-	-	11	5.8	2.0	9-11	5.6	4.0
X	e	-	-	32	5.0	1.5	32	4.8	0.8
X'	e	-	-	30	4.9	0.4	29	n.d.	0.4

Note: a. Data of Hodo and Blatti (1977).  
b. Data presented in this chapter.  
c. MW in kD  $\pm$  6 %; pI  $\pm$  0.2 pH units.  
d. The stoichiometric ratios (St) are relative to the largest polypeptide that appears in purified RNAP II.  
e. Peptides X and X' are not mentioned by Hodo and Blatti.  
f. The pI was in the range of 6.3 to 8.5.  
n.d: Could not be determined.

### Discussion

The peptide patterns of CT RNAP II and PL RNAP II indicate that both RNAP II enzymes belong to subclass "B". The polypeptide compositions of CT RNAP II and PL RNAP II are rather similar with respect to the MWs, although polypeptides K and L in PL RNAP II did not separate well. Robbins et al. (1984) observed that CT RNAP II and human (HeLa cell) RNAP II were similar with respect to polypeptide composition, except that the MW of the largest polypeptide of the HeLa cell RNAP II was 220 kD. Table III shows some differences between CT RNAP II and PL RNAP II with respect to the stoichiometric ratios. Since the amount of binding of CBB-R250 to proteins on a protein mass basis can vary from protein to protein, the polypeptide stoichiometry is still tentative. The only way to obtain exact stoichiometric ratios would be to isolate each polypeptide in mg amounts and prepare a calibration curve, correlating the increase in absorbance at 590 nm of stained polypeptides versus increasing amounts of the stained polypeptide on the basis of weight.

Among the peptides that are present here in CT RNAP II is peptide D, which was reported to be removed from the RNAP II during Biogel 1.5m chromatography, but not during glycerol gradient centrifugation (Hodo and Blatti, 1977). However, upon repeating the purification of CT RNAP II, Hodo was not able to remove peptide D by Biogel filtration (Hodo, personal communication). This peptide D in purified CT RNAP II was also seen by Benson et al. (1978), Kadesh and Chamberlin (1982), Dahmus (1981b), and by Smith et al. (1979) in yeast RNAP II. Dahmus reported that peptide D did not migrate with the CT RNAP II band under non-denaturing conditions. Smith et al. proposed that peptide D is actin, which is a major

cellular skeletal protein with a MW of 46 kD. Other peptides with similar molecular weights in the calf thymus are one peptide of CT RNAP I (43 kD) or casein kinase II (Chapter Five).

Bands X and X', with a MW of 30-32 kD (Fig 14), are also present in purified CT RNAP II isolated by Benson et al. (1978), when they analyzed 30 µg purified enzyme by SDS-PAGE. The purified preparation of PL RNAP II shows polypeptides D, X, and X' as well, although in different stoichiometric ratios (Figure 15).

Polypeptide E is interesting, because this peptide in both CT RNAP II and PL RNAP II was specifically labeled by azido-purine NTPs (Chapter Six), which resulted in a small shift of the pI in the acidic direction during isoelectric focusing (Figure 20). The polypeptide E sometimes appears as a doublet (Figure 16), which was also observed by Benson et al. (1978).

The gel patterns based on non-denaturing PAGE show that CT RNAP II and PL RNAP II consist of one and two protein species, respectively. The enzymes are rather pure because no polypeptide was detected on the non-denaturing gradient PAGE gels with a higher electrophoretic mobility than the major intact protein bands. When electrophoresis was continued for 2 hours for CT RNAP II instead of one hour (Figure 18), the protein dissociated into several polypeptides of lower MW (not shown). Non-denaturing gels containing PL RNAP II were sliced and analyzed for the presence of enzyme activity and [<sup>3</sup>H]-DeMeABGG binding, after elution of the enzyme from the gel slices by reverse electrophoresis as described by Otto and Snejdarkova (1981). Radiolabeled amanitin derivative binds to and enzyme activity could be eluted from the region of the gel where the protein

bands migrated (Waechter et al., 1984). However, after extended electrophoresis, no active enzyme could be detected. This is perhaps due to the decrease of the ionic strength that occurs during PAGE, which causes several polypeptides to dissociate. A similar observation was made earlier when RNAP II lost its activity (irreversibly) upon dialysis against a low ionic strength buffer. Because it is possible for contaminating polypeptides to comigrate with the RNAP II under the non-denaturing conditions used, an exact degree of purity cannot be given. However, based on the "consensus" subunit composition of RNAP II from the higher eukaryotes, both the purified CT RNAP II and PL RNAP II appear to be rather pure. However, until a specific role during transcription in vivo can be assigned to each one of the relevant polypeptides, no definition of purity can be truly valid.

The discrepancy in MWs between CT RNAP II and PL RNAP II can be due to differences in size or due to non-ideal electrophoretic behaviour of CT RNAP II because of, e.g., phosphorylation of some of the polypeptides (see Chapter Five).

The 2D-IEF-SDS-PAGE of CT RNAP II shows polypeptides B, C, D, E, X, F, G, J, and L as major bands, whereas polypeptides X', H, and I were faintly visible or stained purple instead of black after silver staining and therefore did not appear in the photograph. Polypeptides B and C stained less than could be expected, which might be due their alkaline pI and/or to some loss of these two proteins that occurred during the focusing in the first dimension, because there is a gradual depletion of basic ampholines during isoelectric focusing. Furthermore, there is a silver stained area around a pI of 7 and with a MW of that of polypeptide B.

Thus, in contrast to the presence of two strongly stained bands representing the polypeptides B and C after 1D-SDS-PAGE, these species do not show up well after 2D-IEF-SDS-PAGE. A similar observation was made by Coulter and Greenleaf (1982) who could not resolve the two largest polypeptides of Drosophila RNAP II by 2D-SDS-IEF-PAGE (unpublished results).

## CHAPTER FIVE ANALYSES ON CALF THYMUS RNAP II FOR KINASES.

### Introduction

When preliminary photoaffinity labeling experiments with [ $^{32}\text{P}_\gamma$ ]- $8\text{N}_3$ -ATP and CT RNAP II (see Chapter Six) showed specific labeling of a low MW (37 kD) protein (E), there was concern that a contaminating kinase was being photolabeled rather than a component of CT RNAP II. The results described in this chapter here suggest that the radiolabeled peptide in the CT RNAP II preparation purified as described in Chapter Two is not a kinase contaminant.

### Materials and Methods

#### Kinase detection

To assay for protein kinase activity, either 1-5  $\mu\text{Ci}$  of [ $^{32}\text{P}_\gamma$ ]-ATP or equal amounts of [ $^{32}\text{P}_\gamma$ ]- $8\text{N}_3$ -ATP (18.8-81 Ci/mmol, ICN Radiochemicals) or [ $^{32}\text{P}_\gamma$ ]- $8\text{N}_3$ -GTP (34.5 Ci/mmol, ICN Radiochemicals), each containing a final concentration of ATP or GTP of 0.08 mM, were incubated with 100  $\mu\text{g}$  of substrate and 6 pmoles of CT RNAP II in a total volume of 100  $\mu\text{l}$  at temperatures ranging from 22°C to 37°C. Since any of several protein kinases could be present (see Table IV), each with its optimal substrate, divalent cation, pH requirements, and dependence on c-AMP, a number of different reaction conditions were used, as described for different protein kinases, see Table IV and references therein.

For example, the substrates tested included the acidic proteins phosvitin or casein, the basic proteins histones or protamine chloride, and native or heat denatured CT RNAP II. Incubations were performed in the presence or absence of 10 mM  $\text{MnCl}_2$  and/or 10 mM  $\text{MgCl}_2$  and/or 2 mM  $\text{CaCl}_2$ , 2  $\mu\text{M}$  c-AMP, different salts (NaCl or ammonium chloride) in a concentration range from 10 to 450 mM, and different buffers, including Tris-HCl, Hepes-NaOH, or  $\beta$ -glycerophosphate-NaOH in a pH range from 7 to 7.9.

Finally, as an additional control, some incubations were performed in the presence of 2.5  $\mu\text{g}/100 \mu\text{l}$  of Walsh inhibitor, which is known to inactivate c-AMP dependent protein kinases (Ashby and Walsh, 1972). All reactions were terminated after 20 minutes by the addition of 20  $\mu\text{g}$  ATP prior to TCA precipitation.

#### Substrate preparation

Histones (Sigma Chemical Company) were dissolved at a concentration of 25 mg/ml, in 1 mM Hepes, pH 8, containing 1 mM EDTA. The solution was then heated for 20 minutes at 70°C, dialyzed overnight against 1 mM Hepes, pH 8, containing 0.1 mM EDTA, filtered through a 45  $\mu\text{m}$  Millipore hypodermic filter, and stored at -20°C (Gordon et al., 1983).

Phosvitin (Sigma Chemical Company) and casein (Sigma Chemical Company) were prepared by adjusting the pH of a solution containing 25 mg protein/ml to 9.0 with 1 M NaOH, heating in a boiling water bath for 10 minutes before neutralization to pH 7 with 1 M HCl, and storage at -20°C (Thornburg and Lindell, 1977). Protamine chloride did not require any specific treatment. CT RNAP II was heated in a boiling water bath for 10 minutes and stored at -20°C.



### Analysis by TCA precipitable counts

To determine the amount of phosphorylated protein in the reaction assay, 90  $\mu$ l of the reaction mixture were spotted on a dry disc of Whatmann 3MM filter paper ( $2.5 \text{ cm}^2$ ), which had previously been soaked in 20 % (w/v) TCA. The disc was then submerged in 10 % TCA at  $4^\circ\text{C}$  for 10 minutes, and washed with stirring six times at room temperature in 5 % TCA containing 20 mM sodium pyrophosphate and 10 mM  $\text{K}_2\text{HPO}_4$ . The disc was then soaked in 95 % ethanol, dried, and counted in Econofluor (New England Nuclear). The background was calculated from reactions containing heat denatured CT RNAP II and was usually 550 cpm. To estimate the sensitivity of the reaction, bovine cardiac muscle protein kinase type II with a specific activity of 140,000 units per mg protein was used as a standard. One unit is defined as the amount of enzyme that catalyzes the transfer of 1 pmole of phosphate from ATP to substrate per minute under the standard assay conditions: 80 mM Tris-HCl, pH 7.3, 100 mM ammonium sulfate, 1 mM EDTA, 4 mM  $\text{MgCl}_2$ , 2  $\mu\text{M}$  c-AMP, 100  $\mu\text{g}$  phosphatidylcholine, 1  $\mu\text{Ci}$  [ $^{32}\text{P}$ ]-ATP, 0.12 mM ATP, and 0.05 mM BME reacting for 20 minutes at  $30^\circ\text{C}$ . The sensitivity of the phosphate transfer assay allowed the detection of 0.5 ng (0.0026 pmoles) of bovine cardiac muscle protein kinase, type II (190 kD for the holoenzyme).

## Results

### Kinase detection

To determine whether or not the purified CT RNAP II preparation contained contaminating protein kinase activity, a number of different incubations were performed. This was necessary because the several reported

kinases (see Table IV and references therein) have preferences for a variety of substrates, divalent cations, salts concentrations, and buffer types. After surveying these reaction conditions as described in the Materials and Methods section, only one gave positive results. This incubation mixture (100  $\mu$ l) contained 7 pmoles of native CT RNAP II, 100  $\mu$ g of phosvitin, 35 mM ammonium sulfate, 0.1 mM EDTA, 4 mM  $\text{MgCl}_2$ , and 50 mM Tris-HCl (pH 7.2). After incubation of the reaction mixture for 20 minutes at 30°C, 2000 cpm precipitable radioactivity were measured above the control (550 cpm), which contained heat denatured CT RNAP II. The addition of 2  $\mu$ M c-AMP, 2 mM  $\text{CaCl}_2$ , 1 mM BME, or 2.5  $\mu$ g Walsh inhibitor had no effect on the activity in this assay. However, the reaction was sensitive to high salt (150 mM ammonium sulfate or 200 mM ammonium chloride). The reaction appeared to be specific for phosvitin, since when 100  $\mu$ g of protamine-chloride, histones, or casein were used, only 500 cpm over background were observed. No radioactivity above background was found when native or heat denatured CT RNAP II was incubated with [ $^{32}\text{P}_\gamma$ ]-ATP, or [ $^{32}\text{P}_\gamma$ ]-8N<sub>3</sub>-ATP, or [ $^{32}\text{P}_\gamma$ ]-8N<sub>3</sub>-GTP under different conditions but in the absence of UV (see Chapter Six).

In order to attempt to quantify the amount of possible kinase activity which may be present in the CT RNAP II preparation, control experiments were done with bovine cardiac muscle protein kinase type II. From a standard curve generated with this enzyme under optimal conditions (see Materials and Methods), it was determined that the 2000 cpm above background is equivalent to 0.005 pmoles of kinase-like activity in 7 pmoles of CT RNAP II, or less than 0.07 % on a mole stoichiometric basis.

In addition to these experiments, reactions specific for demonstrating c-AMP dependent protein kinase activity were performed by incubating 10 pmoles of CT RNAP II or PL RNAP II, each with 4 mM  $\text{MgCl}_2$  and 1.8  $\mu\text{Ci}$  [ $^{32}\text{P}$ ]-8N<sub>3</sub>-c-AMP (8 Ci/mmol), followed by UV irradiation, as described in the Materials and Methods section of Chapter Six. After analysis of the incubation mixture by 1D-SDS-PAGE followed by autoradiography, no labeling could be detected.

Comparison of the reaction characteristics of the kinase activity found here, i.e., preference for phosvitin and c-AMP independence, and of the MW of the peptide (E) in CT RNAP II that was photoaffinity labeled (Chapter Six) with those results summarized in Table IV and references therein led to the examination of the CT RNAP II preparation for the presence of casein kinase I (CK I) activity as the most likely possible contaminant. Three approaches were used.

CT RNAP II and purified CK I were run in parallel on a 1D-SDS-PAGE system to compare molecular weights. The electrophoretic mobility of peptide E was less than that of CK I, see Figure 22.

CT RNAP II and CK I were run on a 2D-IEF-SDS-PAGE system to compare the pI of CT RNAP II peptide E and CK I, see Figure 23. The pI of CK I was 9, whereas the pI of peptide E was 5.2.

Dr M.E. Dahmus kindly tested the purified preparation of CT RNAP II for the presence of CK I. An  $^{125}\text{I}$ -labeled antibody against CK I was incubated with a "Western" blot of CT RNAP II (Dahmus et al., 1984), and no crossreaction with peptide E was found, see Figure 24.

Table IV. Summary of properties of calf thymus protein kinases.

Calf Thymus:	PK I	PK II	CK I	CK II	SF I
Pi donor	ATP	ATP	ATP	ATP/GTP	ATP
Substrate	Protamine Chloride CTRNAPII	Protamine Chloride CTRNAPII	Phos-vitin CTRNAPII	Phos-vitin CTRNAPII	Phos-vitin
MW CTRNAP II peptide-Pi	25, (180)	25, (180)	20.5	20.5	?
c-AMP dep.	Yes	No	No	No	No
Effect on RNAP II	Activates	Activates	None	None	(yes)
Autophosphorylation	No	No	Yes	Yes	?
MW C	40	55	34-37	26/40/44	36-38 27
MW R	50	-	-	-	-
Total MW	80	-	-	138	55-65
pI	?	?	g*	?	9.1
Salt elution <sup>#</sup>	<40	120-150	<75	75-135	-
Reference	(1)	(2)	(3)	(4)	(5)

Note: \*, (Chapter Five); #, mM of ammonium sulfate required to elute enzyme from DE-52 cellulose. The pI of 9.1 for SF I (stimulating factor) is based on the 60 kD species. PK:protein kinase; CK: casein kinase. References: (1) Kranias et al., 1977, (2) Kranias and Jungman, 1978, (3) Dahmus, 1981a, c. (4) Dahmus, 1981a, b, c and 1984, (5) Gordon et al., 1983, Kranias and Jungman 1978.

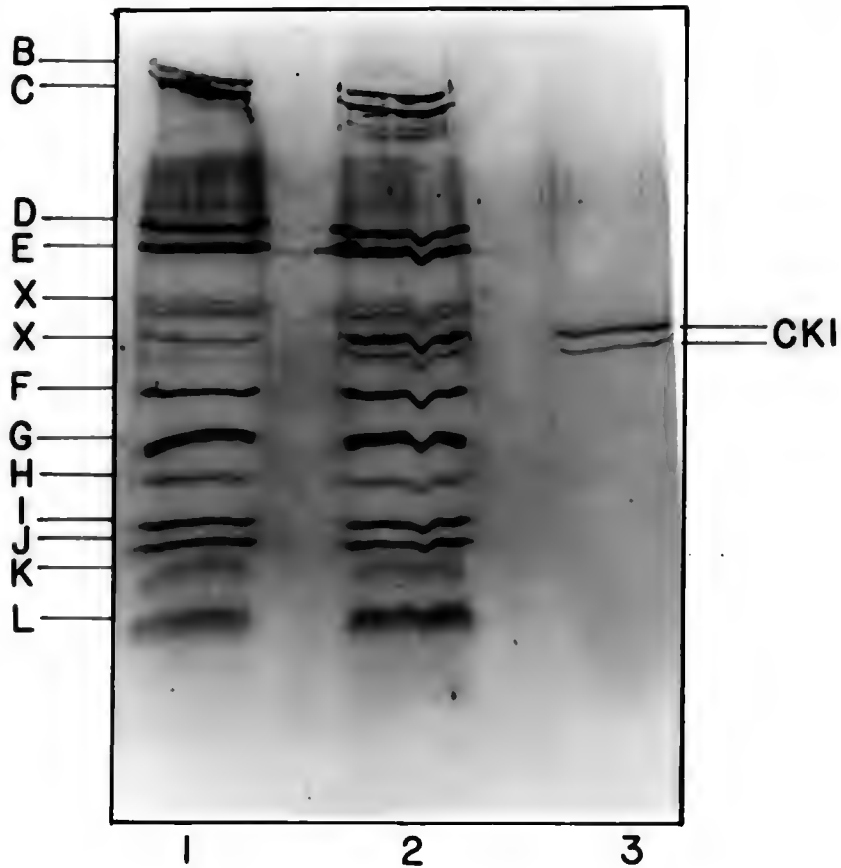


Figure 22. Polypeptide analysis of CT RNAP II and casein kinase I.

CT RNAP II and casein kinase were analyzed by 1D-SDS-PAGE on a 0.75 mm thick gel and silver stained as described in the Materials and Methods section of Chapter Four. Lane 1: 7.5 pmole CT RNAP II. Lane 2: 7.5 pmole CT RNAP II and 1.6 pmole casein kinase. Lane 3: 1.6 pmole casein kinase.

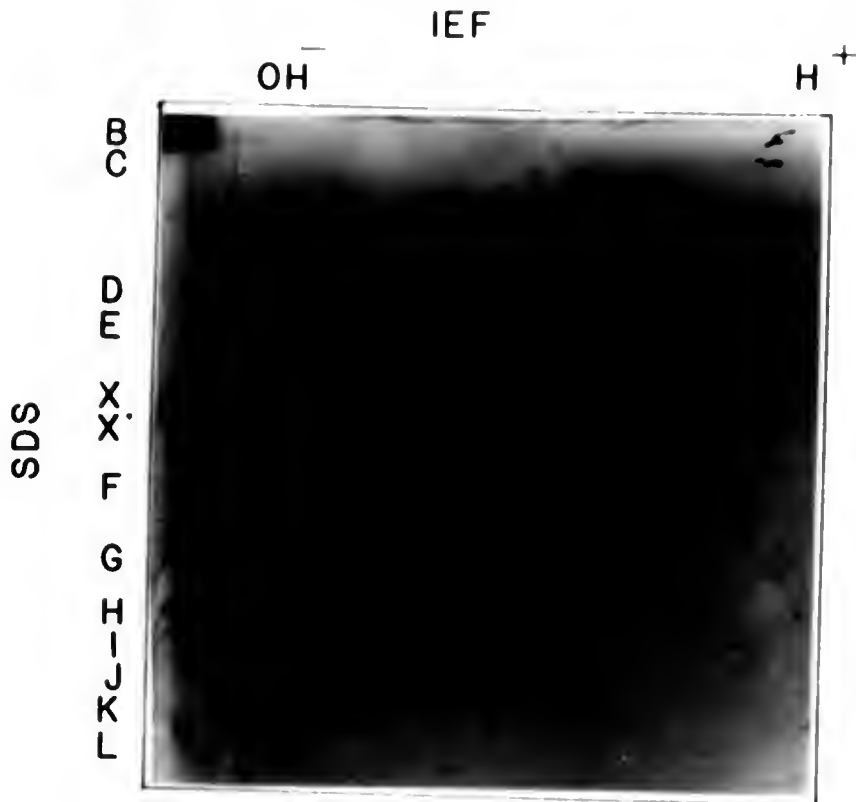


Figure 23. Polypeptide analysis of casein kinase I.

To determine the pI of the casein kinase polypeptides, 9 pmole of casein kinase I were analyzed by 2D-IEF-SDS-PAGE as described in the Materials and Methods section of Chapter Four. Thirty pmole of CT RNAP II were run in parallel during the second dimension. The arrow points to the position of CK I, which has a pI of 9.0.



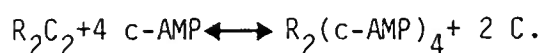
Figure 24. Western blot of CT RNAP II with [ $^{125}$ I] labeled antibodies directed against casein kinase I.

CT RNAP II was analyzed with respect to contamination by casein kinase I. Shown is an autoradiograph of a western blot that was incubated with radiolabeled antibodies against casein kinase I. Lane 1: 3.4  $\mu$ g CT RNAP II. Lane 2: 3.4  $\mu$ g of CT RNAP II but from another preparation. Lane 3: 10  $\mu$ g CT RNAP II. Lane 4: control with 0.1  $\mu$ g casein kinase I. The position of the polypeptide E of CT RNAP II in lanes 1 to 3 is indicated. The 2 bands in lane 4 coincide with casein kinase I.

### Discussion

Since it is possible that the protein band (37 kD) found to be radiolabeled with [ $^{32}\text{P}_\gamma$ ]- $8\text{N}_3$ -ATP or [ $^{32}\text{P}_\gamma$ ]- $8\text{N}_3$ -GTP in the purified CT RNAP II preparation (Chapter Six) is not an essential component of the polymerase, but rather a contaminating activity which can interact with the photoprobes, several control experiments were done. The likely contaminating enzyme activity surveyed here was protein kinase, because radiolabeling of a 37 kD peptide could be obtained if the CT RNAP II preparation contained a contaminating protein kinase. In this case, the radiolabeled azido probe might not only produce a radiolabeled peptide by binding to the active site of the kinase, but might also produce a labeled band either by using the gamma  $^{32}\text{P}_\text{i}$  in an autophosphorylation reaction, or by transferring the  $^{32}\text{P}_\text{i}$  to peptide E of the CT RNAP II. Because of the variety of pathways by which a kinase could radiolabel a peptide and because there are several classes of protein kinases as potential contaminants, each with its own substrate specificity, cation, salt, buffer, and pH preferences, sensitivity to inhibitors, and requirement for c-AMP (see Table IV), a number of these variables were tested here.

The properties of several classes of kinases have been reviewed (Krebs and Beavo, 1979 and Bramson et al., 1983). For example, the c-AMP dependent multisubunit (Catalytic and Regulatory) protein kinases have a total MW of 90-190 kD, but dissociate upon c-AMP binding:





The MWs of the R and C subunits are 40-55 and 33-42 kD, respectively (Bramson et al., 1983). The C protein phosphorylates mostly basic proteins, transferring a gamma phosphate from ATP to serine or threonine. Some of these enzymes are  $\text{Ca}^{2+}$  dependent. They are inhibited by the Walsh inhibitor, which binds to the C subunit. Of interest here, the R subunit of both type I and type II enzymes has been labeled with [ $^{32}\text{P}$ ]- $8\text{N}_3$ -c-AMP (Schoff et al., 1982). The type II enzymes phosphorylate themselves on one unique serine on the R subunit in vitro. This class of c-AMP dependent protein kinases is responsible for many, if not all, c-AMP mediated effects (Murdoch and Rosenfeld, 1982), perhaps through phosphorylation of a 23 kD chromatin-associated basic protein in the eukaryotic nucleus, perhaps a component of RNAP II (Kranias et al., 1977).

The c-AMP independent protein kinases, on the other hand, phosphorylate mainly acidic proteins using either ATP or GTP as phosphate donor. Of interest here, they consist of one protein and have been photo-inactivated by  $8\text{N}_3$ -ATP (Gordon et al., 1983). They have been shown to phosphorylate nonhistone proteins like RNAP. Indeed, differences in phosphorylation have sometimes been accompanied by an increased gene transcription (Duceman et al., 1981). Several studies have shown this to occur in vitro for RNAP I (Thornburg and Lindell, 1977, Duceman et al., 1981, Rose et al., 1981) and for RNAP II (Kranias et al., 1977, Kranias and Jungman, 1978, Spindler, 1979, and Thornberg and Lindell, 1977). In contrast, Dahmus (1981a, c) could not demonstrate any stimulation of RNAP II. In the reports describing stimulation, no clear correlation was found between amount, i.e., stoichiometry, of phosphorylation and enzyme activation in those cases in which activation occurred.

The third class of protein kinases is a mixture of enzymes that phosphorylate mostly metabolic enzymes, are most often c-AMP dependent, and can occur either as C or  $R_2C_2$  proteins.

With regard to potential contaminants from the tissue under study here, five calf thymus nuclear protein kinases have been well-characterized (see Table IV). Nevertheless, the data presented here suggest that the CT RNAP II preparation, purified as described in Chapter Two and radiolabeled with azido purine nucleoside triphosphates as described in Chapter Six, contains no protein kinase of a MW of 37 kD and a pI of 5.4 which could be radiolabeled by autophosphorylation or which could radiolabel peptide E.

Specifically, assuming that 7 pmoles of CT RNAP II are contaminated with 0.005 pmoles of a fully active PK, it is unlikely that this contamination could cause specific labeling of peptide E by the photoaffinity probe, because:

If peptide E is labeled by the PK using the photoprobe as phosphate donor, then this should be independent of the presence of UV light. However, in the absence of UV light no phosphorylation of any peptide occurred with either  $[^{32}P\gamma]$ -ATP or  $[^{32}P\gamma]$ - $8N_3$ -ATP or  $[^{32}P\gamma]$ - $8N_3$ -GTP under the conditions described (see the references in Table IV), when analyzed by TCA precipitable counts or 1D-SDS-PAGE followed by autoradiography (Chapter Six).

If peptide E is labeled because of contamination by a protein kinase with an identical MW, which binds the photoprobe, then the efficiency of labeling could not exceed 0.07 %. However, results presented in Chapter Six demonstrate up to 45 % efficiency in radiolabeling with respect to stoichiometry.

All our attempts to demonstrate contamination by the most likely protein kinase, i.e., casein kinase I, in our purified CT RNAP II, failed.

For example peptide E is homogeneous by 2D-IEF-SDS-PAGE mapping (Chapter Four). The pIs of peptide E and CK I differ, i.e., they are 5.4 and 9, respectively. In addition, peptide E shows a shift of its pI by 0.2 pH units in the acidic direction as a result of the addition of an acidic phosphate group by photoaffinity labeling (Chapter Six), which is consistent with a similar shift in pI upon phosphorylation of polypeptides in other systems (Matsumoto and Pak, 1984).

Likewise, peptides X and X', which are present in the CT RNAP II preparation and were first thought to be potential casein kinase I contaminants, showed pIs of 4.9 to 5.0, which are again different from CK I and the catalytic subunit of c-AMP dependent protein kinases (7-7.8, Bramson et al., 1983).

CT RNAP II peptide E and CK I do not have identical electrophoretic mobilities (Figure 22). Ferguson (1964) showed that ideally a correlation exists between electrophoretic mobility and protein size. This correlation holds true in the absence of added carbohydrate or phosphate moieties, which will slow down mobility in an electric field. Since Dahmus showed that after autophosphorylation, the mobility of casein kinase changes (Dahmus, 1981a), experiments were done which tested whether or not the electrophoretic mobility of casein kinase I decreased slightly, as compared to that of peptide E, by incubating CKI under the autophosphorylation conditions of Dahmus (1981a). Again, when

run in parallel with CT RNAP II on a 1D-SDS-PAGE system, the mobilities of peptide E and CK I were different.

Finally there was no cross reaction of the casein kinase I antibody with CT RNAP II peptide E, under conditions described by Dahmus, (1984). Collectively, these data suggest that the CT RNAP II preparation, purified as described in Chapter Two and radiolabeled with azido NTP photo-probes as described in Chapter Six, contains no kinase contaminant which can account for the specific labeling of a 37 kD polypeptide. These results support the conclusion that CT RNAP II peptide E is within the NTP binding domain of this enzyme.

## CHAPTER SIX DETECTION OF A NUCLEOSIDE TRIPHOSPHATE BINDING SITE

### Introduction

Although much is known about eukaryotic RNAPs, several problems remain unsolved. The regulation of transcription with respect to gene expression is not very well understood. For example, using defined templates in vitro, none of the purified RNAPs isolated thus far is able to initiate or to terminate at correct (in vivo) sites in the absence of added factors. Furthermore, it is not known which subunits confer specificity to each class of RNAP (see Chapter One).

These problems are currently under investigation in many laboratories using a variety of genetic (Greenleaf, 1983 and Ruet et al., 1980), biochemical (Brodner and Wieland, 1976 and Cho and Kimball, 1982) and immunological approaches (Breant et al., 1983, Tsai et al., 1984, Young and Davis, 1983, and Guilfoyle et al., 1984a, b). An even more fundamental question regarding RNAP activity is which of the polypeptides that copurify with this complex enzyme are required for catalytic activity. In prokaryotes, several approaches, including extensive genetic analysis, crosslinking studies, and reconstitution experiments (see Chapter One), were used to elucidate the function of each peptide in the core and the holoenzyme complex. With regard to eukaryotic RNAP activity progress has been slow. For example, to date, all attempts to dissociate and reassociate eukaryotic RNAP "subunits", i.e., reconstitution

experiments, have failed (Burgess, 1976, Guilfoyle et al., 1983, Lewis and Burgess, 1982, and Robbins et al., 1984). Thus, except for the likely involvement of the two largest peptides in binding  $\alpha$ -amanitin (see Chapter One), the subunit composition required for core type catalytic activity for eukaryotic RNAP remains unknown. This chapter describes the results of research which attempts to locate a NTP binding site on CT RNAP II and PL RNAP II using photoaffinity labeling.

### Structure of the active site

From studies with nucleotide analogues, it was concluded that the stereochemical basis of substrate selection during the elongation step is the geometry of the Watson/Crick base pairs, and that the enzyme exerts little control in the selection of the proper NTP (Rackwitz and Scheit, 1977 and Wu and Tweedy, 1982). However, the preferential incorporation of purine NTPs into the 5'-terminus of the nascent RNA chain may at least in part be controlled by the stereochemical requirements of the initiation site (Armstrong and Eckstein, 1979). Modak and Gillerman-Cox (1982) suggested that perhaps ionic interactions between polypeptides and substrates do not play a major role in substrate binding or selection of substrates, whereas the intrinsic Zn does (Chatterji et al., 1984). In specific initiation experiments using truncated templates and a strong, well-defined promoter, proper initiation occurred with Mg but not with Mn (Paule et al., 1984 and Sekimizu et al., 1982). Furthermore, the error rate of E. coli RNAP in the transcription process was found to decrease upon substitution of Mn by Mg (Mildvan and Loeb, 1979). These results suggest that Mg is somehow involved in selecting

the proper start site and/or purine NTP. However, the precise role of metal ions in DNA and RNA polymerases is, to date, still controversial (Williams, R.P., personal communication).

With regard to the structure of the active site of RNAP, the most widely accepted model is derived from studies of E. coli RNAP. This model is based on a number of experimental approaches, including cross-linking with affinity reagents, kinetic analyses (Anthony et al., 1969, Rhodes and Chamberlin, 1974, and Rhodes and Chamberlin, 1975), experiments using equilibrium dialysis (Wu and Goldthwait, 1969b), and studies on fluorescence quenching (Wu and Goldthwait, 1969a). Collectively, these data suggest a two site model for the catalytic center (Nixon et al., 1972, Krakow and Fronk, 1969, Wu and Wu, 1974, Spoor et al., 1970, and Wu and Tweedy, 1982), where the definition of a site is not necessarily limited to one domain on one subunit.

One site is involved with binding of the template, orienting the RNAP II in the 3'-5' direction with respect to the sense strand of DNA. The other site is a catalytic site and is composed of two subsites, one for initiation and one for elongation. The initiation subsite binds the 3'-OH terminus of the first incoming purine NTP and later the 3'-terminus of the growing RNA chain even in the absence of Mg, Mn, or template (Wu and Goldthwait, 1969). This site can also bind dinucleotides that can serve as initiators (Lynwood and Yarbrough, 1982, and Samuels et al., 1984).

The other subsite is an elongation subsite that binds, in the presence of Mn or Mg, purine as well as pyrimidine NTPs. However, unlike the initiation subsite, it does not catalyze the incorporation of

dinucleotides (Samuels et al., 1984). For E. coli RNAP it was found that dinucleotides are competitive inhibitors towards initiation but not towards elongation (Hsu and Dennis, 1982). In addition, the kinetic parameters for the initiation and elongation subsites in the E. coli enzyme differ. For example, the apparent  $K_M$  for NTP for initiation and elongation are approximately 500  $\mu M$  and 20-50  $\mu M$ , respectively (Chamberlin, 1976). Furthermore, there is evidence that the elongation rate with Mn as divalent cation is higher than with Mg (Roeder, 1976), which might explain the higher error rate by the RNAP in presence of Mn compared to the error rate in presence of Mg.

The data supporting the catalytic model are, however, neither complete nor conclusive. For example, the basic two subsite model has been modified to suggest that the elongation site might itself be made up of two subsites, one for purine and one for pyrimidine NTPs (Woody et al., 1984). Yet another version of the two site model was proposed by Dennis and Sylvester (1981), who described a model for rotational translocation in which the active region on RNAP contains two functionally equivalent elongation active sites which are utilized alternatively during elongation, while there is only a unique site for initiation.

#### Crosslinking studies with prokaryotic RNAP and NTP

The results that one obtains with any chemical affinity label, either a substrate or a competitive inhibitor of the enzyme, depend on the localization of the reactive group on the affinity label. Indeed, reactive groups have been attached on various locations of the same affinity probe to map not only the active site but also the neighboring



peptides. For example, with NTP, there are three groups available to attach a reactive group: the base moiety, the pentose sugar, and the 5' phosphate terminus. The last involves a functional group on the 5' terminus of the growing RNA chain and has been used to follow its path across the surface of the enzyme during elongation (Hanna and Meares, 1983).

Several affinity labels derived from NTP have been used (Armstrong and Eckstein, 1979) to locate the NTP binding site for E. coli RNAP. These include: dialdehyde linkage to enzyme amino groups by reduction of periodate oxidized NTPs with  $\text{NaBH}_4$  (Cho et al., 1982 and Malcolm, 1978), mercapto-NTP derivatives that link to cysteine-SH on the enzyme after  $\text{H}_2\text{O}_2$  exposure (Cho and Kimball, 1982), and azido ( $\text{N}_3$ ) containing NTPs that will, upon UV irradiation, link themselves with any nearby group, whether solvent or solute (Woody et al., 1984). In addition, other reagents have been used including formyl, glyoxal, bromoacetyl-amido, and isothiocyanate groups (Armstrong et al., 1977 and Armstrong and Eckstein, 1979) and even direct UV crosslinking (Modak and Gillerman-Cox, 1982).

Collectively, results on the crosslinking of subunit  $\beta$  (Spoor et al., 1970, Armstrong et al., 1976, Frischauf and Scheit, 1973, Cartwright and Hutchinson, 1980, Sverdlov, 1978, Sverdlov et al., 1980, Grachev and Zaychikov, 1981, Hanna and Meares, 1983, and Wu and Wu, 1974) by NTP analogues led the authors of two reports (Wu and Wu, 1974 and Spoor et al., 1970) to the conclusion that it contained the initiation site, while the crosslinking of subunit  $\beta'$  (Armstrong and Eckstein, 1979, Woody et al., 1984, Frischauf and Scheit, 1973, Cartwright

and Hutchinson, 1980, Sverdlov, 1978, Sverdlov et al., 1980, DeRiemer and Meares, 1981a, b, Hanna and Meares, 1983, and Miller et al., 1980) led the authors of two other reports (Woody et al., 1984 and Miller et al., 1980) to the conclusion that it contained the elongation site. Unfortunately, these simple conclusions are not supported by other experimental results showing crosslinking of NTPs to subunit  $\sigma$  (Woody et al., 1984, Cartwright and Hutchinson, 1980, Sverdlov, 1978, and Sverdlov, et al., 1980), as well as to the  $\alpha$  subunit (Malcolm and Moffat, 1978).

In general, however, it is thought that the catalytic domain of E. coli RNAP is probably made up of a contact area between the  $\beta$  and  $\beta'$  subunits and that each contains a NTP binding site, i.e., the initiation and elongation site, respectively.

#### Crosslinking studies with eukaryotic RNAP to assign peptide function

Crosslinking of eukaryotic RNAP to DNA by UV irradiation was reported by Gundelfinger (1983). He studied the interaction of all three RNAP classes (I, II and III) from Drosophila with the DNA template and with the nascent RNA. The two largest polypeptides (140 and 180 kD) appear to be involved in non-specific binding of both DNA and RNA. When a ternary complex with adenovirus type 2 DNA was investigated, the 180 kD peptide seemed to bind the nascent RNA better, while the 140 kD polypeptide bound better to the DNA template. Thus, these two large peptides may play a role in template and nascent RNA binding.

With regard to NTP binding site(s) on eukaryotic RNAP, a number of approaches have been used including a non-analogue approach. For example, since pyridoxal-5'-phosphate, at low concentrations, is known to

inhibit yeast RNAP activity, because the aldehyde can form a Schiff's base with amino groups of the enzyme's lysine residues, Valenzuela (1978) used this reagent to study the substrate binding site in this enzyme. By reducing the enzyme with [ $^3\text{H}$ ]- $\text{NaBH}_4$  in the presence of pyridoxal-5'-phosphate and NTPs, he found a selective reduction of  $^3\text{H}$  incorporation into the largest (185 kD) subunit (Valenzuela, 1978). These results suggest the presence of a NTP binding site on this polypeptide. It was also noted that a single nucleotide gave much less protection than when three different nucleotides were present at the same total concentration. This suggests that the different nucleotide substrates may bind RNAP at different sites. Unfortunately, these results, in the absence of kinetic data, are difficult to interpret, since when a similar approach was used with E. coli DNA polymerase (DNAP), it was found that pyridoxal-5'-phosphate showed noncompetitive inhibition towards dNTP (Hazra et al., 1984).

The first nucleotide affinity analogue used (Cho and Kimbal, 1982) to study eukaryotic RNAP was the anti-tumor agent 9- $\beta$ -D-arabinofuranosyl-6-mercaptapurine (ara-6-MP), which was used to label wheat germ RNAP II. This analogue has a structural alteration in the pentose portion (trans-diol instead of cis-diol) of the ribonucleosides, which inhibits the growth of cultured mammalian cells by inhibiting DNAP. However, the compound (used without the 6 mercapto group) did not inhibit a crude extract of CT RNAP in vitro or RNA synthesis in vivo (Furth and Cohen, 1967a, b). Furthermore, it was not a substrate for CT DNAP. Nevertheless, the ara-6-MC was found to be a competitive inhibitor with respect to [ $^3\text{H}$ ]-UMP incorporation using purified wheat germ RNAP with

CT DNA template. Wheat germ RNAP II could be covalently labeled, and inactivated, by treating the RNAP ara-6-MC complex with 0.1 mM  $H_2O_2$  in vitro. This chemical inactivation could be partially prevented by DTT or by co-incubation with the natural substrates, suggesting that the ara-6-MC binds the elongation site. Further analysis of the labeled enzyme showed a cysteine residue to be crosslinked, which the authors interpret to be an amino acid in the active site. 1D-SDS-PAGE of the labeled wheat germ RNAP II showed more than 80 % of the label to be in the 140 kD polypeptide.

In a subsequent paper (Cho et al., 1982), these authors use two purine nucleoside dialdehydes (Kimball, 1977) to probe wheat germ RNAP II. Both probes showed noncompetitive inhibition with respect to [ $^3H$ ]-UMP incorporation and inhibition was reversed with purine NTPs, but the effect of pyrimidine NTPs was not studied. By [ $^3H$ ]- $NaBH_4$  reduction of these probes it was shown that they both labeled the 180 kD subunit of wheat germ RNAP through a lysine residue. With regard to the possibility of a cysteine residue in the NTP binding site, Modak and Gillerman-Cox reported that no cysteine residue is present in the ATP binding site of terminal deoxynucleotidyl transferase, which has a catalytic mechanism similar to that of RNAP and DNAP.

#### Genetic approach to identifying eukaryotic RNAP subunits

Ruet et al. (1980) described a mutation ( $rpo B_1$ ) in a yeast gene coding for the 220 kD peptide in RNAP II, which affected the structure and function of the enzyme in vitro. The mutant enzyme was less

efficient in both RNA chain initiation and elongation; its specific activity was 8 to 20-fold lower than that of wild type enzyme. In addition to an altered 220 kD polypeptide, this mutation also changed the properties of the enzyme during purification, namely, both the 16.5 kD and 32 kD peptides were lost during its isolation, yielding an enzyme with reduced catalytic activity. Furthermore, it was noticed that the wild type RNAP II lost the 16.5 and 32 kD polypeptides upon a mild urea treatment, whereupon the enzyme lost 50 % of its activity. Collectively, these results present evidence that the mutation in the large polypeptide plays a role in the association of the two small polypeptides and suggests that the large and at least one of the small polypeptides are essential for activity and may, indeed, be true subunits.

Several investigators have isolated  $\alpha$ -amanitin resistant cell lines (Bryant et al., 1977) or  $\alpha$ -amanitin resistant Drosophila (Greenleaf et al., 1977). However, subsequent analyses by 1D and 2D-SDS-PAGE (Greenleaf, 1979 and Coulter and Greenleaf, 1982) revealed no differences in electrophoretic mobility between the wild type and mutant enzyme. Kinetic analyses showed that although the mutant Drosophila RNAP II had a 259 fold reduced activity for  $\alpha$ -amanitin, it retained its specific activity, and ionic strength and metal requirements. The  $K_M$  values for UTP and GTP from the wild type and mutant enzymes were similar when Mn was used as divalent cation, but upon substitution with Mg, the  $K_M$  of the mutant enzyme differed from that of the wild type RNAP II. Coulter and Greenleaf (1982) mapped the locus for  $\alpha$ -amanitin resistance to the X-chromosome and provided evidence that this locus is a structural gene for an RNAP II subunit, since different mutations

(temperature sensitive, lethal) at that locus affected the enzyme properties. This was confirmed by Ingles et al. (1983) and Greenleaf (1983) who isolated a 7 kb fragment which was found to contain the coding region for the largest subunit (215 kD) of Drosophila RNAP II. This conclusion was based on the use of RNAP II-polypeptide specific antibodies, one of which reacted specifically with a hybrid protein produced by an E. coli expression strain containing the 7 kb fragment. Interestingly, the probe developed from Drosophila cross hybridized with a DNA fragment isolated from a human cell line, which suggests that there is a similarity in the structure of the largest peptide between human and Drosophila RNAP II.

#### The use of antibodies to identify eukaryotic subunits

A number of investigators have used monoclonal antibodies to study the structure of a number of RNAPs. For example, Rose et al. (1983), using monoclonal antibodies against rat hepatoma RNAP I, found that the antibody, which bound to the 190 kD peptide of this enzyme, also inhibited the elongation rate of hepatoma RNAP III but not RNAP II. Furthermore the presence of NTPs prevented inactivation of the enzyme by antibodies. These results suggested that this polypeptide in RNAP I and III is essential for catalytic activity during RNA chain elongation. Young and Davis (1983) isolated the yeast RNAP II genes coding for the two largest subunits by using antibodies against products of a lambda phage recombinant DNA expression library.

### Photoaffinity labeling

Several reviews have been published on the subject of photoaffinity labeling (Baylay and Knowles, 1977, Guillory, 1983, Czarnecki et al., 1979, and Potter and Haley, 1983). Although any chemical affinity labeling approach is inferior to x-ray crystallography in defining the structure of the enzyme because the results obtained vary with the probe used, this method is very useful in cases in which the molecular complexes are either too large to subject to crystallographic calculations, or in which no crystal of the macromolecular complex can be obtained (Plapp, 1983). In addition, affinity labeling may be especially limited when the functional groups used on the probe are restricted to reacting with only a few amino acids whose reactivity may be further reduced by steric hindrance and the micro-environment (Plapp, 1983). For this reason the use of photoaffinity labeling is recommended, as photoprobes do not suffer from selective reactivity. In photoaffinity labeling, a chemically inert but photolabile ligand is converted upon irradiation to a species of very high chemical reactivity. Ideally this takes place only at the ligand binding site on the macromolecule (RNAP), and the compound reacts indiscriminately with whatever group it finds there (Bayley and Knowles, 1977). Due to the short half life of the reactive intermediate, however, the reaction efficiency is comparatively low. The short half life of the reactive intermediate is, however, advantageous in cases in which the affinity of the photoprobe for the enzyme is not in the  $\mu\text{M}$  range, because high concentrations of the probe can be used during incubation with less nonspecific photoaffinity labeling (see Discussion).

Azides ( $\text{RNN}_2$ ) are rapidly converted upon irradiation with UV light (photo excitation) to very reactive nitrenes (electron-deficient monovalent nitrogen species) through fragmentation of the double bond and nitrogen elimination (Turro, 1980). The half life of the reactive intermediates is approximately 100  $\mu\text{seconds}$  (Hanna and Meares, 1981 and Guilory and Jeng, 1983). Nitrenes have two different non-resonant electronic structures, which influences their chemistry. The most competent structures are the electrophilic singlet nitrenes  $\text{R}-\ddot{\text{N}}\uparrow\downarrow$ , or  $\text{R}-\overset{+}{\text{N}}^-$  which contain two paired but antiparallel electron spins and follow "zwitterion chemistry" or "two-electron chemistry", resulting in insertion reactions into single bonds (mostly C-H), cyclo addition to multiple bonds, or addition to nucleophiles. The triplet nitrenes  $\text{R}-\ddot{\text{N}}\uparrow\uparrow$  contain two individual unpaired but parallel electron spins which result in diradical reactions by insertions into single bonds (mostly C-H) after hydrogen abstraction and coupling. Of all these pathways, covalent insertion reactions are most common and result in the formation of secondary amines in a first order reaction. Advantages of azides include their excellent stability in neutral solution in the dark and their low susceptibility to intra-molecular rearrangement after photolysis. Another advantage is that no crosslinking of enzyme molecules or subunits will occur under irradiation conditions used with azido-NTP probes. This makes azides very attractive for use as probes in studying protein structure.

Radical scavengers in the form of thiols are sometimes added to inactivate those UV induced azido-photoprobes that are free in the solution. Thiols reduce free azides rapidly to the corresponding amines



(Staros et al., 1978) and thus lower nonspecific labeling. The scavenging reaction is especially rapid in the presence of DTT at pH 8.5-11.5 (Cartwright et al., 1976). Although water competes with the enzyme for the nitrene radicals, resulting in a low yield, this can be partially offset by the very high specific radioactivity of the linker.

The introduction of  $8N_3$ -ATP/GTP as a photoprobe by Haley and Hoffman (1974) has already aided in elucidating the role of many polypeptides, since it is a good affinity probe, this photoprobe could either serve as a substrate or compete with the natural substrate (Haley, 1983). For example,  $8N_3$ -ATP/GTP serves as a substrate for rabbit skeletal muscle phosphorylase kinase (King et al., 1982), sheep brain tubulin (Gaehlen and Haley, 1979), bacterial  $F_1$ -ATPase (Scheurich et al., 1978), rat liver fructose-6-P<sub>1,2</sub>-kinase (Sakakibara et al., 1984) and rabbit muscle c-AMP dependent protein kinase (Hoppe and Freist, 1979), and acts as a competitive inhibitor in the case of bovine  $F_1$ -ATPase (Holleman et al., 1983), Chlamydomonas dynein ATPase (Pfister et al., 1984), E. coli RNA polymerase (Woody et al., 1984), E. coli DNA polymerase (Abraham and Modak, 1984), and calf thymus terminal deoxynucleotidyltransferase (Abraham et al., 1983). In addition, the ADP analogue,  $8N_3$ -ADP, is a competitive inhibitor of polynucleotide phosphorylase, (Cartwright and Hutchinson, 1980).

Furthermore, it was shown that  $8N_3$ -ATP and its 2',3'-dialdehyde derivative labeled the same polypeptide of rabbit skeletal muscle phosphorylase kinase, when UV light or  $NaBH_4$  reduction was used, respectively (King et al., 1982). Also relevant was the observation by Abraham and Modak (1984) that UV light induced a labeling pattern of

E. coli terminal deoxynucleotidyl transferase that was identical when using either radiolabeled azido ATP or GTP.

Collectively, these results demonstrate that  $8N_3$ -purine NTPs are well designed photoaffinity probes. Furthermore, since they have been used successfully with enzymes of similar catalytic properties as eukaryotic RNAP, e.g., E. coli RNAP and DNAP, and calf thymus terminal deoxynucleotidyl transferase, their use in the system under study here seems most appropriate.

There are several conditions that a photoaffinity label has to meet if the results are to indicate labeling of a true substrate NTP binding site in an enzyme like RNAP II (Woody et al., 1984). For example, the photoaffinity probe should, in the absence of light, be either a competitive inhibitor or a substitute for the natural substrate; the photoprobe should inactivate RNAP II irreversibly and the natural substrates should protect RNAP II against photoinactivation or labeling. Finally, UV light must be absolutely necessary to label the enzyme. If  $8N_3$ -ATP can fulfill those conditions, then it would allow the analysis of a polypeptide(s) that is unequivocally a part of a mammalian RNAP II. The purpose of this section is to provide evidence that these criteria have been satisfied in studies on a NTP binding site of eukaryotic RNAP II, using  $8N_3$ -purine NTP probes. These experiments have characterized the molecular weight and iso-electric point of at least one NTP binding polypeptide from two mammalian RNAP II enzymes. Finally an attempt was made to isolate those peptides that are labeled from the rest of RNAP II.

## Materials and Methods

### Photolysis

Both the radiolabeled and unlabeled photoaffinity compounds were regularly tested by spectrophotometric analysis and TLC to quantify the amount of degradation that occurred (Potter and Haley, 1983). The average useful life (at  $-20^{\circ}\text{C}$ ) of the radiolabeled probes was two weeks. The nonradiolabeled probes were stable for up to a year at  $-20^{\circ}\text{C}$ .

All operations were performed under a red safety light. The indicated amounts of [ $^{32}\text{P}_{\gamma}$ ]- $8\text{N}_3$ -ATP/GTP were added to a 1.5 ml microcentrifuge tube and the solvent methanol removed by a stream of nitrogen. The photolabeling occurred in a solution with a volume of 30-100  $\mu\text{l}$ , containing RNAP II, 50 mM Tris-HCl (7.9), 4 mM  $\text{MnCl}_2$  or  $\text{MgCl}_2$ , and the indicated amounts of ammonium sulfate and DTT in a concentration range of 5-120 mM and 0-0.3 mM, respectively.

Preincubation time was 5 minutes at room temperature in total darkness. The conditions for the crosslinking reaction were exposure of the preincubated mixture at  $4^{\circ}\text{C}$  for 20 minutes to short or long UV light from a distance of 2 cm from the filter surface to the microcentrifuge tube. Tubes were rotated every 5 minutes to ensure equal sample exposure to UV light. The UV light source (multiband UV mineral light, Type UVSL-25, UV-Products, Inc.) when set on the long wave (366nm) mode produced UV light energetically equivalent to  $3.5\text{-}4.5\text{ mWatt/cm}^2$ , or  $35,000\text{-}45,000\text{ ergs/second cm}^2$ , when measured with a Blak-Ray long wave UV intensity meter (Type J-221, UV-Products, Inc. with a peak sensitivity of 365 nm). The same UV source when set on the short wave mode produced

approximately  $0.63 \text{ mWatt/cm}^2$ , equivalent to  $6,300 \text{ ergs/second cm}^2$  (Woody et al., 1984). The photoaffinity labeling reaction was terminated by the addition of concentrated DTT and SDS to a final concentration of 25 mM and 1 %, respectively.

The labeled photoaffinity nucleotides were obtained from the Chemical & Radioisotope Division of ICN. The specific activities of [ $^{32}\text{P}_\gamma$ ]- $8\text{N}_3$ -ATP, [ $^{32}\text{P}_\gamma$ ]- $8\text{N}_3$ -GTP, and [ $^{32}\text{P}$ ]-cAMP were 18.8-81 Ci/mmole, 13-34 Ci/mmole, and 8 Ci/mmole, respectively. When indicated in the text, the labeled isotopes were diluted with unlabeled compounds. The  $8\text{N}_3$ -ATP and  $8\text{N}_3$ -GTP were gifts from Dr B.E. Haley and Dr. A. Kemp, respectively.

Analysis of the photoaffinity labeled RNAP II enzyme took place by 1D or 2D-IEF-SDS-PAGE (see the Materials and Methods section in Chapter Four), followed by drying and autoradiography. In general, photoproducts derived from a UV irradiated mixture containing 6 pmoles of RNAP II and 1  $\mu\text{Ci}$  [ $^{32}\text{P}_\gamma$ ]- $8\text{N}_3$ -ATP or [ $^{32}\text{P}_\gamma$ ]- $8\text{N}_3$ -GTP became visible on x-ray film (Cronex 4, Dupont) within one day of exposure.

In those experiments in which the photolabeling was to be performed in the absence of DTT, 1 ml of RNAP II was chromatographed at  $4^\circ\text{C}$  over a PD-10 column (1.2 cm diameter x 5.5 cm) filled with Sephadex G-50 (Pharmacia) equilibrated with 50 mM Tris-HCl, pH 7.9, 25 % glycerol, 5 mM  $\text{MnCl}_2$ , 100 mM ammonium sulfate, and 0.1 mM EDTA. The peak containing RNAP II activity appeared at an elution volume of 4-5 ml.

## Results

### Photolysis kinetics of $8N_3$ -ATP/GTP

The absorption spectrum of  $8N_3$ -ATP has a specific maximal absorbance at 281 nm (Potter and Haley, 1983), which upon photolysis, i.e., UV light-induced nitrogen elimination resulting in nitrene formation, decreases by approximately 30 %. The molar extinction coefficient of  $8N_3$ -ATP is  $13,300 \text{ cm}^{-1} \text{ M}^{-1}$  at 281 nm. In addition to a decrease in absorption at 281 nm, a spectral shift occurs upon photolysis to 274 nm. Thus, an absorption spectrum with a maximum optical density (O.D.) measured at 281 nm is an indication that the azido group is intact and this O.D. 281 nm can be used to determine the photoprobe concentration. The upper scan in Figure 25, shows the absorption spectrum from 230-330 nm. The absorbance was measured in 1 ml quartz cuvettes in a Varian Cary 210 spectrophotometer. The reference cuvette contained the sample buffer.

The half life of  $8N_3$ -ATP during photolysis is an indication of the rate of formation of the nitrene, which is the reactive species that can crosslink to amino acid residues in RNAP II. To calculate the half life of  $8N_3$ -ATP, a solution was exposed to the UV light source under the conditions described in Materials and Methods, and the rate of decrease of the O.D. 281 nm measured as a function of irradiation time. Figure 25 shows the absorption spectra of  $8N_3$ -ATP after exposure to UV light with the source in the long wave mode (peak output at 366 nm) as a function of irradiation time. After 40 minutes no further decrease of O.D. 281 nm could be observed, indicating completion of photolysis. The percent photolysis was calculated from the relative decrease of the O.D.

at 281 nm and plotted as a function of time (Figure 26). Longwave irradiation was more efficient than the short wave irradiation, because the time required to obtain 50 % conversion at room temperature was 6 minutes when the long wave mode was selected, and 18 minutes when the short wave mode was used. This difference in reaction rate is due to the lower energy output of the UV source at 254 nm and not because  $8N_3$ -ATP absorbs more at 366 nm than at 254 nm.

The photolysis of  $8N_3$ -GTP was also studied, using a similar experimental design. Upon photolysis the  $8N_3$ -GTP (molar extinction coefficient is  $12,000 \text{ cm}^{-1} \text{ M}^{-1}$  at 278 nm) shows a decrease in O.D. at 278 nm and a spectral shift as described previously. The rates of photolysis at 366 and 254 nm are shown in Figure 27. The half lives at room temperature were 5 and 18 minutes with 366 and 254 nm, respectively. Both Figures show that the rate of nitrene formation under the conditions used is approximately three fold higher with the UV light in the long wave mode. A control reaction, with  $8N_3$ -ATP or  $8N_3$ -GTP exposed to a red safety light for several hours at 4°C, did not show any photolysis. Furthermore, the UV light in the spectrophotometer did not photolyze the azido probe during the time it took to scan the solution.

The results shown in Figures 25, 26, and 27 were obtained using water as solvent. Substitution by 95 % methanol or a buffer containing 50 mM Tris-HCl, pH 7.9, 5 mM  $MnCl_2$ , 200 mM ammonium sulfate and 50  $\mu\text{g}$  BSA/ml, did not change the results significantly. The time needed for complete photolysis of the azido-photoprobes by long wave UV light of a 65  $\mu\text{M}$  solution was 40 minutes but, due to self-absorption increased to approximately 60 and 120 minutes when concentrations of 0.6 and 2.2 mM photo-probes were used, respectively.

Substitution of ATP by Azido-ATP in a CT RNAP II activity assay

An experiment was performed to test whether or not ATP could be replaced by  $8N_3$ -ATP in the standard RNAP II activity assay with  $[^3H]$ -UTP (Materials and Methods in Chapter Two). If positive, this would indicate not only specific binding of the photoprobe to the RNAP II, but also incorporation of  $8N_3$ -AMP into RNA. An incubation was performed with 0.6 mM  $8N_3$ -ATP instead of 0.6 mM ATP. The reaction took place in the presence of a red safety light. The overall transcription reaction rate was only 2 % of that of the standard control reaction done in the presence of 0.6 mM ATP. However, when both ATP and  $8N_3$ -ATP were omitted from the reaction, the transcription rate was also approximately 2 % of the control reaction. When the experiment was repeated with prephotolyzed  $8N_3$ -ATP, the resulting activity was equally low. Apparently,  $8N_3$ -ATP was not a substrate that could be incorporated into nascent RNA by CT RNAP II.

The possibility that  $8N_3$ -ATP was an inhibitor was investigated using the standard transcription assay in the absence of light to prevent photoinactivation. Identical standard transcription reaction mixtures, each containing 6 pmoles of CT RNAP II, were titrated with increasing amounts of  $8N_3$ -ATP to a final concentration as indicated in Figure 28 and the enzyme activity plotted as shown. The experiment was repeated using 1.2  $\mu Ci$   $[^3H]$ -ATP diluted to a final concentration of 0.1 mM, instead of  $[^3H]$ -UTP, see Figure 28. The inhibition observed in the absence of UV light was not irreversible. In presence of 0.6 mM ATP, a 0.6 mM concentration of  $8N_3$ -ATP inhibited the  $[^3H]$ -UMP

incorporation rate by 40 %, but only by 20 % when the reaction was repeated in presence of 1.2 mM ATP and 0.6 mM  $8N_3$ -ATP. Prephotolyzed  $8N_3$ -ATP did not inhibit the CT RNAP II activity as much as intact  $8N_3$ -ATP, see Figure 28.

#### Mode of inhibition by Azido-ATP

Since the results of Figure 28 show that  $8N_3$ -ATP is an inhibitor of the transcription reaction by CT RNAP II with respect to [ $^3H$ ]-AMP and [ $^3H$ ]-UMP incorporation into RNA, it is important to determine whether the inhibition was competitive or non-competitive, which indicates the type of interaction between RNAP II and azido-ATP. There are several problems associated with the transcription reaction conditions if one wishes to study inhibition kinetics by a substrate analogue. These problems were detailed in the Materials and Methods section in Chapter Two and will be reviewed only briefly here. First the enzyme requires four different substrates in a sequence determined by a heterogeneous template like CT DNA and not by the individual substrate concentrations present during the assay. The overall rate of incorporation, as determined by measuring the incorporation of, for example [ $^3H$ ]-AMP, is composed of two separate events that occur during the transcription assay; initiation and elongation are known to occur at different velocities. For example, initiation is the rate-limiting step because of the time needed to form a ternary complex composed of RNAP II, template, and two nucleotides, and to form the first phosphodiester bond. Furthermore, once the RNAP has dissociated from the template, reinitiation can take place, causing another lag in the transcription rate. To facilitate the



study of inhibition kinetics here, several experimental modifications were made in an attempt to measure the reaction velocity only during the elongation phase of the transcription reaction. Instead of CT DNA, a synthetic poly d(T) template was used, simplifying the kinetics to a single substrate assay. A preformed ternary complex composed of polyd(T), CT RNAP II and ApA, was used to start the reaction. Dinucleotides like ApA are efficient initiators of transcription reactions (see Chapter Two) and are used often for kinetic studies and are not incorporated during elongation (DeRiemer and Meares, 1981a, b, Yarbrough, 1982, Wilkinson and Sollner-Webb, 1982, and Samuels et al., 1984). Finally, the assay mixture incubation time was limited to seventy-five seconds instead of the usual ten minutes, because this limits reinitiation as well as substrate depletion. When all reactants were warmed to 37°C prior to mixing, no initial lag in enzyme velocity occurred. The results of experiments using these modifications are shown in Figure 29. The apparent  $K_M$  for ATP was 0.77 mM with a turnover number of 2.9 mole AMP incorporated per enzyme molecule per second, assuming all enzymes present in the assay participated simultaneously. The  $K_i$  of  $8N_3$ -ATP was  $400 \pm 40$   $\mu$ M. The pattern shown in the Lineweaver-Burk plot shows intersection of the lines on the ordinate, indicating competitive inhibition.

The effect of the presence of ApA in the ternary complex was studied by repeating the experiment in the absence of ApA and  $8N_3$ -ATP. The results (Figure 30) show an apparent  $K_M$  of 3.57 mM and a turnover number of 3.8 mole AMP incorporated per enzyme molecule per second.

Irreversible light-induced inactivation of CT RNAP II by azido-ATP

If  $8N_3$ -ATP binds to a domain of CT RNAP II that is part of a NTP binding site, the  $8N_3$ -ATP should, after crosslinking to amino acid residues in the NTP binding site(s), inactivate the enzyme irreversibly. CT RNAP II was mixed with increasing concentrations of  $8N_3$ -ATP in a standard reaction mixture containing 60 mM ammonium sulfate and 0.1 mM DTT and exposed to UV light (366 nm) for 90 minutes. This extended exposure was necessary due to self absorption by  $8N_3$ -ATP at the concentrations used. The activity of CT RNAP II after UV irradiation was assayed immediately and corrected for two types of inhibition not caused by irreversible photoinactivation. The first inhibition resulted from exposure of the enzyme to UV light and amounted to a loss of 10 % of the enzyme activity under the conditions used. The remaining 90 % activity was arbitrarily set at 100 % activity for comparison. The second noncovalent inhibition was caused by the presence of photolyzed  $8N_3$ -ATP during the enzyme activity assay after UV irradiation, see control in Figure 31. The data showing irreversible photoinactivation were obtained by subtracting the percent enzyme inhibition obtained with prephotolyzed  $8N_3$ -ATP from the percent inhibition determined using intact  $8N_3$ -ATP. The resulting values were plotted as a function of the  $8N_3$ -ATP concentration with respect to  $[^3H]$ -UMP and  $[^3H]$ -AMP incorporation and are shown in Figures 31 and 32, respectively. The photoinactivation by  $8N_3$ -ATP was irreversible, because addition of ATP to the 0.6 mM ATP already present in the activity assay did not increase the activity of the enzyme. Additional control experiments were performed by preincubating CT RNAP II with ATP and GTP at the concentrations indicated for

$8N_3$ -ATP, followed by UV irradiation, but no inhibition of enzyme activity was observed. When prephotolyzed  $8N_3$ -ATP was used, no photoinactivation occurred.

#### Protection of CT RNAP II by NTPs against photoinactivation

True photoaffinity labeling requires that the probe interacts with the natural substrate binding site, which in the case of RNAP II is the NTP binding site. Previous experiments (Figures 31 and 32) indicated that CT RNAP II could be irreversibly photoinactivated by  $8N_3$ -ATP and that its mode of inhibition is competitive with respect to ATP binding during the elongation phase of transcription. Therefore, photoinactivation by  $8N_3$ ATP should be partially preventable by co-incubation of RNAP II with the natural substrates.

In the design of the experimental assay, several complications had to be addressed. For example, added NTPs will absorb UV light, thus decreasing the number of photons available for absorption by the photoprobe. This in turn would decrease the rate of photoinactivation merely by lowering the rate of nitrene formation. As a control then, adenosine was added to a final concentration, calculated to result in an identical absorbance as that present in solutions containing 3 mM of NTP. The calculations were based on the molar extinction coefficients at 260 nm, which are for ATP, GTP, UTP, CTP, and  $8N_3$ -ATP; 15,400; 11,700; 7,500; 9,900, and 7,100  $\text{cm}^{-1} \text{M}^{-1}$ , respectively. It was established that no photoinactivation of CT RNAP II was caused by UV irradiation of a mixture containing CT RNAP II and 1.5 mM adenosine. Furthermore, the effect of the added adenosine during standard transcription assays

(Chapter Two) was determined and shown in Figure 33. The inhibition was minor, e.g., at 1 mM adenosine, only a 10 % loss of activity occurred. In addition to the added adenosine, another factor that had to be corrected was the presence of photolyzed  $8N_3$ -ATP, which was shown to inhibit CT RNAP II activity, see Figure 28.

The design of the "photoinactivation protection" experiment is based on three independent assays, yielding three values representing CT RNAP II activity when measured under three different conditions. Reaction "A" is the control value, because it represents total CT RNAP II activity when measured with the standard transcription assay as described in Chapter Two, i.e., using denatured CT DNA as template and either undiluted  $[^3H]$ -UTP or  $[^3H]$ -ATP (diluted with ATP to a final concentration of 0.1 mM ATP). The final concentrations of the other NTPs were 1.2 mM. Reaction "B" is the amount of enzyme activity left after photoinactivation, and reaction "C" is the amount of enzyme activity remaining under the conditions of "B", but in the presence of one of the natural substrates, i.e., ATP, GTP, CTP, or UTP. The percentage protection ("% P") is calculated from the three parameters, A, B, and C, using the following equation:

$$\% P = 100 \times \{(C-B)/(A-B)\}.$$

For example, when "A" equals "C", the percentage protection is 100 %, whereas it is 0 % when "C" equals "B". The experimental conditions to derive the value for "A" were as follows: CT RNAP II was incubated with prephotolyzed  $8N_3$ -ATP, adenosine, and  $MnCl_2$  for 5 minutes at room temperature, exposed to UV light at 4°C and the reaction mixture

completed to measure enzyme activity under standard conditions. To measure "B", CT RNAP II was incubated with adenosine,  $8N_3$ -ATP, and  $MnCl_2$  for 5 minutes at room temperature and exposed to UV light at  $4^\circ C$  and the reaction mixture completed to measure remaining enzyme activity under standard conditions. "C" was determined by mixing CT RNAP II with  $8N_3$ -ATP,  $MnCl_2$ , and one NTP, i.e., either ATP, GTP, UTP, or CTP. The reaction mixture was incubated for 5 minutes at room temperature, exposed to UV light at  $4^\circ C$  and the reaction mixture completed (including the addition of adenosine) to measure the partial recovery of enzyme activity under the standard conditions.

The initial concentration of  $8N_3$ -ATP was 0.55 mM and the NTP concentration 3 mM during preincubation and UV irradiation. After incubation of reaction mixtures "A", "B", and "C" (in the dark) in a total volume of 20  $\mu l$ , the mixture was irradiated with UV light for 40 minutes. Additional assay components were added including denatured CT DNA and either 0.6  $\mu Ci$  [ $^3H$ ]-ATP or 0.6  $\mu Ci$  [ $^3H$ ]-UTP in the final reaction volume of 50  $\mu l$ . After additions were made to complete the reaction mixtures (50  $\mu l$ ), the final concentration of the NTP was 1.2 mM. Because of this concentration, neither could UTP be tested as a protective agent in case of the [ $^3H$ ]-UMP incorporation assay nor could ATP be tested in the [ $^3H$ ]-AMP incorporation assays, due to excessive isotope dilution. The typical values obtained for reaction "A" were 110,000 cpm or 23,000 cpm above background (200 cpm), when measured in the [ $^3H$ ]-UMP or [ $^3H$ ]-AMP incorporation assay, respectively.

The amount of protection provided by the presence of the four NTPs, used individually, was calculated after correction for self-absorbance by adenosine addition and after correction for inhibition by the addition of prephotolyzed  $8N_3$ -ATP in the control reactions.

NTP :	ATP	GTP	CTP	UTP	substrate
%P :	45 $\pm$ 10	41 $\pm$ 9	12 $\pm$ 5	-	[ $^3H$ ]-UTP
%P :	-	25 $\pm$ 9	5 $\pm$ 3	9 $\pm$ 3	[ $^3H$ ]-ATP

#### Photoaffinity labeling of RNAP II and subunit analysis

UV irradiation of a reaction mixture containing CT RNAP II and [ $^{32}P_\gamma$ ]- $8N_3$ -ATP or [ $^{32}P_\gamma$ ]- $8N_3$ -GTP and  $MnCl_2$  induced covalent crosslinking of the radioactive  $8N_3$ -ATP or  $8N_3$ -GTP into RNAP II, whereas no incorporation of label occurred in the absence of UV irradiation (Figure 34). The experiments when repeated with PL RNAP II yielded similar results, see Figure 35. Specific labeling of peptide E occurred, and this pattern did not change after preincubation of the RNAPs before UV irradiation with 4  $\mu$ g of various templates (denatured or native CT DNA, polyd(T), and polyd(C) or with 10 ng  $\alpha$ -amanitin/ml. The information derived from 1D-SDS-PAGE analysis was equivalent to the data obtained from 2D-IEF-SDS-PAGE (Figures 36 and 37), but in addition the latter showed a small shift of 0.2 pH units in the pI of the polypeptide E in the acidic direction after crosslinking of the photoprobes. Comparison of the silver stain pattern (before and after photoaffinity labeling) and autoradiography revealed that after radiolabeling a small amount of new silver stainable material (protein) appeared up to 0.2 pH

units away from the main body of silver stained protein with a pI of 5.4. This new spot contained most of the radiolabel (Figure 37, panel C). No photolabeling of the largest polypeptides was observed after 2D-IEF-SDS-PAGE, which might be due to prolonged exposure of the gamma  $^{32}\text{P}$  of the label on the two basic polypeptides B and C to the alkaline environment present during electrophoresis in the first dimension. This complication does not apply to analysis of the polypeptide E, because it is slightly acidic (Discussion section of Chapter Four).

No photoaffinity labeling occurred when either the RNAPs were inactivated by heat denaturation (80°C for 5 minutes) or the photoprobes were prephotolyzed with UV light.

The photoaffinity labeling occurred more efficiently when either  $\text{MgCl}_2$  or  $\text{MnCl}_2$  was present during the preincubation (Figure 38). No difference was observed between Mn and Mg with respect to their role in enzyme photolabeling (Figure 39).

The photoaffinity labeling experiments described thus far were done in the presence of the quencher DTT (with the exception of the 2D-IEF-SDS-PAGE) at a concentration of 0.3 mM. To determine the effect of this thiol on the specific radiolabel incorporation pattern seen by 1D-SDS-PAGE analysis, the experiment described in the legend of Figure 34 (panel A, lane 1) was repeated in the absence of DTT. The two largest polypeptides present in CT RNAP II (B and C) were now labeled in addition to polypeptide E, but the latter remained the principal target of the photolabeling. When the experiment was repeated with PL RNAP II, no labeling of any peptide except E was observed.

#### Optimization of conditions for crosslinking of probes to RNAP II

The efficiency of crosslinking of [ $^{32}\text{P}_\gamma$ ]- $8\text{N}_3$ -ATP and [ $^{32}\text{P}_\gamma$ ]- $8\text{N}_3$ -GTP to RNAP II was determined as a function of increasing time of UV irradiation. A time course of irradiation versus the extent of crosslinking of [ $^{32}\text{P}_\gamma$ ]- $8\text{N}_3$ -ATP and [ $^{32}\text{P}_\gamma$ ]- $8\text{N}_3$ -GTP to CT RNAP II and PL RNAP II is shown in Figures 40 and 41, respectively. Also shown are the autoradiographs from which the data were derived. The maximal amount of radioactivity incorporated at 30 minutes was typically 3 to 4.5 kcpm. The efficiency of counting [ $^{32}\text{P}_\gamma$ ]- $8\text{N}_3$ -ATP and [ $^{32}\text{P}_\gamma$ ]- $8\text{N}_3$ -GTP in Aquasol (New England Nuclear) was 90 %.

#### Stoichiometric analysis of photo affinity labeling

The extent of covalent attachment of the photoprobes [ $^{32}\text{P}_\gamma$ ]- $8\text{N}_3$ -ATP and [ $^{32}\text{P}_\gamma$ ]- $8\text{N}_3$ -GTP to CT RNAP II and PL RNAP II were measured using different amounts of the photoprobes to determine at which concentration saturation of labeling occurs. The standard reaction mixtures contained the RNAP II and photoaffinity label which was diluted by adding unlabeled photoprobe to a final concentration as indicated in the Figures. The mixtures were preincubated and UV irradiated (30 minutes). The extent of crosslinking was determined as described in the legend of Figure 40. The number of pmoles of photoprobe molecules bound per pmole of RNAP II was plotted as a function of total photoprobe concentration. The stoichiometry of the [ $^{32}\text{P}_\gamma$ ]- $8\text{N}_3$ -ATP and [ $^{32}\text{P}_\gamma$ ]- $8\text{N}_3$ -GTP incorporation to CT RNAP II is shown in Figures 42 and 43, respectively. The stoichiometry of [ $^{32}\text{P}_\gamma$ ]- $8\text{N}_3$ -ATP and [ $^{32}\text{P}_\gamma$ ]- $8\text{N}_3$ -GTP incorporation to PL RNAP II is shown in Figures 44 and 45, respectively.



Protection against photoaffinity labeling by the natural substrate

If the labeling of RNAP II by photoprobes is specific with respect to binding in a domain of the enzyme that is part of the substrate binding site, then one would expect the natural substrate to protect the enzyme from photoaffinity labeling. The amount of crosslinking of the enzyme from photoaffinity labeling. The amount of crosslinking of the labeled photoprobe onto RNAP II was determined as described in Figure 40, in presence of different concentrations of one of the NTPs during preincubation and UV irradiation. The results were plotted as a function of concentration and are shown in Figures 46 and 47 for CT RNAP II incubated with [ $^{32}\text{P}_\gamma$ ]-8N<sub>3</sub>-ATP and [ $^{32}\text{P}_\gamma$ ]-8N<sub>3</sub>-GTP, respectively, and in Figures 48 and 49 for PL RNAP II incubated with [ $^{32}\text{P}_\gamma$ ]-8N<sub>3</sub>-ATP and [ $^{32}\text{P}_\gamma$ ]-8N<sub>3</sub>-GTP, respectively. The purine NTPs offer better protection than the pyrimidine NTPs. UV light absorption by the addition of natural substrates is not responsible for the protection, since the addition of adenosine to CT RNAP II and [ $^{32}\text{P}_\gamma$ ]-8N<sub>3</sub>-ATP as shown in Figure 33 hardly affects incorporation of the photoprobe under the conditions used. Also included in these Figures is the effect of the addition of nonradioactive photoprobe (8N<sub>3</sub>-ATP and 8N<sub>3</sub>-GTP) on the amount of crosslinked label.

With respect to quantification of the the amount of crosslinked material, the radioactivity present in the excised protein bands was compared to the radioactivity crosslinked to RNAP II in the absence of any other NTP or unlabeled photoprobe and was arbitrarily set at 100 % labeling efficiency. The average optimal incorporation found was 3000-4500 cpm.

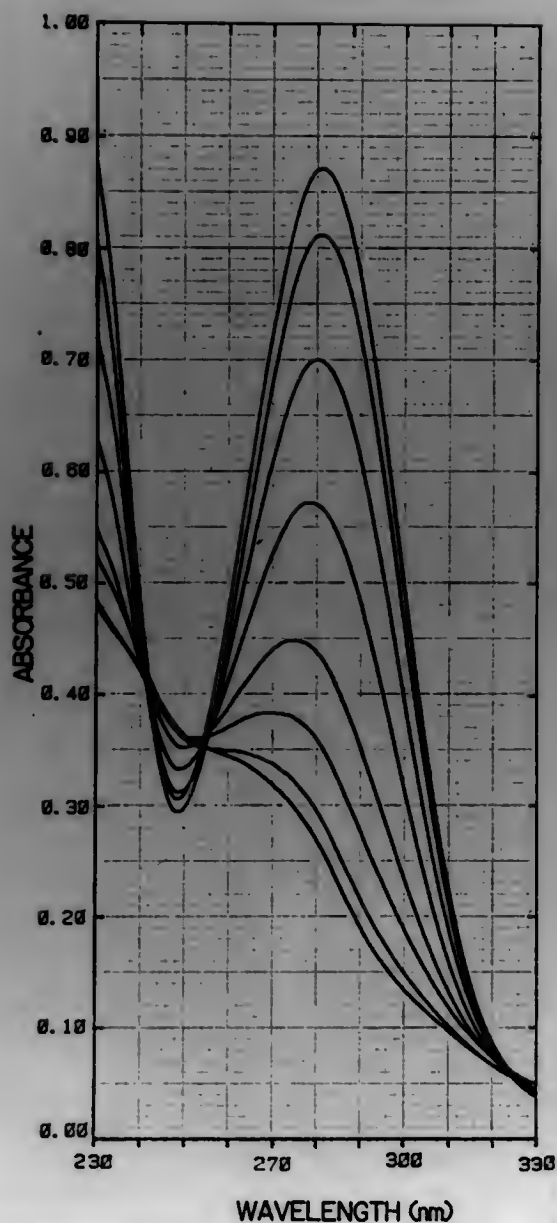


Figure 25. Absorption spectra of 8N<sub>3</sub>-ATP before and after UV irradiation.

A mixture of 65  $\mu$ M azido-ATP in 100  $\mu$ l water was exposed to UV light as described in Materials and Methods. After 0, 1, 2.5, 5, 9, 15, 25, and 40 minutes, the absorbance spectrum was determined using a Varian Cary 210 spectrophotometer. Upon increasing photolysis, the absorbance at 281 nm decreases and the peak shifts as shown.

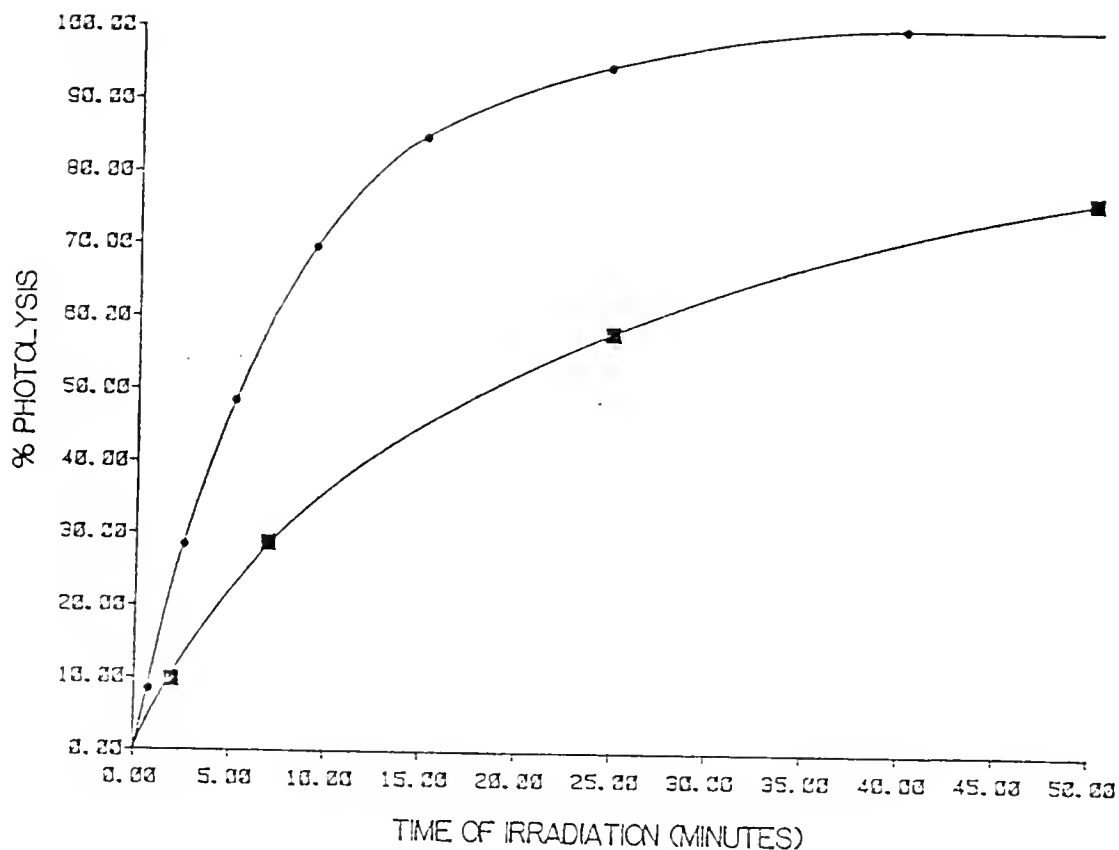


Figure 26. Rate of photolysis of  $8N_3$ -ATP as a function of the time of UV irradiation.

The data obtained in Figure 25 were used to calculate the rate of photolysis. The relative decrease of the absorbance at 281 nm was converted to % photolysis and plotted as a function of irradiation time with the UV light source, used with either the peak output at 366 nm (●) or 254 nm (■).

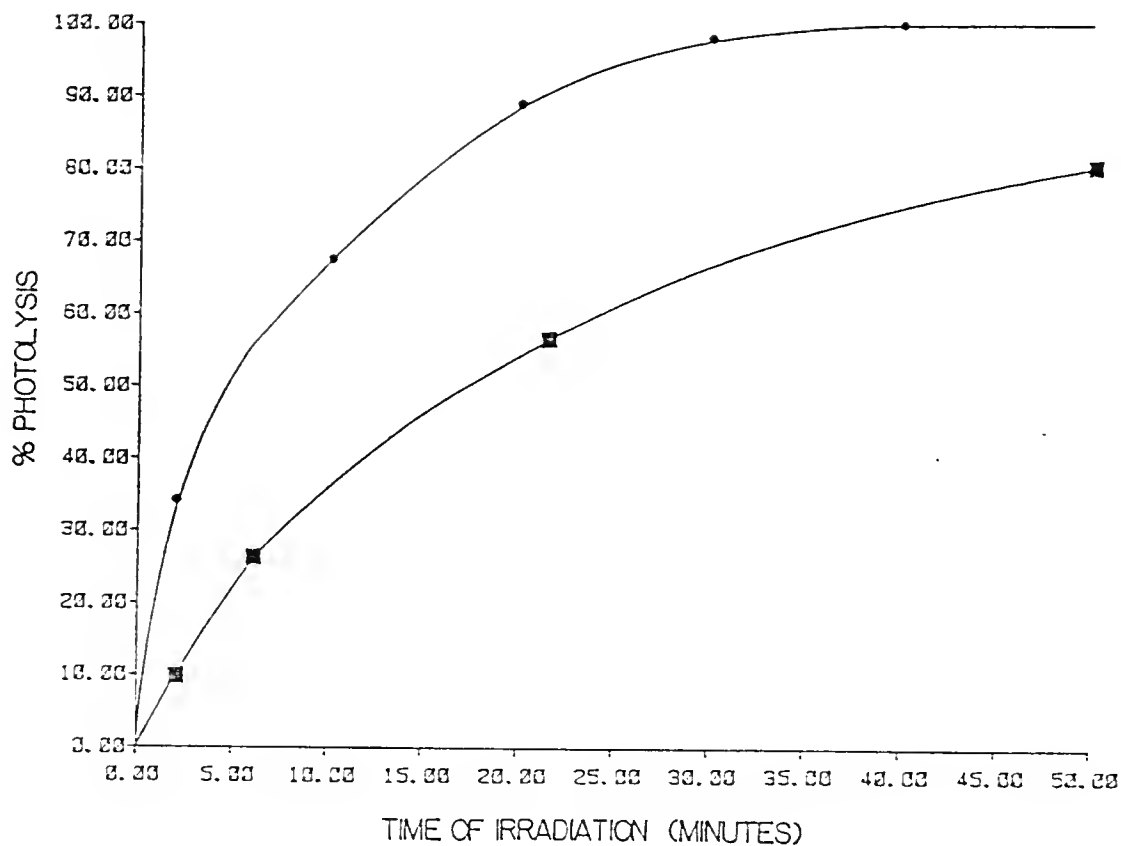


Figure 27. Rate of photolysis of  $8N_3$ -GTP as a function of UV irradiation time.

The experimental design was as described for Figure 26 and the relative decrease of the absorbance at 278 nm was converted to % photolysis and plotted as a function of irradiation time with the UV light source, used with either the peak output at 366 nm (●) or 254 nm (■).

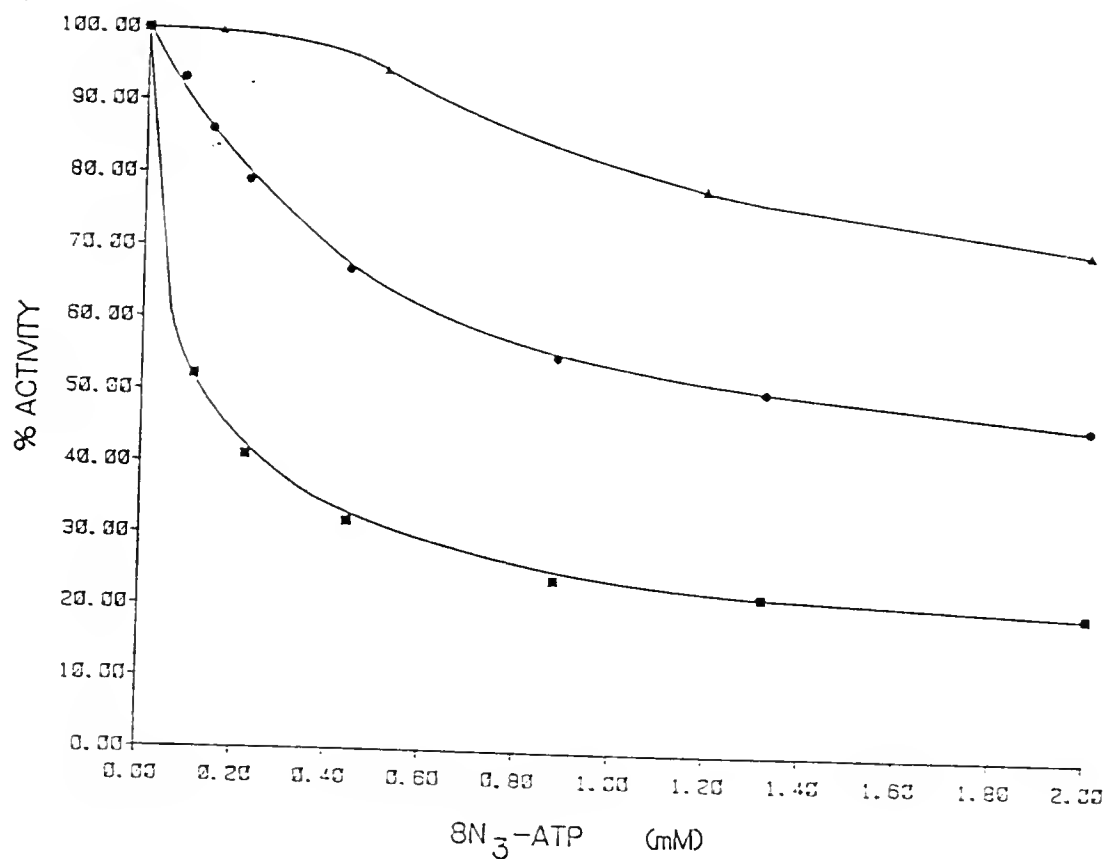


Figure 28. Non-covalent inhibition of CT RNAP II activity by 8N<sub>3</sub>-ATP.

Standard transcription assays, each containing 6 pmole of CT RNAP II, were titrated with increasing concentrations of azido-ATP and the enzyme activity was measured in presence of 1.2  $\mu$ Ci tritiated UTP (—●—) or 1.2  $\mu$ Ci tritiated ATP (diluted to 0.1 mM with ATP) per reaction (—■—), described in the Materials and Methods section of Chapter Two. The effect of addition of prephotolyzed azido-ATP was also measured with respect to tritiated AMP incorporation (—▲—) and its concentration is indicated on the abscissa.

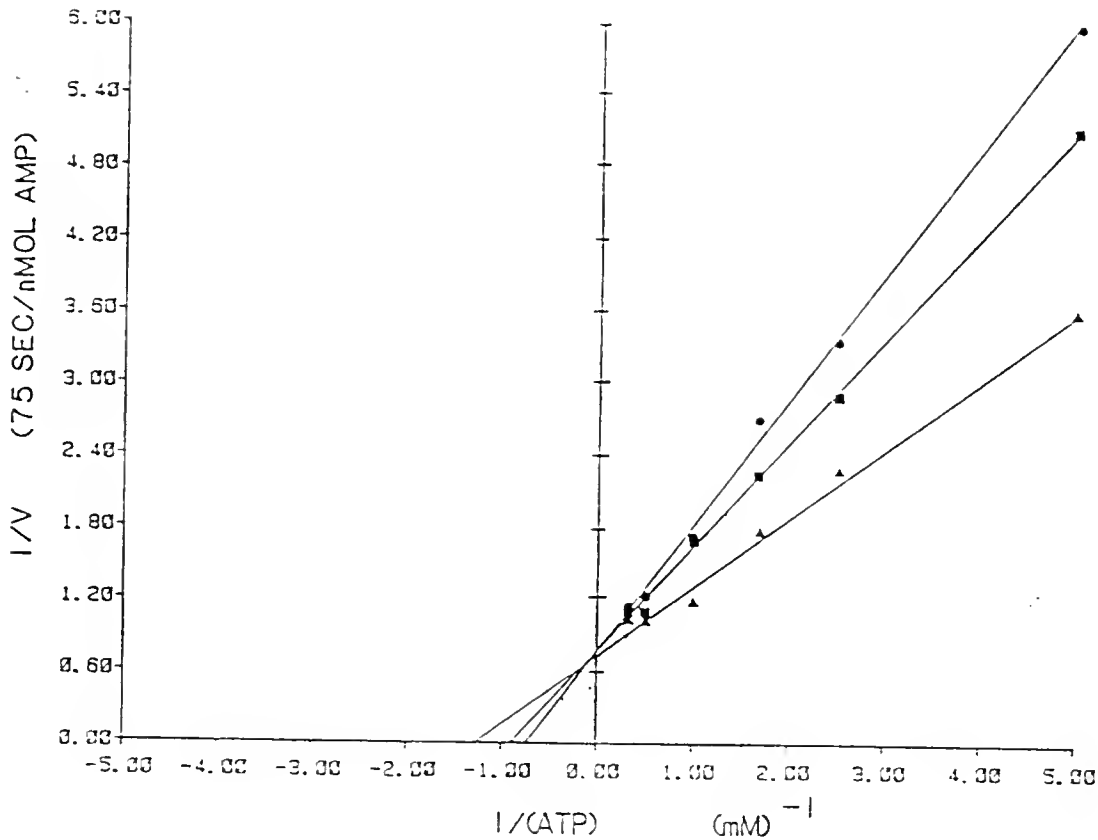


Figure 29. Inhibition of RNA synthesis by  $8\text{N}_3\text{-ATP}$  in the absence of UV light.

Shown are three double reciprocal plots of initial velocity versus ATP concentration. Solution I contained 6 pmole CT RNAP II, 2  $\mu\text{g}$  poly d(T) (13-20 pmoles, based on a MW of 100-150 kD), and 0.55 mM ApA in 27  $\mu\text{l}$ . Solution II (23  $\mu\text{l}$ ) contained ammonium sulfate, manganese chloride, Tris-HCl, pH 7.9, 1  $\mu\text{Ci}$  tritiated ATP, ATP and azido-ATP. Solutions I and II were incubated at 37°C for 6 and 3 minutes, respectively, and mixed (50  $\mu\text{l}$ ). The final concentrations of Tris-HCl, ammonium sulfate, manganese chloride, CT RNAP II, ApA, and poly d(T) were 50 mM, 100mM, 2 mM, 0.12  $\mu\text{M}$ , 0.3 mM, and 0.3  $\mu\text{M}$ , respectively. The ATP concentrations used are indicated in the figure. The final concentrations of the inhibitor azido-ATP were 0 mM (▲), 0.15 mM (■), and 0.3 mM (●). The reactions were terminated after seventy-five seconds by the addition of 40  $\mu\text{l}$  of 20 mM EDTA and 5 % TCA. The amount of tritiated AMP incorporated into product RNA was determined as described in the Materials and Methods section in Chapter Two.

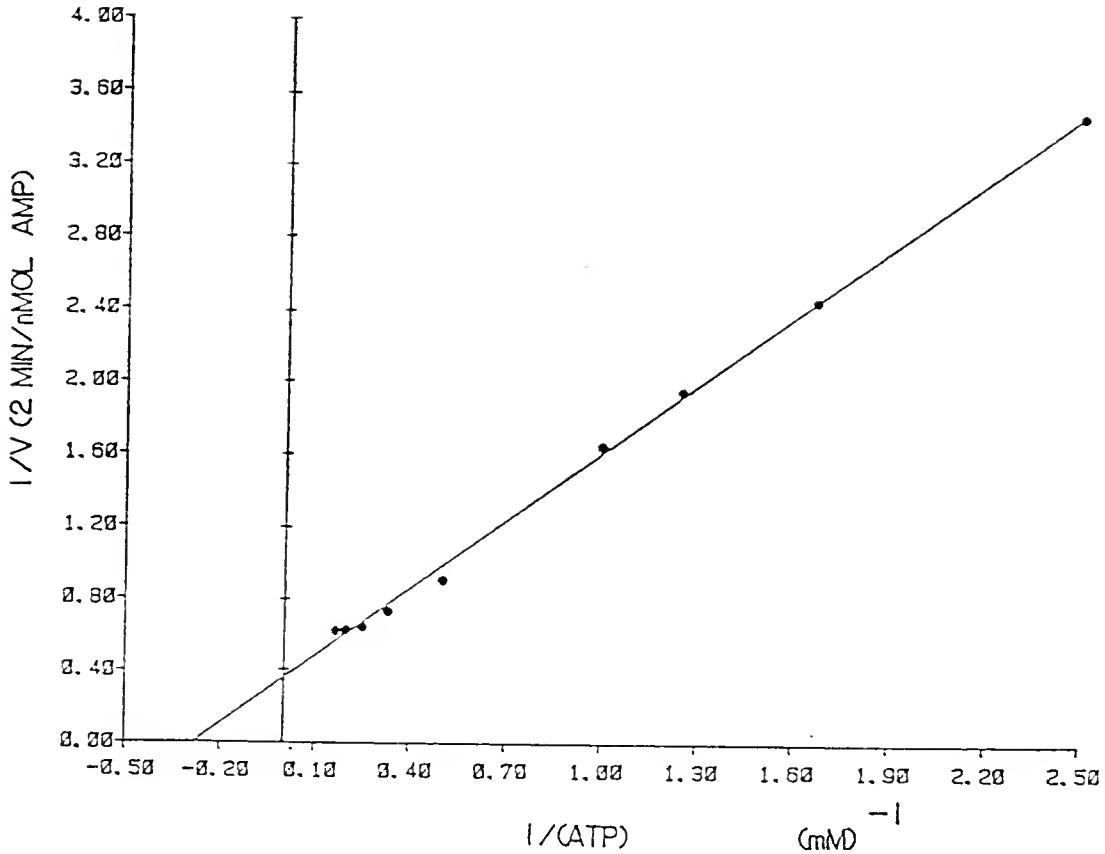


Figure 30. Double reciprocal plot of the velocity versus ATP concentration.

The standard reaction mixture (100  $\mu$ l) contained 1  $\mu$ Ci of tri-  
tiated ATP diluted with ATP as indicated. To start the reaction, a  
preincubated mixture (37°C for 6 minutes) of 6 pmoles CT RNAP II and  
4  $\mu$ g of polyd(T) were added. The reaction continued for two minutes,  
and the rate was determined as described in the legend of Figure 29.

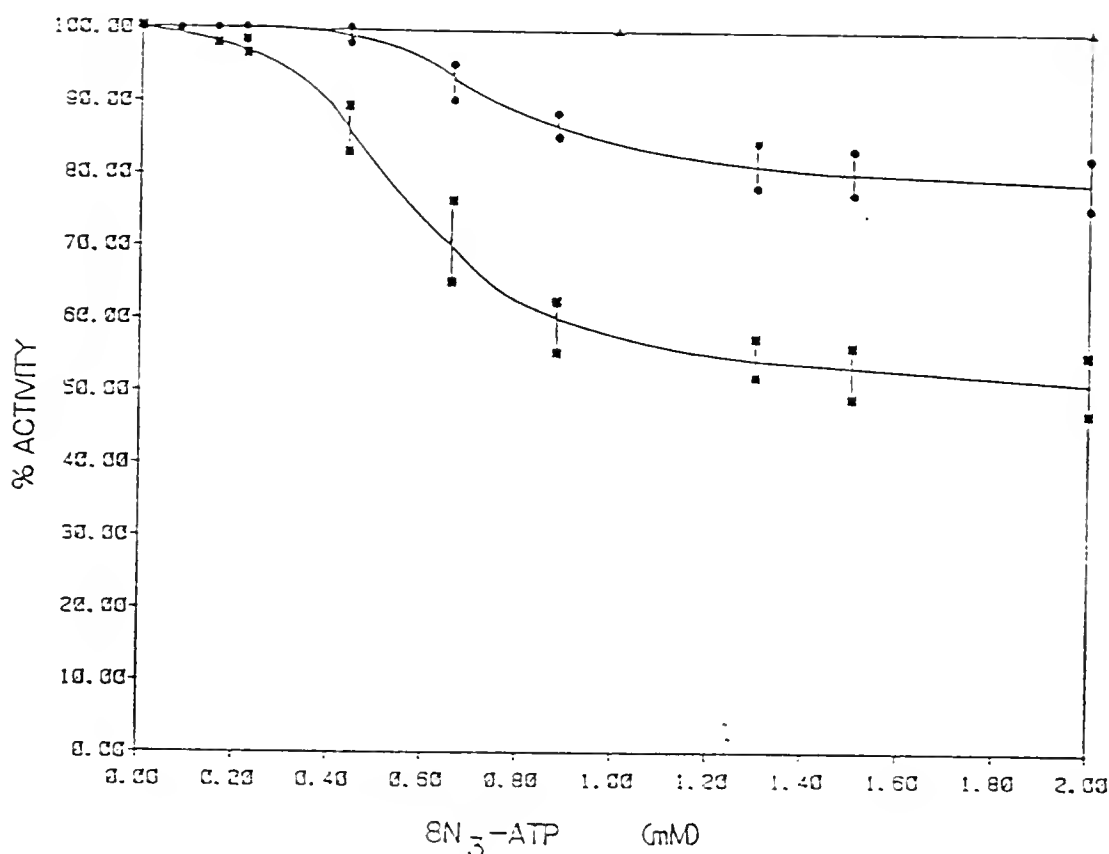


Figure 31. Photoinactivation of CT RNAP II by  $8N_3$ -ATP measured with respect to UMP incorporation.

Azido-ATP was added to standard reaction mixtures, containing 3 pmoles of CT RNAP II and 4 mM manganese chloride, to the final concentrations within the preincubation mixture as indicated. After preincubation, the reaction mixtures were exposed to UV light (366 nm) for 90 minutes at 4°C. The activity of the enzyme was assayed immediately, using undiluted tritiated UTP as described in the Materials and Methods section of Chapter Two. After ten minutes at 37°C, the reaction was terminated. The experiment was repeated using prephotolyzed azido-ATP as a control. The percentage inhibition obtained from the control experiment were subtracted from the inhibitions measured by using intact azido-ATP, and the resulting enzyme activities expressed as percent activity relative to RNAP II that had been exposed to UV irradiation in absence of azido-ATP. Shown are the plots indicating enzyme activity remaining after incubation and UV irradiation of CT RNAP II with prephotolyzed azido-ATP (—●—) and the results obtained with intact azido-ATP, after correction for inhibition by the prephotolyzed azido probe (—■—). As another control, the experiment described above was repeated by preincubating and UV irradiating CT RNAP II with ATP at final concentrations as indicated (—▲—) on the abscissa.



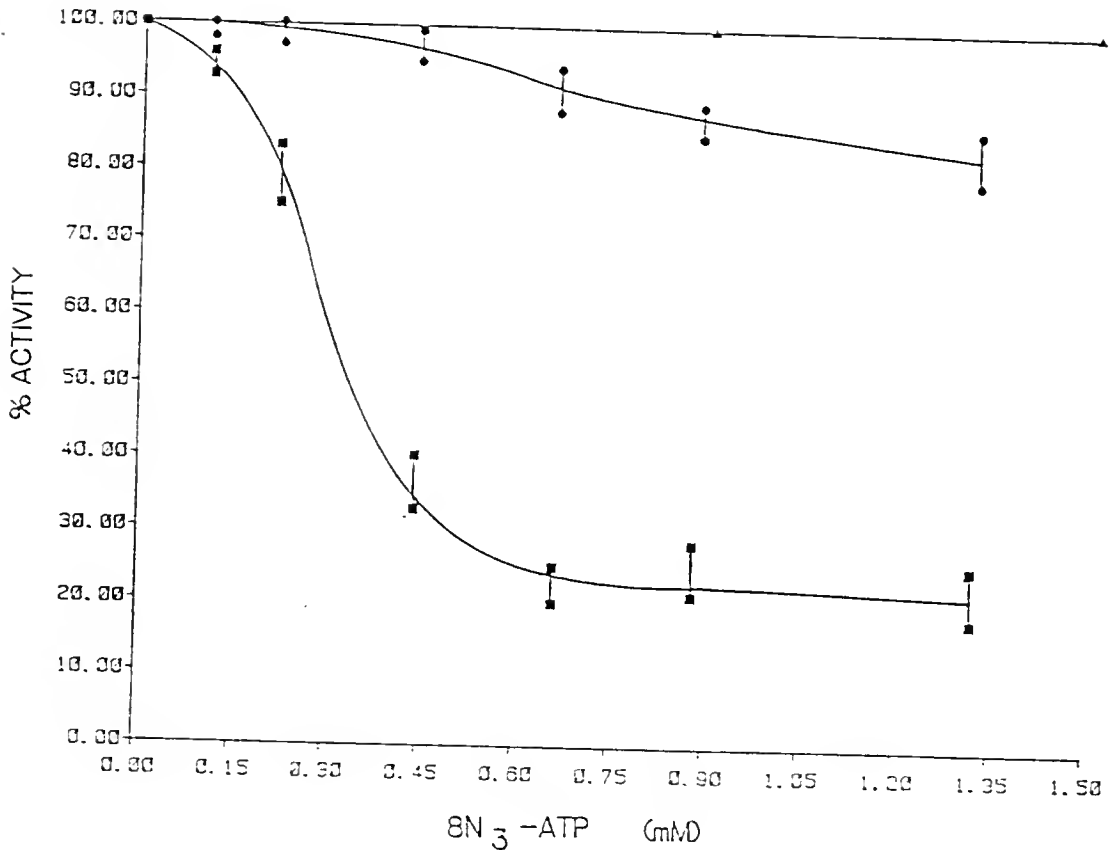


Figure 32. Photoinactivation of CT RNAP II by 8N<sub>3</sub>-ATP, with respect to AMP incorporation.

The assay was performed as described in the legend of Figure 31, with the exception that tritiated AMP instead of tritiated UMP was used. The 1.2  $\mu$ Ci of labeled ATP was diluted to a final concentration of 0.1 mM. Shown are the plots indicating enzyme activity remaining after incubation and UV irradiation of CT RNAP II with prephotolyzed azido-ATP (—●—) and intact azido-ATP, after correction for inhibition by the prephotolyzed azido probe (—■—). As another control, the experiment described above was repeated by preincubating and UV irradiating CT RNAP II with GTP instead of ATP, since the last compound would dilute the labeled ATP too much at the concentrations used (—▲—) as indicated on the abscissa.

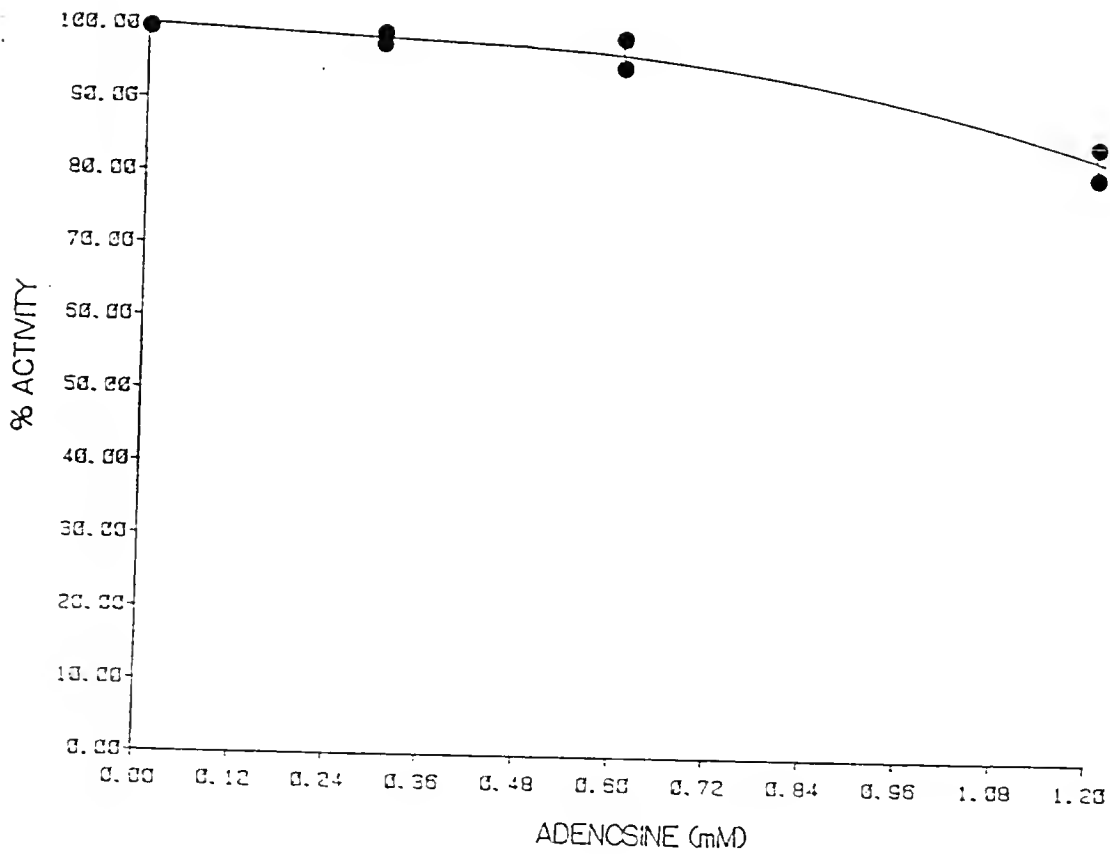


Figure 33. Inhibition of CT RNAP II activity by adenosine.

The standard reaction mixture contained 6 pmole CT RNAP II and 1.2  $\mu$ Ci tritiated UTP and the indicated final concentrations of adenosine. The assay was performed twice, as described in the Materials and Methods section of Chapter Two.

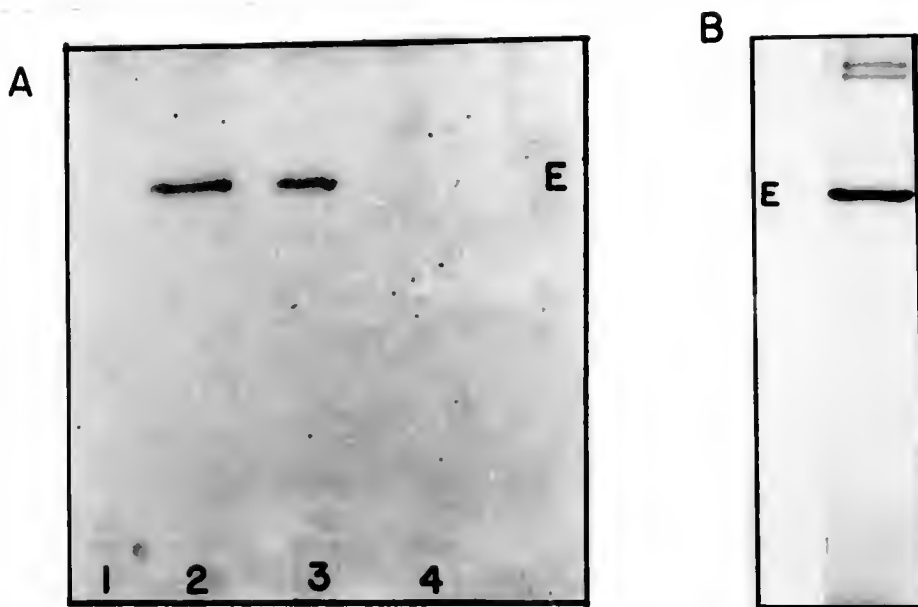


Figure 34. Photoaffinity labeling of CT RNAP with radiolabeled azido-ATP or with radiolabeled azido-GTP.

Shown is an autoradiograph of a dried 1D-SDS-PAGE gel of RNAP II enzyme. Panel A. Lane 1: 7 pmole CT RNAP II were incubated with 2  $\mu$ Ci radiolabeled azido-ATP and 4 mM manganese chloride and incubated in the dark for 30 minutes at 22°C. Lane 2: as lane one, but irradiated with long wave UV light for 15 minutes at 4°C. Lane 3: as lane two, but with radiolabeled azido-GTP. Lane 4: as lane one, but with radiolabeled azidoGTP. All mixtures contained 0.3 mM DTT. Panel B: Autoradiogram of CT RNAP II labeled with radiolabeled azido-ATP in the presence 4 mM manganese chloride, but in the absence of DTT.

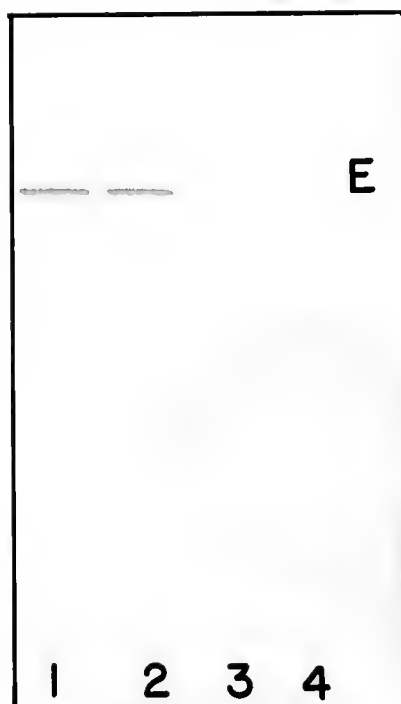


Figure 35. Photoaffinity labeling of PL RNAP with radiolabeled azido-ATP or with radiolabeled azido-GTP.

Shown is an autoradiograph of a dried 1D-SDS-PAGE gel of RNAP II enzymes. Lane 1: 3 pmole PL RNAP II were incubated with 1  $\mu$ Ci radiolabeled azido-ATP and 4 mM manganese chloride and irradiated with long wave UV light for 15 minutes at 4°C. Lane 2: as lane one, but in the presence of radiolabeled azido-GTP. Lane 3: as lane one, but incubated for 30 minutes at 22°C in the absence of UV light. Lane 4: as lane three, but with radiolabeled azido-GTP. All mixtures contained 0.3 mM DTT.

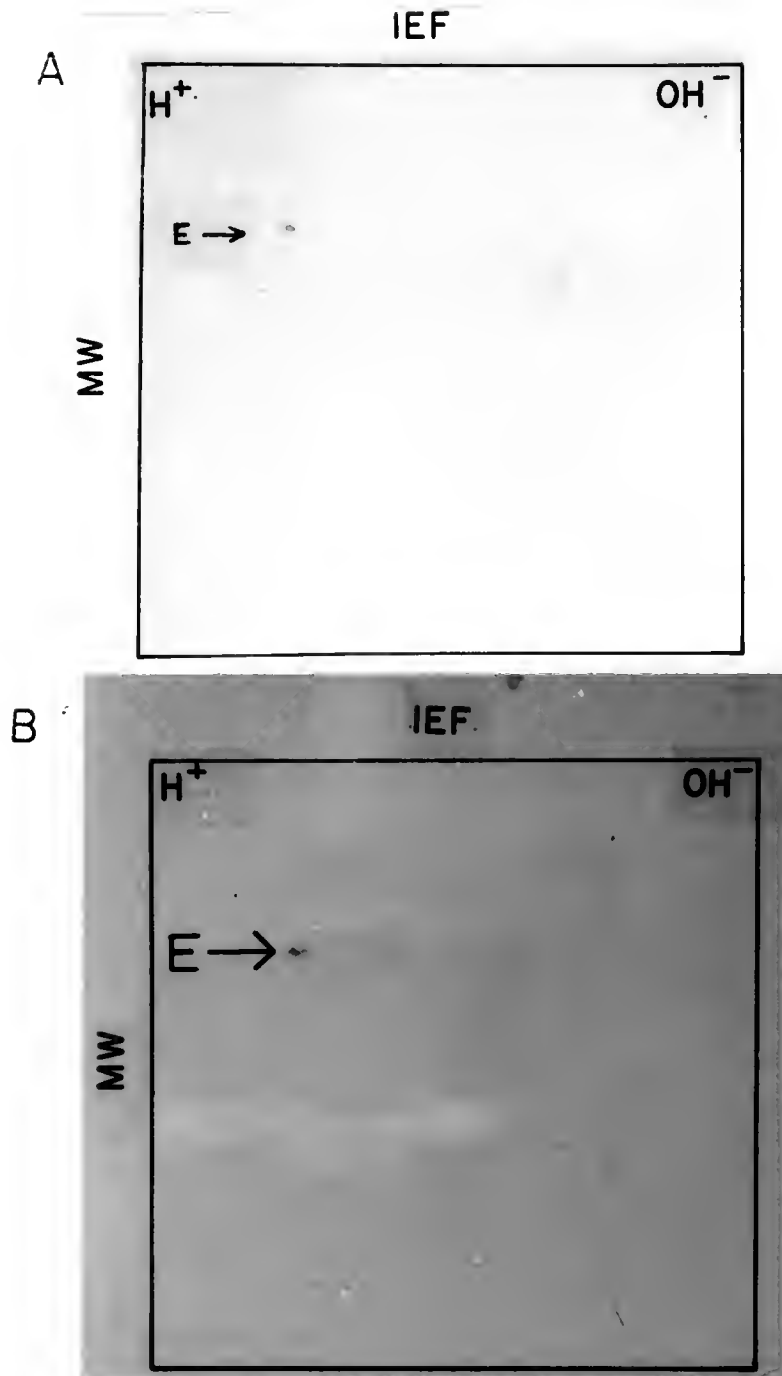


Figure 36. Analysis of polypeptides from CT RNAP II, modified by photoaffinity labeling.

Panel A. CT RNAP II (10  $\mu$ g, DTT free) was incubated with 1  $\mu$ Ci radiolabeled azido-ATP and 4 mM manganese chloride and UV (long wave) irradiated for 30 minutes at 4°C, followed by 2D-IEF-SDS-PAGE and autoradiography.

Panel B. CT RNAP II (10  $\mu$ g, DTT free) was incubated with 3  $\mu$ Ci radiolabeled azido-GTP and 4 mM manganese chloride and analyzed as described in panel A.

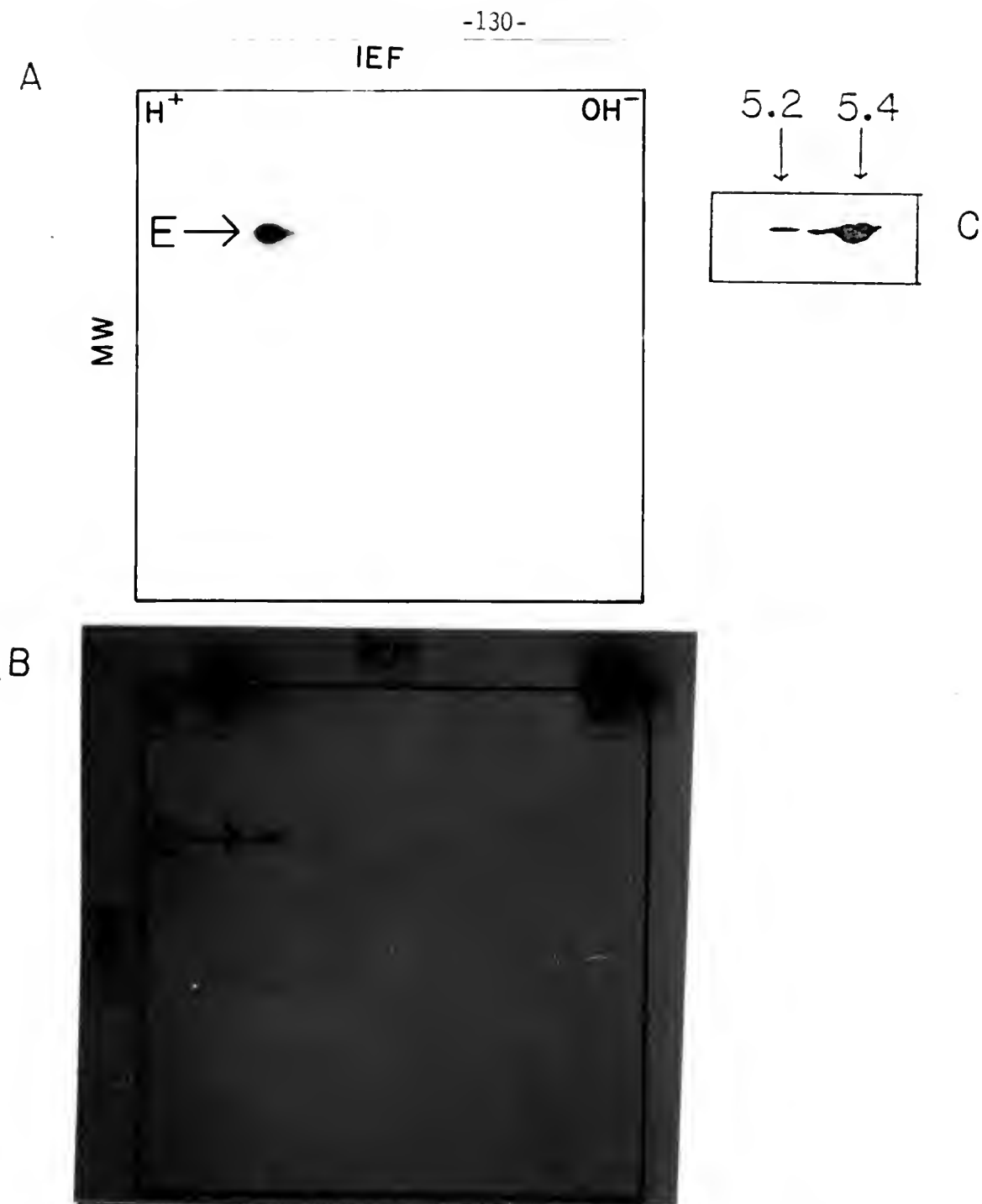


Figure 37. Analysis of polypeptides from PL RNAP II, modified by photoaffinity labeling.

Panel A: PL RNAP II (17  $\mu$ g, DTT free) was incubated with 5  $\mu$ Ci radiolabeled azido-GTP and 4 mM manganese chloride and UV (long wave) irradiated for 30 minutes at 4°C, followed by 2D-IEF-SDS-PAGE and autoradiography. Panel B: PL RNAP II (10  $\mu$ g, DTT free) was incubated with 1  $\mu$ Ci radiolabeled azido-ATP and 4 mM manganese chloride and analyzed as described in panel A. Panel C: Close-up of silver stained polypeptide E after the insertion of the photoprobe azido-ATP (Panel A).

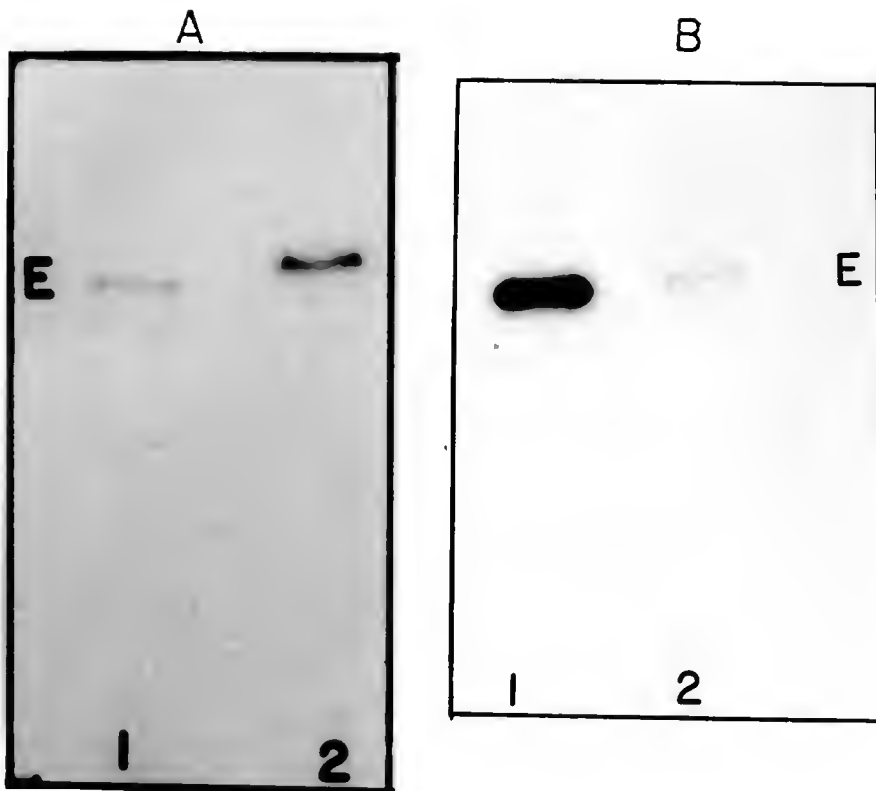


Figure 38. Photoaffinity labeling of CT RNAP II and PL RNAP II.

Shown are autoradiographs of RNAP II labeled in the absence or presence of divalent cations in the incubation mixture. Panel A, lane 1: 4 pmole CT RNAP II were incubated with 0.8  $\mu$ Ci radiolabeled azido-ATP in the absence of manganese chloride and irradiated with long wave UV light as described in the Materials and Methods section. Lane 2: As lane 1, but with the incubation in the presence of 4 mM manganese chloride. Panel B, lane 1: 7 pmole of PL RNAP II were incubated with 2  $\mu$ Ci radiolabeled azido-ATP in the presence of 4 mM manganese chloride and irradiated with long wave UV light as described for panel A. Lane 2: as lane 1, but in the absence of manganese chloride.



Figure 39. Photoaffinity labeling of CT RNAP II.

The autoradiograph compares the amount of photoaffinity labeling of CT RNAP II by radiolabeled azido-GTP in the absence or presence of two different metal ions. Lane 1: Six pmole of CT RNAP II were incubated with 1  $\mu$ Ci of radiolabeled azido-GTP in the presence of 4 mM manganese chloride and irradiated with long wave UV light as described in Figure 38. Lane 2: as lane 1, but with 4 mM magnesium chloride. Lane 3: as lane 1, but in the absence of metal ions. Lane 4: as lane 1, but in the presence of 8 mM EDTA.



Figure 40. Time course of photoaffinity labeling of CT RNAP II by radiolabeled  $8N_3$ -ATP and  $8N_3$ -GTP.

A standard reaction mixture of 50  $\mu$ l included 10 pmoles CT RNAP II (free of DTT), 1  $\mu$ Ci azido photoprobe, and 4 mM manganese chloride. After preincubation as described in the Materials and Methods section, the identical reaction mixtures were exposed to UV light (366 nm) for the indicated amount of time. After termination of the reaction, the samples were analyzed by 1D-SDS-PAGE and stained as described in Chapter Four. After autoradiography, the appropriate bands were excised and the amount of crosslinked radiolabeled azido-ATP or azido-GTP was determined by liquid scintillation counting in 10 ml Aquasol (New England Nuclear). The amount of labeling obtained during different time intervals is expressed as the percent of optimal labeling achieved by irradiation for 30 minutes. Both the autoradiographs and radiolabel incorporation time plots are shown for CT RNAP with radiolabeled azido-ATP (—●—) and azido-GTP (—■—). The numbers under each band indicate the time of UV irradiation in minutes.

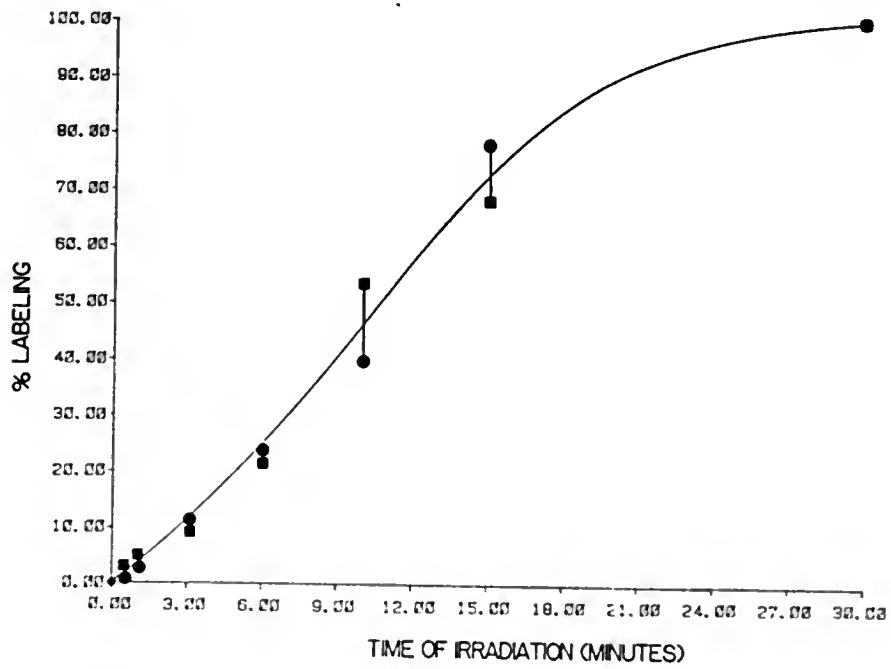
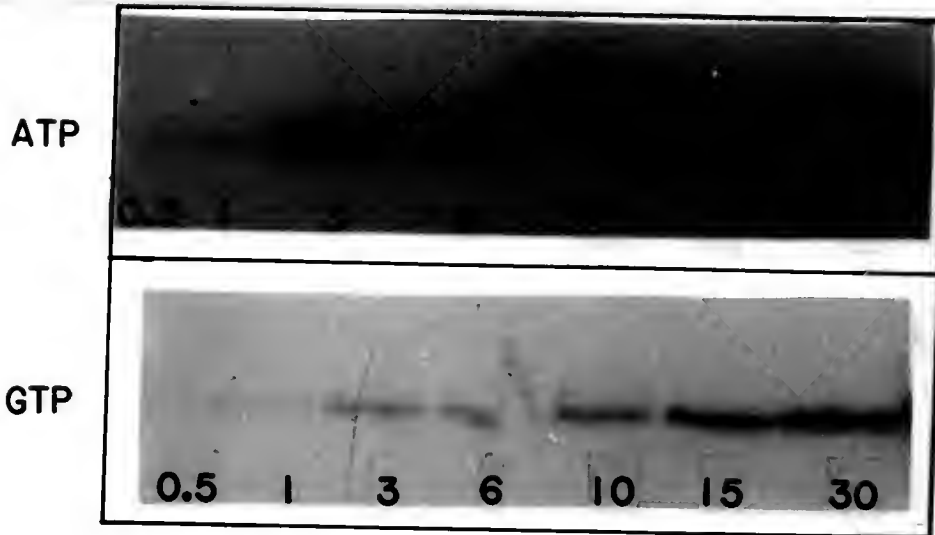
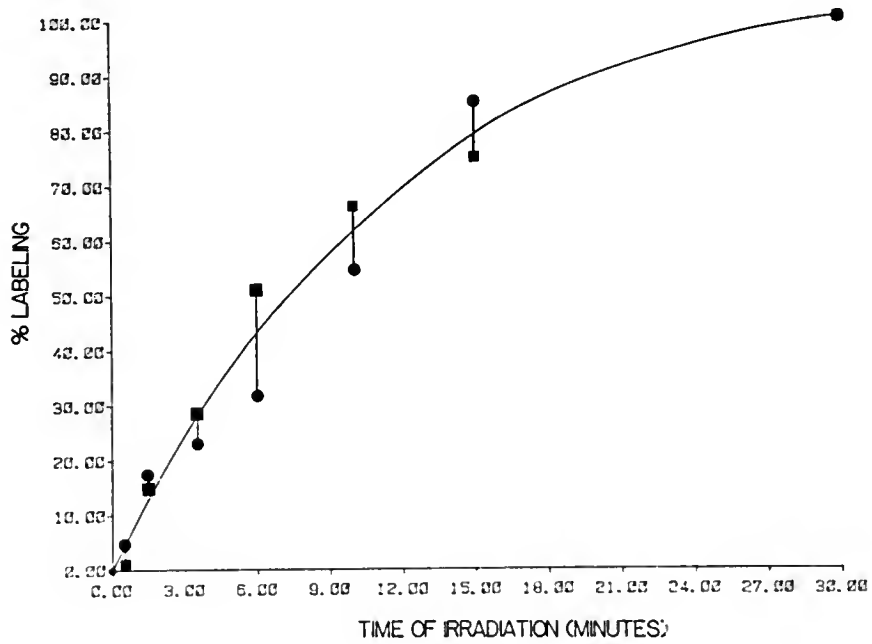
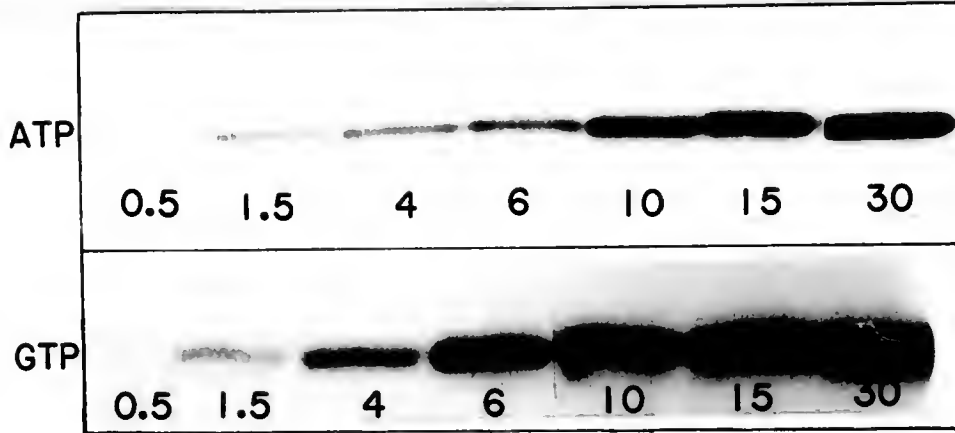


Figure 41. Time course of photoaffinity labeling of PL RNAP II by radiolabeled  $8N_3$ -ATP and  $8N_3$ -GTP.

A standard reaction mixture of 50  $\mu$ l included 20 pmoles PL RNAP II (free of DTT), 2  $\mu$ Ci azido photoprobe, and 4 mM manganese chloride. The experimental design was as described in the legend of Figure 40. Both the autoradiographs and radiolabel incorporation time plots are shown for PL RNAP with radiolabeled azido-ATP (—●—) and azido-GTP (—■—). The numbers under each band indicate the time of UV irradiation in minutes.



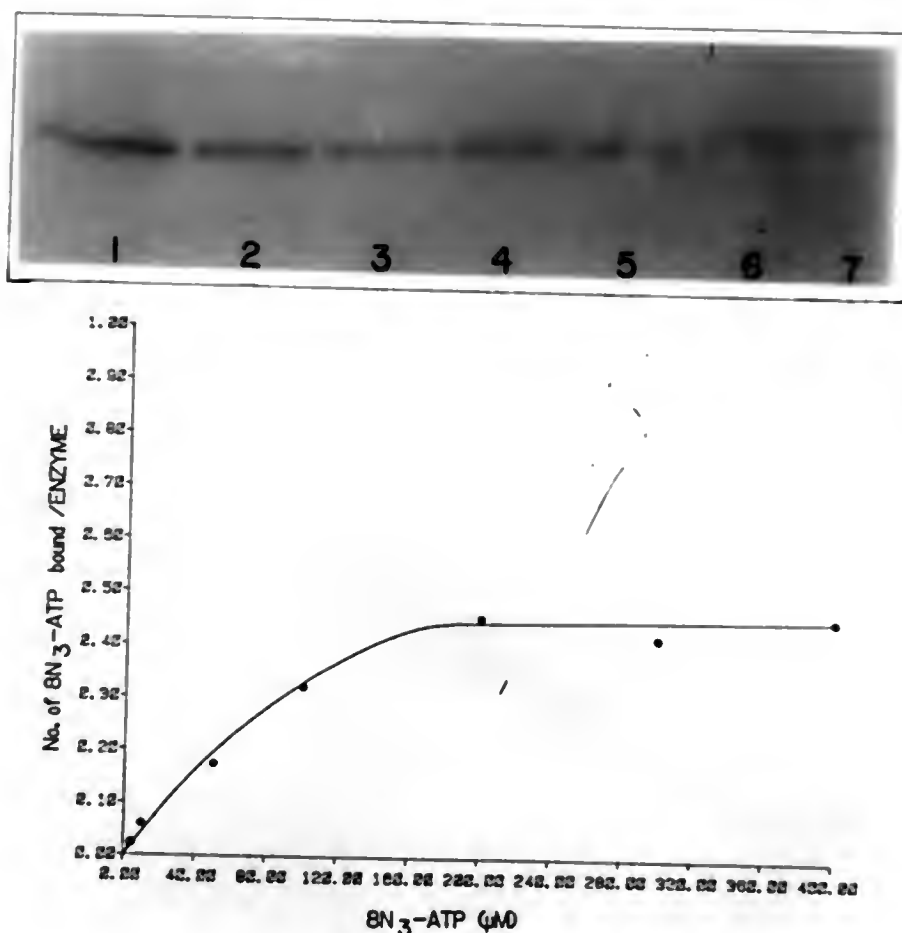


Figure 42. Number of radiolabeled azido-ATP molecules bound per CT RNAP II versus the azido-ATP concentration.

The standard reaction mixture contained 10 pmole CT RNAP II (free of DTT) and 1  $\mu$ Ci of radiolabeled azido-ATP, which was diluted by addition of unlabeled azido-ATP to final concentrations as indicated. After preincubation and exposure to UV light (366 nm) for 30 minutes, the samples were analyzed by 1D-SDS-PAGE, stained and autoradiographed as described in the legend of Figure 40. The amount of crosslinked radiolabeled azido-ATP was quantified by excising the appropriate bands, followed by liquid scintillation counting. The number of photoprobe molecules covalently crosslinked per molecule of CT RNAP II was plotted as a function of the photoprobe concentration. The number under each band in the autoradiograph indicates the increasing concentration of the photoprobe as shown on the abscissa.

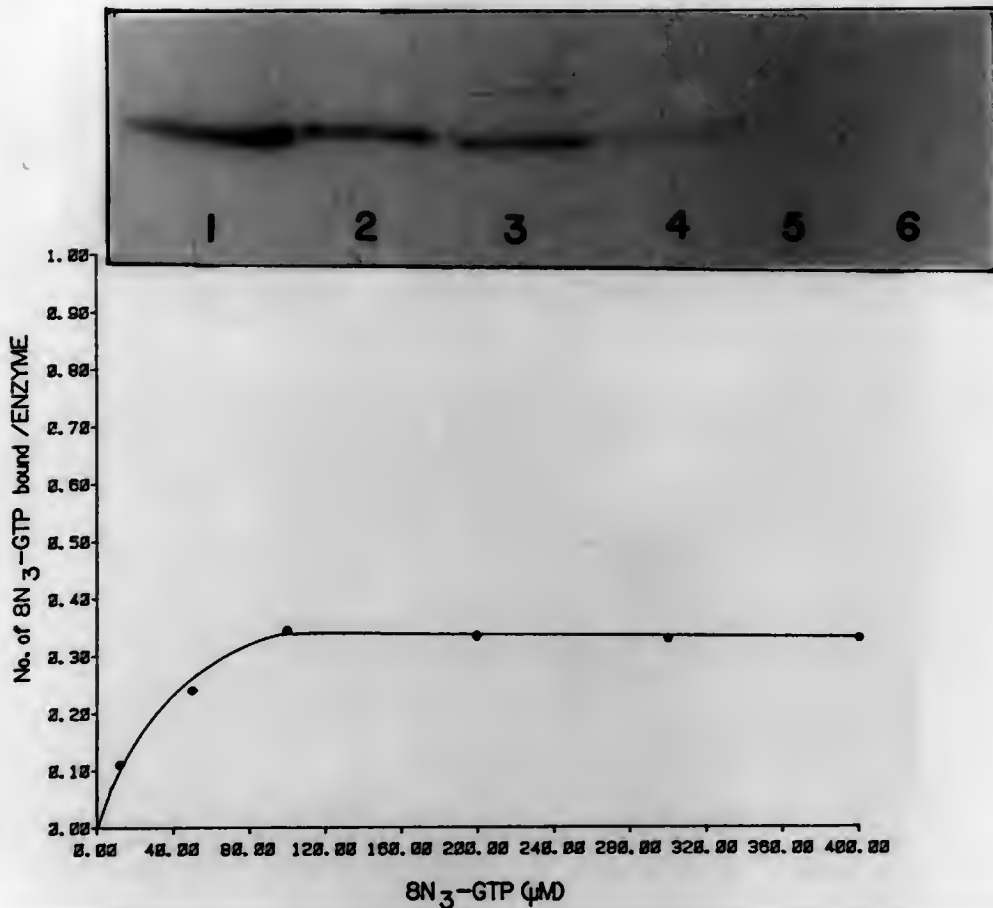


Figure 43. Number of radiolabeled azido-GTP molecules bound per CT RNAP II versus the azido-GTP concentration.

The standard reaction mixture contained 10 pmole CT RNAP II (free of DTT) and 1  $\mu$ Ci of radiolabeled azido-GTP, which was diluted by addition of unlabeled azido-GTP to final concentrations as indicated. After preincubation and exposure to UV light (366 nm) for 30 minutes, the samples were analyzed by 1D-SDS-PAGE, stained and autoradiographed as described in the legend of Figure 40. The amount of crosslinked radiolabeled azido-GTP was quantified by excising the appropriate bands, followed by liquid scintillation counting. The number of photoprobe molecules covalently crosslinked per molecule of CT RNAP II was plotted as a function of the photoprobe concentration. The number under each band in the autoradiograph indicates the increasing concentration of the photoprobe as shown on the abscissa.

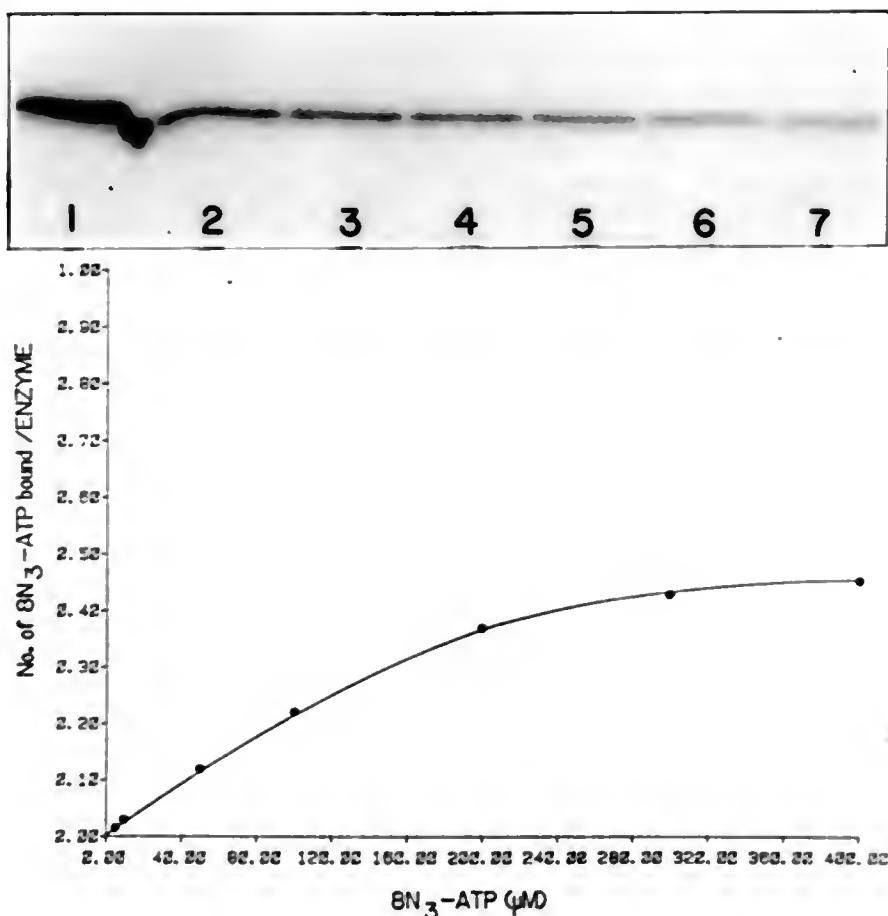


Figure 44. Number of radiolabeled azido-ATP molecules bound per PL RNAP II versus the azido-ATP concentration.

The standard reaction mixture contained 20 pmole PL RNAP II (free of DTT) and 1  $\mu$ Ci of radiolabeled azido-ATP, which was diluted by addition of unlabeled azido-ATP to final concentrations as indicated. After preincubation and exposure to UV light (366 nm) for 30 minutes, the samples were analyzed by 1D-SDS-PAGE, stained and autoradiographed as described in the legend of Figure 40. The amount of crosslinked radiolabeled azido-ATP was quantified by excising the appropriate bands, followed by liquid scintillation counting. The number of photoprobe molecules covalently crosslinked per molecule of PL RNAP II was plotted as a function of the photoprobe concentration. The number under each band in the autoradiograph indicates the increasing concentration of the photoprobe as shown on the abscissa.

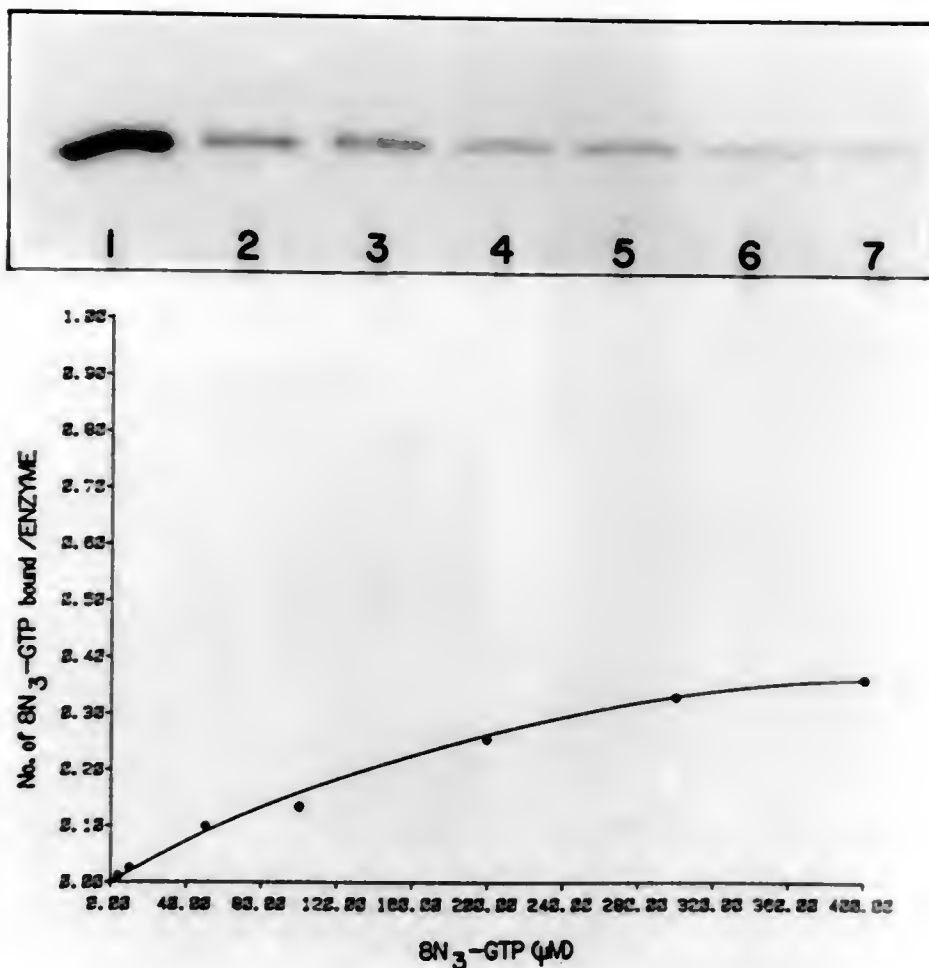


Figure 45. Number of radiolabeled azido-GTP molecules bound per PL RNAP II versus the azido-GTP concentration.

The standard reaction mixture contained 20 pmole PL RNAP II (free of DTT) and 1  $\mu$ Ci of radiolabeled azido-GTP, which was diluted by addition of unlabeled azido-GTP to final concentrations as indicated. After preincubation and exposure to UV light (366 nm) for 30 minutes, the samples were analyzed by 1D-SDS-PAGE, stained and autoradiographed as described in the legend of Figure 40. The amount of crosslinked radiolabeled azido-GTP was quantified by excising the appropriate bands, followed by liquid scintillation counting. The number of photoprobe molecules covalently crosslinked per molecule of PL RNAP II was plotted as a function of the photoprobe concentration. The number under each band in the autoradiograph indicates the increasing concentration of the photoprobe as shown on the abscissa.



Figure 46. Effect of homologous and heterologous NTPs on the cross-linking of  $8N_3$ -ATP to CT RNAP II.

Standard reaction mixtures of 50  $\mu$ l contained 10 pmoles CT RNAP II (free of DTT) and 1  $\mu$ Ci of radiolabeled azido-ATP, which was either diluted with unlabeled azido-ATP as indicated or to which was added either ATP, GTP, CTP, or UTP, before the preincubation, to final concentrations as indicated. The reaction mixtures were exposed to UV light (366 nm) as described in the Materials and Methods section and the amount of crosslinked radiolabel determined by counting the radioactivity in excised band E from 1D-SDS-PAGE as described in the legend of Figure 40. Included are the autoradiographs that show the effect of adding the 4 different NTPs at increasing concentrations. "C" is the control experiment because nothing was added to decrease the efficiency of photoaffinity labeling. The autoradiograph showing the effect of adding unlabeled azido-ATP is shown in Figure 42.

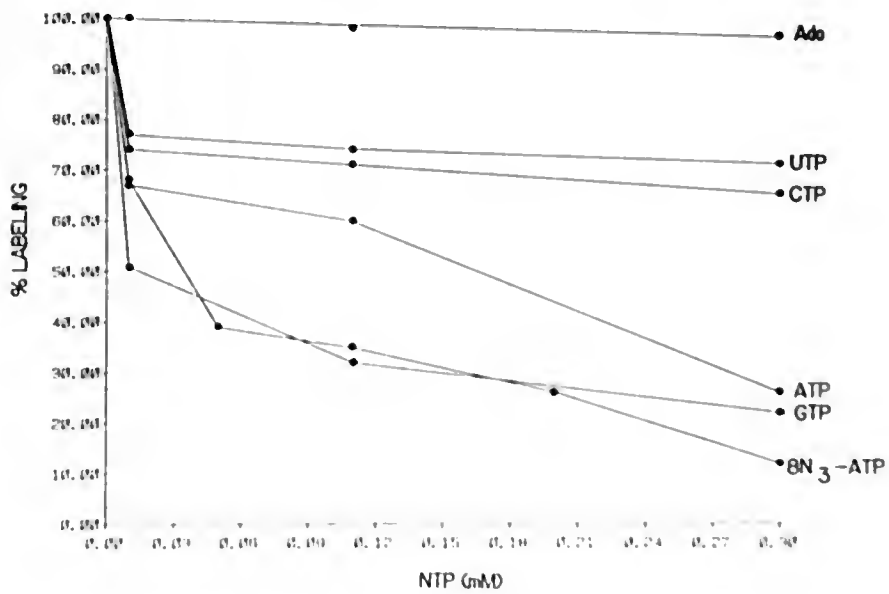
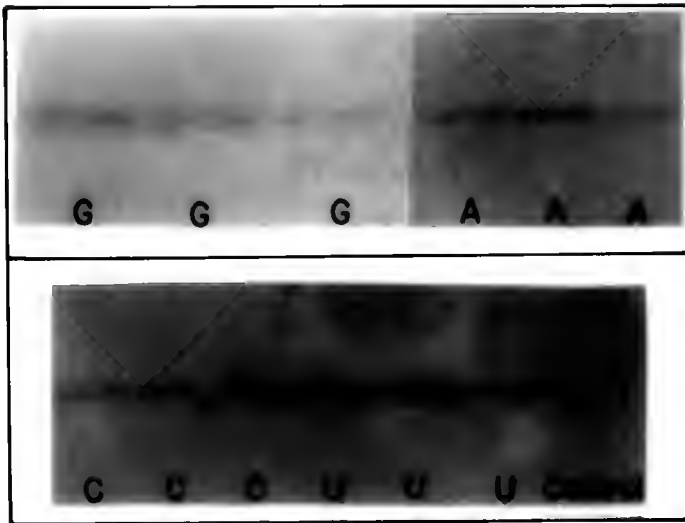


Figure 47. Effect of homologous and heterologous NTPs on the cross-linking of  $8N_3$ -GTP to CT RNAP II.

Standard reaction mixtures of 50  $\mu$ l contained 10 pmoles CT RNAP II (free of DTT) and 1  $\mu$ Ci of radiolabeled azido-GTP, which was either diluted with unlabeled azido-GTP as indicated or to which was added either ATP, GTP, CTP, or UTP, before the preincubation, to final concentrations as indicated. The reaction mixtures were exposed to UV light (366 nm) and the amount of crosslinked radiolabel determined as described in the legend of Figure 40. Included are the autoradiographs that show the effect of adding the 4 different NTPs at increasing concentrations. "C" is the control experiment because nothing was added to decrease the efficiency of photoaffinity labeling. The autoradiograph showing the effect of adding unlabeled azido-GTP is shown in Figure 43.

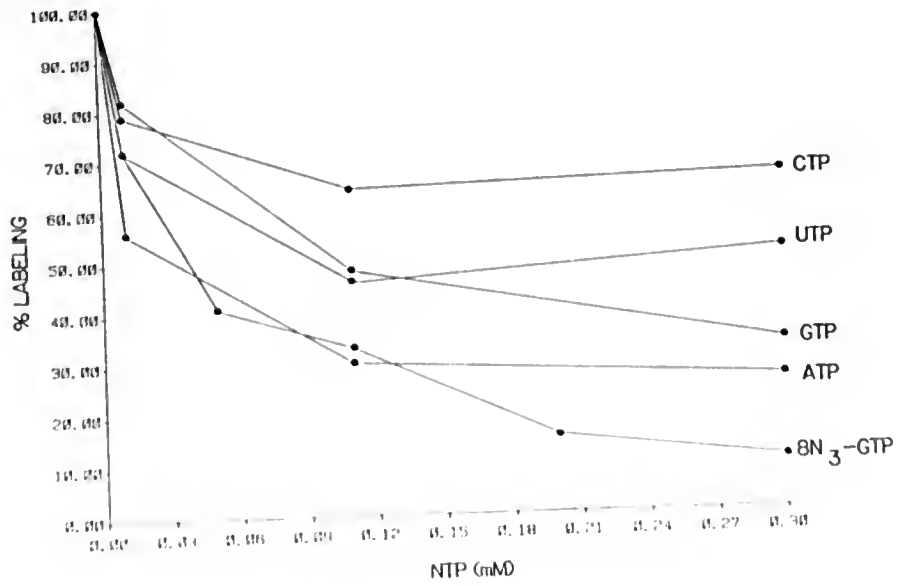
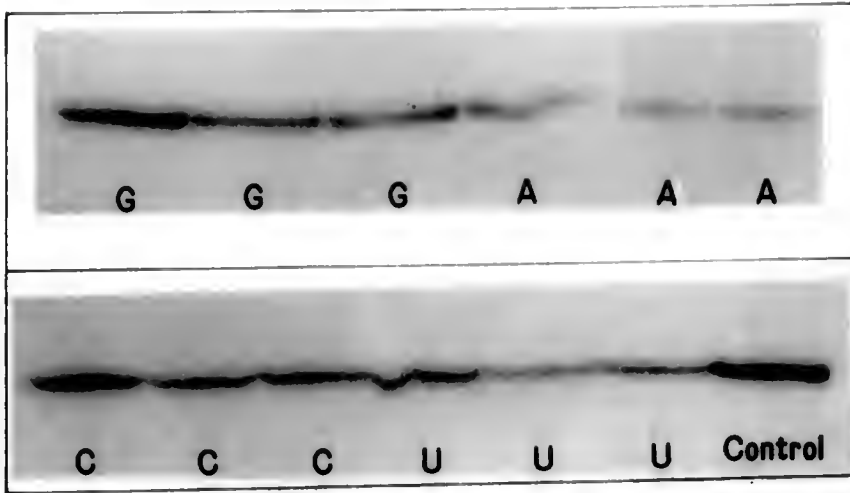


Figure 48. Effect of homologous and heterologous NTPs on the cross-linking of  $8N_3$ -ATP to PL RNAP II.

Standard reaction mixtures of 50  $\mu$ l contained 20 pmoles PL RNAP II (free of DTT) and 1  $\mu$ Ci of radiolabeled azido-ATP, which was either diluted with unlabeled azido-ATP as indicated or to which was added ATP, GTP, CTP, or UTP, before the preincubation, to final concentrations as indicated. The reaction mixtures were exposed to UV light (366 nm) and the amount of crosslinked radiolabel determined as described in the legend of Figure 40. Included are the autoradiographs that show the effect of adding the 4 different NTPs at increasing concentrations. The control experiment is shown in lane 1 of Figure 44. The autoradiograph showing the effect of adding unlabeled azido-ATP is shown in Figure 44.

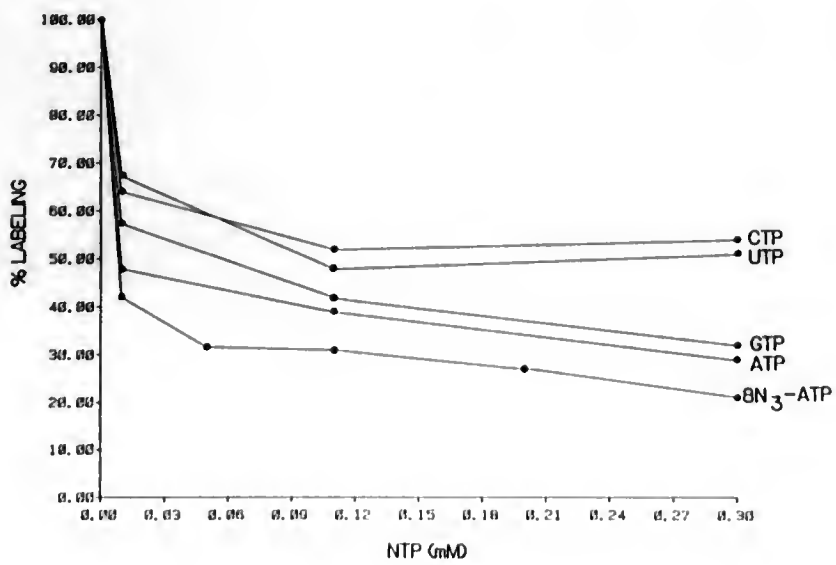
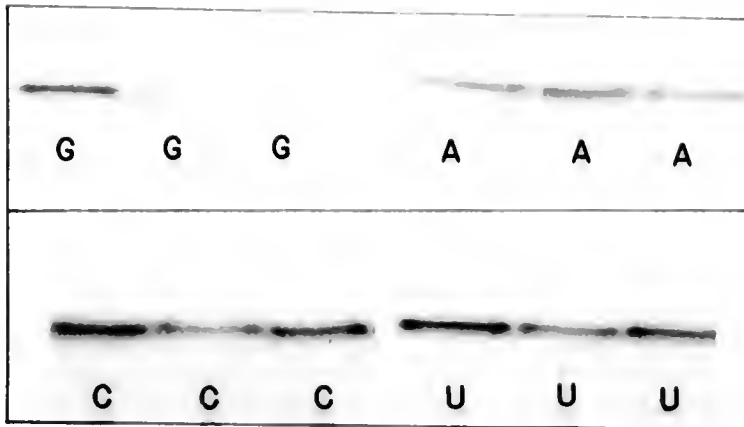
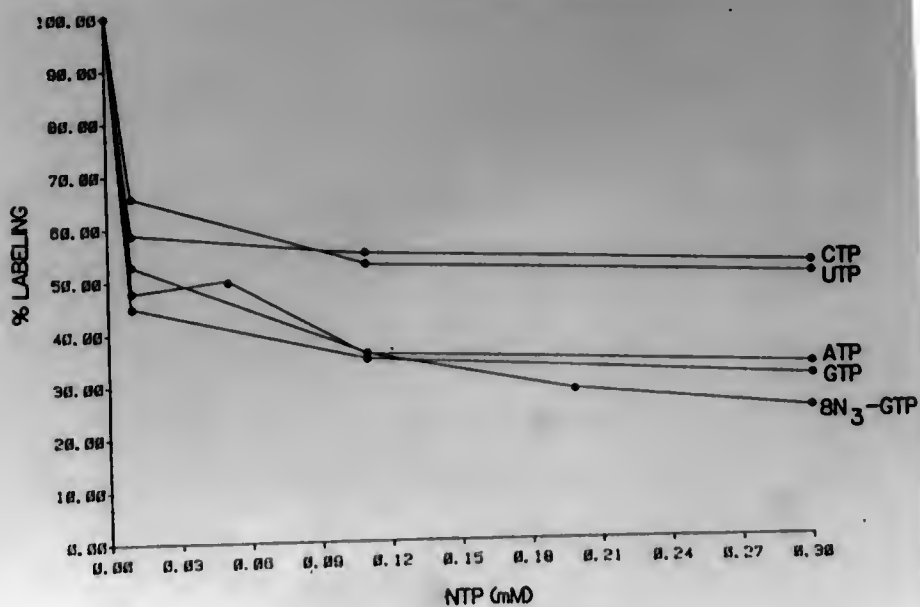
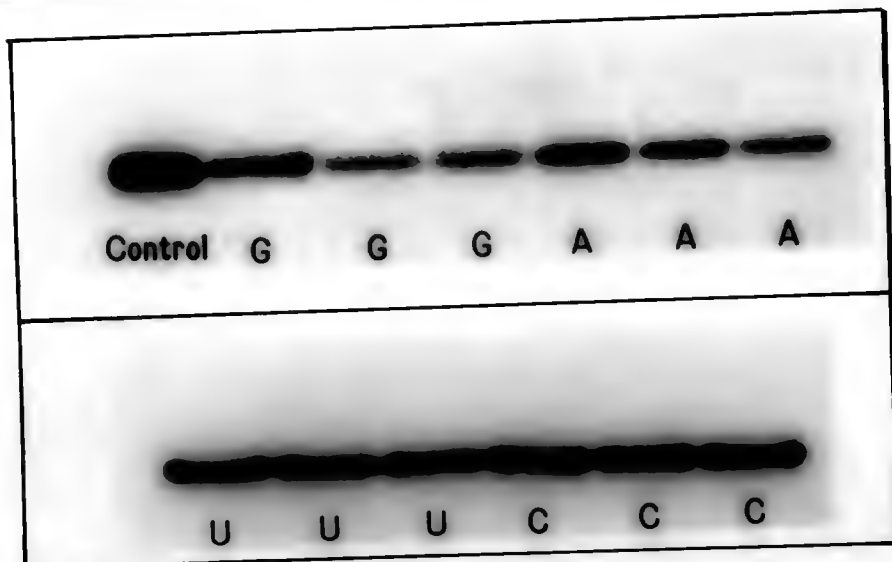


Figure 49. Effect of homologous and heterologous NTPs on the cross-linking of  $8N_3$ -GTP to PL RNAP II.

Standard reaction mixtures of 50  $\mu$ l contained 20 pmoles PL RNAP II (free of DTT) and 1  $\mu$ Ci of radiolabeled azido-GTP, which was either diluted with unlabeled azido-GTP as indicated or to which was added either ATP, GTP, CTP, or UTP, before the preincubation, to final concentrations as indicated. The reaction mixtures were exposed to UV light (366 nm) and the amount of crosslinked radiolabel determined as described in the legend of Figure 40. Included are the autoradiographs that show the effect of adding the 4 different NTPs at increasing concentrations. The effect of adding unlabeled  $8N_3$ -GTP on photoaffinity labeling is shown in Figure 45.





### Discussion

The UV light photolyzed both  $8N_3$ -ATP and  $8N_3$ -GTP with a first order rate constant of approximately  $0.002 \text{ seconds}^{-1}$ , when the long wave mode was used (Figures 26 and 27). This rate constant was twice as fast as the observed rate constant of approximately  $0.001 \text{ seconds}^{-1}$  of photoaffinity labeling (Figures 40 and 41). This difference is possibly due to dissociation of the photoprobes from the RNAP II during UV irradiation.

Since  $8N_3$ -ATP is not incorporated into the RNA product by CT RNAP II, and since this agent both photoinactivates the enzyme irreversibly and inhibits CT RNAP II in the absence of UV light, it was necessary to determine whether or not  $8N_3$ -ATP binds to the natural substrate binding site(s) of RNAP II. If so, this agent should, when added to a transcription reaction in the absence of light, display a competitive inhibition pattern. When the inhibition kinetics of  $8N_3$ -ATP were studied in the standard reaction assay based on  $[^3H]$ -UMP or  $[^3H]$ -AMP incorporation with CT DNA as template as described in the Materials and Methods section of Chapter Two, the Lineweaver-Burk plots indicated a mixed-type inhibition and substrate (ATP) inhibition at or above 2 mM (not shown). Furthermore, the progress curve was not linear during the first few minutes. For these reasons, the reaction assay was modified to exclude multi-substrate and initiation problems. The results obtained with  $8N_3$ -ATP using poly d(T) and ApA show competitive inhibition, indicating that at least under the conditions used,  $8N_3$ -ATP interferes with binding of the natural substrate ATP to the NTP binding site(s) on

CT RNAP II. A similar observation was made by Woody et al. who studied the mode of inhibition by  $8N_3$ -ATP of E. coli RNAP in a elongation transcription assay incorporating the same features as described in Figure 29.

The apparent  $K_M$  for ATP is much higher (0.77 mM) with polyd(T) as template than the apparent  $K_M$  measured for ATP using CT DNA as template (0.136 mM, Chapter Two). Since the apparent  $K_M$  for ATP with poly(dT) and ApA during preincubation was also 0.75 mM when the incubation was continued for 30 minutes (not shown), the short incubation time of seventy-five seconds used in the elongation assay alone could not be responsible for the discrepancy in  $K_M$  values. The difference in  $K_M$  is probably the result of the differences in template, as well as the use of dinucleotides during initiation. The presence of ApA in the ternary complex has a profound influence on the elongation kinetics, because the  $K_M$  for ATP was 3.57 mM when ApA was omitted from the preincubation assay.

In order to understand the observed differences in interactions of the NTP binding site of CT RNAP II with ATP or with  $8N_3$ -ATP, it is necessary to compare the stereochemistry of the two different purine nucleotides. The rotational position (torsion angle "X") of the base relative to the pentose in nucleic acids is sterically restricted, and two conformational states are preferred, i.e., the anti and the syn form (Saenger, 1984). Due to the flexibility of the furanose ring, there is an association between "X" and the furanose pucker. The  $C_{2'}$ endo pucker is associated more with the syn conformation. Due to the low energy barrier, there is a dynamic equilibrium with a rapid conversion from one

state into another. The pyrimidine NTPs favor the  $C_{3,endo}$  pucker, i.e., 60 % to 80 % are in the anti form. The purine NTPs favor the  $C_{2,endo}$  pucker, and about half of them are in the syn form. This means that the ribose adopts the  $C_{2,endo}$  pucker, resulting in a shift of the equilibrium towards the syn conformation. For example 8-Cl-Guanosine and 8-Br-Guanosine are 90 % to 95 % syn (Birnbaum et al., 1984), and the same is true for  $8N_3$ -ATP/GTP (Woody et al., 1984). Therefore it is important to ask whether that conformation impedes the binding of  $8N_3$ -ATP to a NTP binding site, since the conformation of the base moiety with respect to the pentose in B-DNA and in native RNA is anti (Chamberlin and Berg, 1964). An exception was found recently in Z-DNA where the conformation of GMP is syn (Saenger, 1984, Birnbaum et al., 1984).

The  $\alpha$ -amanitin did upon binding to CT RNAP II not prevent the enzyme from being photoaffinity labeled. This result correlates with the observation that amatoxins are non-competitive inhibitors (Chapter One).

When the radical scavenger DTT was omitted and CT RNAP II photoaffinity labeled, approximately one percent of the radiolabeled photoprobe was incorporated into the two largest polypeptides (Figure 34 B). This might be due to non-specific labeling or pseudo affinity labeling which arises from diffusion of the reactive nitrenes away from the NTP binding site. This is not significant, because the life time of the (RNAP-DNA-RNA)-NTP complex is approximately 300 mseconds (if the turnover number is three), which is much longer than the life time of the nitrene of approximately 0.1 mseconds (DeRiemer and Meares, 1981a, b).

The  $K_i$  of 0.4 mM for  $8N_3$ -ATP was lower than the apparent  $K_M$  of 0.77 mM for ATP for CT RNAP II, in experiments using polyd(T).

A similar observation was made by Kapular and Reich (1971) in inhibition studies with 8Br-GTP using E. coli RNAP. Those experiments were designed to study the prokaryotic enzyme's stereochemical requirements for substrates and utilized 8Br-CTP, which like 8Br-ATP (Tavale and Sobell, 1970) and  $8N_3$ -ATP (Woody, et al., 1984) prefers the syn conformation. The 8Br-GTP was found to inhibit RNAP strongly and to be competitive with GTP, when CT DNA was used as template. Furthermore, in a poly-d(C) directed reaction, its rate of incorporation was only 1 % of that found with CT DNA template, and even this low rate of incorporation requires the presence of GTP. These results indicated that 8Br-GTP (syn) can bind to the active site of the enzyme-template complex during elongation in a manner apparently similar to GTP, but that binding only rarely results in phosphodiester bond formation. The authors found that the  $K_M$  for GTP (45  $\mu$ M) was greater than  $K_i$  (18  $\mu$ M) for  $8N_3$ -GTP when an [ $^3$ H]-GMP incorporating assay was used with CT DNA as template.

Based on studies such as these with syn nucleotide analogues, it has been suggested that the initial binding of nucleotides to RNAP requires a conformation at the glycosyl bond that could be syn or intermediate between the syn and anti conformation (Chatterji et al., 1984). It is also possible that the syn conformation precludes this analogue of NTP from participating in Watson/Crick base pairing, but that some intrahelical constraint causes the  $8N_3$ -ATP to adopt the anti conformation (Cartwright and Hutchinson, 1980). This change in conformation, although not yet shown for RNAP, was demonstrated when it was observed that the ATP analogue, 8Br-ATP (syn), when binding to the  $NAD^+$  site of alcohol dehydrogenase, adopts the anti conformation of  $NAD^+$  (Abdallah, 1975).

The photoinactivation protection experiments showed that natural substrates could partially prevent the inactivation of CT RNAP II by  $8N_3$ -ATP. Concentrations of the natural substrates in excess of the concentration of  $8N_3$ -ATP were required to protect the enzyme partially from photoinactivation. This was also observed by Woody et al., (1984) who used a ten-fold excess of ATP to protect E. coli RNAP by 29 % to 52 % against photoinactivation by  $8N_3$ -ATP. In earlier experiments (Figures 31 and 32) it was observed that photoinactivation of CT RNAP II by  $8N_3$ -ATP inhibited the rate of [ $^3H$ ]-AMP incorporation to a greater extent than the rate of [ $^3H$ ]-UMP incorporation. Similarly, the photoinactivation protection data show that the natural substrates prevent photoinactivation to a greater extent when measured with respect to [ $^3H$ ]-UMP than with [ $^3H$ ]-AMP incorporation. Finally, the data show that purine NTPs protect CT RNAP II better against photoinactivation than pyrimidine NTPs, which agrees with the "photoaffinity-labeling protection" experiments. This is probably due to the presence of two binding sites for purine nucleoside triphosphates on RNAP II, whereas there is only one binding site for pyrimidine nucleoside triphosphates.

Saturation of photoaffinity labeling occurred at 200  $\mu M$   $8N_3$ -ATP (Figure 42) and resulted in a labelings efficiency of 45 %. The concentration required for saturation of photoinactivation was 600  $\mu M$  (Figure 32) and resulted in 75 % inactivation of the enzyme. The difference between the efficiency of photoaffinity labeling and photoinactivation is probably due to some hydrolysis of the  $^{32}P$  from the incorporated photoprobe during 1D-SDS-PAGE, because the pH of the running gel is alkaline. The measurement of photoinactivation is more precise because

the remaining activity of the RNAP II was determined, which is independent on the presence of a terminal Pi in the incorporated photoprobe. There is however, a correlation between photoaffinity labeling and photo-incorporation, because at 200  $\mu$ M concentration of the photoprobe, 45 % of the enzyme was labeled and 40 % of the enzyme was photoinactivated.

## CHAPTER SEVEN GENERAL DISCUSSION

Eukaryotic RNA polymerases are complex multi-polypeptide enzymes that transcribe the DNA template by polymerization of 4 different NTPs into complementary RNA products. The enzyme contains several sites which bind the DNA template, NTPs, and the product RNA. The study of the molecular structure of such an enzyme should answer three fundamental questions. Which polypeptides are subunits? Which polypeptides are adjacent to each other in the native enzyme? How do these subunits interact during the four stages of transcription, i.e., recognition of promoter sequences, initiation, elongation, and termination. This dissertation presents research that focuses on the first question.

Saraste (1983) and Robbins et al. (1984) stated several criteria which could be used to distinguish real subunits in polymeric enzymes from contaminating polypeptides: (1) copurification, (2) stoichiometric ratios that should give integral numbers, (3) reconstitution experiments, (4) genetic mapping of mutants with a defective enzyme activity, (5) localization of sites that bind either a specific inhibitor or the natural substrate, and (6) crossreactivity of a single antibody with similar polypeptides from different organisms.

Copurification of polypeptides is a weak argument, which can, however, be strengthened somewhat by showing integral stoichiometric ratios. Even this is not enough for a polypeptide to qualify as a functional subunit, and at least one more criterion should be tested before a polypeptide can be placed among the subunits. The research presented

in this dissertation addressed the fifth criterion, which is also the most common test applied to multimeric enzymes in general. Most research on the localization of true subunits in eukaryotic RNA polymerases has used tests satisfying the fifth criterion, by using the specific inhibitor  $\alpha$ -amanitin. These tests have pointed to the two largest subunits in eukaryotic RNAP II for binding this inhibitor. The research presented here attempts to locate true subunit(s) by determining which polypeptide, among the polypeptides that copurify in CT RNAP II or PL RNAP II, binds NTP. The conclusions drawn from these experiments should, however, be further corroborated by other experiments that test the third and fourth criteria, for which the experimental approaches reported in studies of prokaryotic RNAP are a good examples.

The NTP derivatives used here were the photoaffinity labels [ $^{32}\text{P}\gamma$ ]- $8\text{N}_3$ -ATP and [ $^{32}\text{P}\gamma$ ]- $8\text{N}_3$ -GTP. These photoprobes are very reactive and do not require the presence of any specific amino acid residue at the active site for covalent incorporation. To show binding site specificity in photoaffinity labeling, the method has to pass several tests. The photoprobe should either be a substrate or a competitive inhibitor of the enzyme. The photoprobe should be able to photoinactivate and photoaffinity label the enzyme, and the natural substrates should at least partially protect the enzyme from both photoinactivation and photoaffinity labeling. The site on which the photoprobe interacts should show saturation kinetics with respect to both photoinactivation and photoaffinity labeling. Finally, control experiments should be performed to show that the photoaffinity labeling is UV light dependent and takes place only under conditions at which both the enzyme and the



photoprobe are intact. For the present studies, it should also be demonstrated that the labeling is not the result of a transfer of the labeled gamma phosphate to a polypeptide of RNAP II by a contaminating kinase activity.

The experimental results presented in this dissertation led to the identification of a single major site of photoaffinity labeling by azidopurine NTP analogues in eukaryotic RNAP II from several sources under the in vitro conditions used. This site is located on a slightly acidic polypeptide with a MW of 37 kD, known otherwise as polypeptide "E", according to the nomenclature used to describe the polypeptide compositions of eukaryotic RNAP II enzymes.

This polypeptide E contains one or more domains that are involved in the binding and/or catalytic stage during transcription. This is based on the following observations:

Azido-ATP inactivated CT RNAP II irreversibly in the presence of UV light.

The mode of inhibition by azido-ATP in the absence of UV light was competitive with respect to the incorporation of [ $^3\text{H}$ ]-AMP during the elongation phase of the transcription.

UV light was absolutely necessary for irreversible inactivation and photoaffinity labeling.

The RNAP II was partially protected from photoaffinity labeling and photoinactivation by the presence of the natural substrate NTPs during both preincubation and UV irradiation.

A native conformation of the RNAP II was absolutely necessary for photoaffinity labeling.

At high concentrations of the photoprobe during UV irradiation, a saturation effect occurred in photoaffinity labeling and photoinactivation.

The concentrations of azido-ATP at which saturation kinetics occurred for photoinactivation and photoaffinity labeling are 600 and 200  $\mu\text{M}$ , respectively. These concentrations are consistent with the  $K_i$  value of 400  $\mu\text{M}$ , indicating that covalent photoaffinity labeling and covalent photoinactivation may occur at the same site at which noncovalent but competitive inhibition occurs by azido-ATP towards AMP incorporation during the elongation phase of a transcription reaction.

The involvement of other domains on different peptides of RNAP II in binding NTPs and/or in the polymerization reaction is by no means excluded, because in the absence of the radical scavenger DTT, some minor labeling of the two largest polypeptides occurred in addition to the labeling of polypeptide E. Furthermore, only azido-purine NTP analogues were used here, since no azido-pyrimidine derivatives are available.

The selectivity and degree of covalent labeling of RNA polymerase by any NTP derivative in vitro will depend on many factors, including the efficiency of Watson/Crick base pairing by the particular NTP analogue with the template strand and the micro-environment, i.e., the ionic strength, pH, and presence of competing NTPs. In addition, there will be the factor of a varying molecular distance between the highly reactive NTP-nitrene intermediates and the peptide chain domains during all four phases of the transcription reaction.

All these factors warrant further studies if one wants to obtain a correlation between enzyme subunits and their actions during transcription. In this study an NTP binding site was identified which is likely to be involved with catalysis. Only the use of more discriminating kinetics and the use of other NTP labels can reveal whether peptide E carries domain(s) for the initiation and/or elongation reactions.

In addition it would be interesting to study the degree of similarity among the "E" class polypeptides from different organisms by analyzing their tryptic fragments by HPLC or by classical 2D-analysis.

Future work should include amino acid sequencing of at least the first 10 amino acids on the amino terminal of polypeptide E and/or the amino acids that are near the residues into which labeled photoprobes inserted themselves during UV irradiation. It is likely that more than one amino acid residue is modified because the binding of the photoprobe to the RNAP II was not in the micromolar range.

Preliminary experiments with preparative electrophoresis described in Chapter Four show that preparative amounts of peptide E can be obtained. This peptide can be studied with respect to the binding of NTPs in the absence of other RNAP II subunits, by using either equilibrium dialysis or fluorescence quenching, since nucleic acids when binding to proteins do change the fluorescence spectrum of tryptophane. In addition, peptide E would permit amino acid sequencing, provided the amino terminal is not blocked. Once the amino terminal sequence has been determined, an DNA sequence can be synthesized by solid phase chemistry, which would provide a probe that allows the isolation of clones containing the cDNA for peptide E from a bovine or human gene

library. This probe could lead to the cloning of components essential for RNAP activity. Alternatively, polyclonal or monoclonal antibodies directed against peptide E could be used to screen a phage Lambda library of bovine sequences (Young and Davies, 1983) to isolate the gene coding for one of the subunits of CT RNAP II. A probe for this gene would allow one to study the regulation of gene expression of an enzyme which is essential to the cell function, or to study the degree of homology in the sequence of polypeptide E among RNAP II enzymes from different eukaryotic sources.

## REFERENCES

- Abraham, K.I., Haley, B.E & Modak, M.J. (1983) *J. Biochemistry* 22, 4197-4203.
- Abraham, K.I. & Modak, M.J. (1984) *Biochemistry* 23, 1176-1182.
- Abdallah, M.A., Biemann, J-F., Nordstrom, B. & Brandin, C-I., (1975) *Eur. J. Biochem.* 50, 475-481.
- Anthony, D.D., Wu, C.W. & Goldthwait, D.A. (1969) *Biochemistry* 8, 246-256.
- Armstrong, V.W. & Eckstein, F. (1979) *Biochemistry* 18, 5117-5122.
- Armstrong, V.W., Sternbach, H. & Eckstein, F. (1976) *Biochemistry* 15, 2086-2091.
- Armstrong, V., Sternbach, H. & Eckstein, F. (1977) In: *Methods in Enzymology* (Jacobus, W.B. and Wilchek, M., eds.) Volume XLVI, pp. 346-353. Academic Press, New York.
- Ashby, C.D. and Walsh, D.A. (1972) *J. Biol. Chem.* 247, 6637-6642.
- Bartlett, P.A. & Eckstein, F. (1982) *J. of Biol. Chem.* 257, 8879-8884.
- Bayley, H. & Knowles, J.R. (1977) In: *Methods in Enzymology* (Jacobus, W.B. & Wilchek, M. eds.) Volume XLVI, pp. 69-114. Academic Press, New York.
- Benson, R.H., Spindler, S.R., Hodo, H.G. & Blatti, S.P. (1978) *Biochemistry* 17, 1387-1396.
- Birnbaum, G.I., Lassota, P. & Shugar, D. (1984) *Biochemistry* 23, 5048-5053.
- Bogenhagen, D.F., Sakonju, S. & Brown, D.D. (1980) *Cell* 19, 27-35.
- Bradford, M.M. (1976) *Anal. Biochem.* 72, 248-254.
- Bramson, H.N., Mildvan, A.S. & Kaiser, E.T. (1983) In: *CRC Critical Reviews in Biochemistry* (Fasman, G.D. ed.) Volume 15, 93-124, CRC Press, Boca Raton.
- Breant, B., Huet, J., Sentenac, A. & Fromageot, P. (1983) *J. of Biol. Chem.* 258, 11968-11973.

- Breathnach, R. & Chambon, P. (1981) *Ann. Rev. Biochem.* 50, 349-383.
- Brodner, O.G. & Wieland, T., (1976) *Biochemistry* 15, 3480-3484.
- Bryant, R., Adelberg, E.A. & Magee, P.T. (1977) *Biochemistry* 16, 4237-4243.
- Burgess, R.R. (1976) In: *RNA Polymerase* (Losick, R. & Chamberlin, M., eds.) pp. 179-191. Cold Spring Harbor Laboratory, Cold Spring Harbor.
- Cartwright, I.L. & Hutchinson, D.W. (1980) *Nucleic Acid Res.* 8, 1675-1691.
- Cartwright, I.L., Hutchinson, D.W. & Armstrong, V.W. (1976) *Nucleic Acid Res.* 3, 2331-2338.
- Chamberlin, M.J. (1976) In: *RNA Polymerase* (Losick, R. & Chamberlin, M., eds.) pp. 179-191. Cold Spring Harbor Laboratory, Cold Spring Harbor.
- Chamberlin, M.J., (1982) In: *The Enzymes*, volume XV, (Boyer, P.D., ed.) part B, third edition, pp. 61-82. Academic Press, New York.
- Chamberlin, M.J. & Berg, P. (1964) *J. Mol. Biol.* 8, 297-313.
- Chatterji, D., Wu, C.-W. & Wu, F.-Y., H. (1984) *J. of Biol. Chem.* 259, 284-289.
- Cho, J.M. & Kimball, A.P. (1982) *Biochem. Pharmacology* 31, 2575-2581.
- Cho, J.M., Carbu, R.K., Evans, J.E. & Kimball, A.P. (1982) *Biochem. Biophys. Res. Comm.* 31, 2583-2589.
- Cleveland, D.W., Fischer, S.G., Kirschner, M.W. & Laemmli, U.K. (1977) *J. of Biol. Chem.* 252, 1102-1106.
- Cochet-Meilhac, M. & Chambon, P. (1974) *Biochim. Biophys. Acta* 353, 160-184.
- Corden, J., Wasylyk, B., Buchwalder, A., Sassone-Corsi, P., Keding, C., & Chambon, P. (1980) *Science*, 209, 1406-1414.
- Coulter, D.E. & Greenleaf, A.L. (1982) *J. of Biol. Chem.* 257, 1945-1952.
- Czarnecki, J., Geahlen, R. & Haley, B. (1979) In: *Methods of Enzymology* (Fleischer, S. & Packer, L. eds.), volume LVI, pp. 642-653. Academic Press, New York.
- Dahmus, G.K., Clover, C.V.C., Brutlag, D.L. & Dahmus, M.E. (1984) *J. of Biol. Chem.* 259, 9001-9006.

- Dahmus, M.E. (1981a) J. of Biol. Chem. 256, 3319-3325.
- Dahmus, M.E. (1981b) J. of Biol. Chem. 256, 3332-3339.
- Dahmus, M.E. (1981c) J. of Biol. Chem. 256, 11239-11243.
- Dahmus, M.E. (1983) J. of Biol. Chem. 258, 3956-3960.
- Dahmus, M.E. & Keding, C. (1983) J. of Biol. Chem. 258, 2303-2307.
- Darnell, J.E., Girard, M., Baltimore, D., Summers, D.F. & Maizel, J.V. (1967) In: The Molecular Biology of Tumor Viruses (Colter, J., ed.) pp. 375-401. Academic Press, New York.
- Davies, G.E. & Stark, G.R. (1970) Proc. Natl. Acad. Sci. USA 66, 651-656.
- Davison, B.L., Egly, J.-M., Mulvihill, E.R. & Chambon, P. (1983) Nature 301, 680-686.
- Dennis, D. & Sylvester, J. (1981) FEBS Lett. 124, 135-139.
- DeRiemer, L.H. & Meares, C.F. (1981a) Biochemistry 20, 1606-1612.
- DeRiemer, L.H. & Meares, C.F. (1981b) Biochemistry 20, 1612-1670.
- Duceman, B.W., Rose, K.M. & Jacob, S.T. (1981) J. of Biol. Chem. 256, 10755-10758.
- Eckstein, F., Romaniuk, P.J. & Connolly, B.A. (1980) In: Methods in Enzymology (Purich, D.L., ed.) Volume 87, pp. 197-212. Academic Press, New York.
- Engelke, D.R., Shastri, B.S. & Roeder, R.G. (1983) J. of Biol. Chem. 258, 1921-1931.
- Faulstich, F. (1980) Progress in Mol. Subcellular Biol. 7, 88-134.
- Faulstich, H., Trischmann, H., Wieland, Th. & Wulf, E. (1981) Biochemistry 20, 6498-6504.
- Ferguson, A.O. (1964) Metabolism 13, 985-1002.
- Frischauf, A.M. & Scheit, K., (1973) Biochem. Biophys. Res. Comm. 53, 1227-1233.
- Furth, J. & Cohen, S. (1967a) Cancer Res. 27, 1528-1533.
- Furth, J. & Cohen, S. (1967b) Cancer Res. 20, 2061-2067.
- Gaehlen, R.L. & Haley, B.E. (1979) J. of Biol. Chem. 254, 11982-11987.

- Gilbert, W. (1976) In: RNA Polymerase (Losick, R. & Chamberlin, M., eds.) pp. 193-205. Cold Spring Harbor Laboratory, Cold Spring Harbor.
- Glass, R.E. (1982) In: Gene Function, E. coli. and its Heritable Elements pp. 5-35. University of California Press, Berkeley.
- Gordon, A.S., Milfay, D. & Diamond, I. (1983) Proc. Natl. Acad. Sci. (USA) 80, 5862-5865.
- Grachev, M.A. & Zaychikov, E.F., (1981) FEBS Lett. 130, 23-26.
- Greenblat, J. & Li, J. (1981) Cell 24, 421-428.
- Greenleaf, A.L. (1983) J. of Biol. Chem. 258, 13403-13406.
- Greenleaf, A.L., Borsett, L.M., Jiamachello, P.F. & Coulter, D.E. (1979) Cell 18, 613-622.
- Guilfoyle, T.J., Malcolm, S. & Hagen, G. (1983) In: Isozymes, Volume 7 (Rattazzi, M.C., Scandalios, J.G. & Whitt, G.S., eds.) pp. 241-259. Alan, R. Liss, New York.
- Guilfoyle, T.J., Hagen, G. & Malcolm, S. (1984a) J. of Biol. Chem. 259, 640-648.
- Guilfoyle, T.J., Hagen, G. & Malcolm, S. (1984b) J. of Biol. Chem. 259, 649-653.
- Guillory, R.J. & Jeng, S.J. (1983) Fed. Proc. 42, 2826-2845.
- Gundelfinger, E.D. (1983) FEBS Lett. 157, 133-138.
- Haley, B.D. & Hofmann, J.F. (1974) Proc. Natl. Acad. Sci. (USA) 71, 3367-3371.
- Haley, B.E. (1983) Fed. Proc. 42, 2831-2835.
- Hanna, M.M. & Meares, C.F. (1983a) Biochemistry 22, 3546-3551.
- Hanna, M.M. & Meares, C.F. (1983b) Proc. Natl. Acad. Sci. (USA) 80, 4238-4242.
- Hayashi, T.T. (1977) Gynecological Investigation 8, 183-194.
- Hayat, M.A. (1981) In: Principles and Techniques of Electron Microscopy, Volume 1, second edition, University Park Press, Baltimore.
- Hazra, A.K., Detera-Wadleigh, S. & Wilson, S.H. (1984) Biochemistry 23, 2073-2078.
- Hillel, Z. & Wu, C.-W. (1977) Biochemistry 16, 3334-3342.



- Hodo, H.G. & Blatti, S.P. (1977) *Biochemistry* 6, 2334-2343.
- Hollemans, M., Runswick, M.J., Fearnley, I.M. & Walker, J.E. (1983) *J. of Biol. Chem.* 258, 9307-9313.
- Hoppe, J. & Freist, W. (1979) *Eur. J. Biochem.* 93, 141-146.
- Horikoski, M., Sekimizu, K. & Natori, S. (1984) *J. of Biol. Chem.* 259, 608-611.
- Horowitz, J.A., Toeg, H. & Orr, G.A. (1984) *J. of Biol. Chem.* 259, 832-838.
- Hsu, C.-Y. & Dennis, D. (1982) *Nucl. Acid Res.* 10, 5637-5647.
- Huet, J., Sentenac, A. & Fromageot, P. (1982) *J. of Biol. Chem.* 257, 2613-2618.
- Ingles, C.J., Biggs, J., Wong, J.K.-C, Weeks, J.R. & Greenleaf, A.L. (1983) *Proc. Natl. Acad. Sci. (USA)* 80, 3396-3400.
- Jankowski, J.M. & Kleczkowski, K. (1980) *Biochem. Biophys. Res. Comm.* 96, 1216-1224.
- Jendrisak, J. (1980) In: *Genome Organization and Expression in Plants* (Leaver, C.J., ed.) pp. 77-92. Plenum Press, New York.
- Jove, R. & Manley, J.L. (1984) *J. of Biol. Chem.* 259, 8513-8521.
- Kadesch, T.R. & Chamberlin, M.J. (1982) *J. of Biol. Chem.* 257, 5286-5295.
- Kapuler, A.M. & Reich, E. (1971) *Biochemistry* 10, 4050-4061.
- Kaufman, R. & Voigt, H.-P. (1973) *Hoppe Seyler's Zeitschrift fur Physiologische Chemie* 354, 1432-1438.
- Kedinger, C. & Chambon, P. (1972) *Eur. J. Biochem.* 28, 283-290.
- Kedinger, C., Gissenger, F. & Chambon, P. (1974) *Eur. J. Biochem.* 44, 421-436.
- Kimball, A.P. (1977) In: *Methods in Enzymology* (Jacobus, W.B. and Wilchek, M., eds.) Volume XLVI, pp. 353-358. Academic Press, New York.
- King, M.M., Carlson, G.M. & Haley, B.E. (1982) *J. of Biol. Chem.* 257, 14058-14065.
- Kohorn, B.D. & Rae, P.M.M. (1983) *Nature* 304, 179-181.
- Knowles, S.R. (1980) *Ann. Rev. Biochem.* 49, 890-907.

- Korn, L.J. (1982) *Nature* 295, 101-105.
- Krakow, J.S. & Fronk, E. (1969) *J. of Biol. Chem.* 244, 5988-5993.
- Krakow, J.S., Rhodes, G. & Jovin, T.M. (1976) In: *RNA Polymerase* (Losick, R. & Chamberlin, M., eds.) pp. 127-157. Cold Spring Harbor Laboratory, Cold Spring Harbor.
- Kranias, E.G. & Jungman, R.A. (1978a) *Biochim. Biophys. Acta* 517, 439-446.
- Kranias, E.G. & Jungman, R.A. (1978b) *Biochim. Biophys. Acta* 517, 447-456.
- Kranias, E.G., Schweppe, J.S. & Jungmann, R.A. (1977) *J. of Biol. Chem.* 252, 6750-6758.
- Krebs, E.G. & Beavo, J.A. (1979) *Ann. Rev. Biochem.* 48, 923-959.
- Kusamran, T., Drake, R., Wunderlich, S.M., Lau, A.S., Baliga, B.S. & Munro, H.N. (1980) *Placenta* 1, 157-167.
- Laga, E.M., Driscoll, S.G. & Munro, H.N. (1973) *Biology of the Neonate* 23, 242-259.
- Larionov, O.A., Gragerov, A.I., Kalyaeva, E.S. & Nikiforov, V.G. (1979) *Mol. Gen. Genet.* 176, 105-111.
- Lau, A.S., Baliga, B.S., Roy, R.K., Sarkar, S. & Munro, H.N. (1980) *Placenta* 1, 168-180.
- Laemmli, U.K. (1970) *Nature* 227, 680-685.
- Lewis, M.K. & Burgess, R.R. (1980) *J. of Biol. Chem.* 255, 4928-4936.
- Lewis, M.K. & Burgess, R.R., (1982) In: *The Enzymes*, volume XV, (Boyer, P.D., ed.) part B, third edition, pp. 109-153.
- Lindell, T.J., Weinberg, F., Morris, P.W., Roeder, R.G. & Rutter, W.J. (1970) *Science* 170, 447-448.
- Lynwood, R. & Yarbrough, R. (1982) *J. of Biol. Chem.* 257, 6171-6177.
- Maizel, J.V. (1971) In: *Methods in Virology* (Maramosch, K. & Kaprowski, H., eds.) Volume V, pp. 180-244. Academic Press, New York.
- Malcolm, A.D.B. & Moffat, J.R. (1978) *Biochem. J.* 175, 189-192.
- Manley, J.L., Fire, A., Cano, A., Sharp, P.A. & Gelfand, M.L. (1980) *Proc. Natl. Acad. Sci. (USA)* 77, 3855-3859.
- Marmur, J. (1961) *J. of Mol. Biol.* 3, 208-218.

- Martial, J., Zaldivar, J., Bull, P., Venegas, A. & Valenzuela, P. (1975) *Biochemistry* 14, 4907-4911.
- Matsui, T., Segall, J., Weil, A. & Roeder, R.G. (1980) *J. of Biol. Chem.* 255, 11992-11996.
- Matsumoto, H. & Pak, W.L. (1984) *Science* 223, 184-186.
- Mertelsmann, R. (1969) *Eur. J. Biochem.* 9, 311-318.
- Mertelsmann, R. & Matthaei, H. (1968) *Biochem. Biophys. Res. Com.* 33, 136-139.
- Mildvan, A.S. & Loeb, L.A. (1979) In: *CRC Critical Reviews in Biochemistry*, Volume 6, pp. 219-244. CRC Press, Boca Raton.
- Miller, J., Serio, G.F., Bear, J.L., Howard, A.R. & Kimball, A.P. (1980) *Biochim. Biophys. Acta* 612, 286-294.
- Modak, M.J. & Gillerman-Cox, E. (1982) *J. of Biol. Chem.* 257, 15105-15109
- Moore, K.L. (1977) In: *The Developing Human*, second edition, pp. 96-110. W.B. Saunders Company, Philadelphia.
- Munro, H.N. (1979) In: *Placenta--A Neglected Experimental Animal* (Beaconsfield, P. & Vिलlee, C. eds.) pp. 62-74. Pergamon Press, New York.
- Murdoch, G.H. & Rosenfeld, M.G. (1982) *Science* 218, 1315-1317.
- Nixon, J., Spoor, T., Evans, J. & Kimball, A. (1972) *Biochem.* 11, 4570-4573.
- Novello, F., (1970) *Eur. J. Biochem.* 15, 505-512.
- O'Farrel, P.H. (1975) *J. of Biol. Chem.* 250, 4007-4021.
- Otto, M., Snejdarkova, M. (1981) *Anal. Biochem.* 111, 111-114.
- Park, C.S., Hillel, Z. & Wu, C.-W. (1980) *Nucl. Acid Res.* 8, 5895-5912.
- Parker, C.S., Ng, S.-Y. & Roeder, R.G. (1976) In: *Molecular Mechanisms in the Control of Gene Expression*, pp. 223-242. Academic Press, New York.
- Paule, M.R. (1981) *Trends in Biochem. Sci.* 6, 128-131.
- Paule, M.R., Calvin, T.I., Perna, P.J., Harris, G.H., Shimer, S.L.B., & Kownin, P. (1983) *Biochemistry* 23, 4167-4172.
- Pedone, F. & Ballario, P. (1984) *Biochemistry* 23, 69-79.

- Pfister, K.K., Haley, B.E. & Witman, G.B. (1984) *J. of Biol. Chem.* 259, 8499-8504.
- Plapp, B.V. (1983) In: *Contemporary Enzyme Kinetics and Mechanism* (Purich, D.L. ed.) pp. 321-351. Academic Press, New York.
- Potter, R.L., and Haley, B.E. (1983) In: *Methods in Enzymology* (Hirs, C.H.W. & Timashef, S.N. eds.) Volume 91, pp. 613-632. Academic Press, New York.
- Preston, J.F., Hencin, R.S. & Gabbay, E.J. (1981) *Arch. of Biochem. and Biophys.* 209, 63-71.
- Rackwitz, H.R. & Scheit, K.H. (1977) *Eur. J. of Biochem.* 72, 191-200.
- Rhodes, G. & Chamberlin, M.J. (1974) *J. of Biol. Chem.* 249, 6675-6683.
- Rhodes, G. & Chamberlin, M.J. (1975) *J. of Biol. Chem.* 250, 9112-9120.
- Robbins, A., Dynan, W.S., Greenleaf, A. & Tjian, R. (1984) *J. of Mol. and Applied Genet.* 2, 343-353.
- Roeder, R.G. (1976) In: *RNA Polymerase* (Losick, R. & Chamberlin, M., eds.) pp. 285-329. Cold Spring Harbor Laboratory, Cold Spring Harbor.
- Rose, K.M., Maguire, K.A., Wurpel, J.N.D., Stetler, D.A. & Marquez, E.D. (1983) *J. of Biol. Chem.* 258, 12976-12981.
- Rose, K.M., Stetler, D.A. & Jacob, S.T. (1981) *Proc. Natl. Acad. Sci. (USA)* 78, 2833-2837.
- Ruet, A., Sentenac, A., Fromageot, P., Winsor, B. & Lacronte, F. (1980) *J. of Biol. Chem.* 255, 6450-6455.
- Sakakibara, R., Kitajima, S. & Uyeda, K. (1984) *J. of Biol. Chem.* 259, 8366-8371.
- Saenger, W. (1984) In: *Principles of Nucleic Acid Structure*, pp. 69-77. Springer Verlag, New York.
- Sakonju, S., Bogenhagen, D.F. & Brown, D.D. (1980) *Cell* 19, 13-25.
- Samuels, M., Fire, A. & Sharp, P.A. (1984) *J. of Biol. Chem.* 259, 2517-2525.
- Saraste, M. (1983) *Trends in Biochem. Sci.* 8, 139-142.
- Sarkar, G.S. & Mukherjee, G. (1974) *Acta Endocrinology* 75, 379-384.
- Sassone-Corsi, P., Dougherty, J.P., Wasylyk, B. & Chambon, P. (1984) *Proc. Natl. Acad. Sci. (USA)* 81, 308-312.

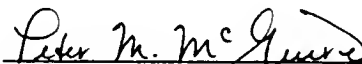
- Scaife, J. (1976) In: RNA Polymerase (Losick, R. & Chamberlin, M., eds.) pp. 207-255. Cold Spring Harbor Laboratory, Cold Spring Harbor.
- Scheurich, P., Schafer, H.J. & Dose, K. (1978) Eur. J. Biochem. 88, 253-257.
- Schoff, P.K., Forrester, I.T., Haley, B.E. & Atherton, R.W. (1982) J. Cell. Biochem. 19, 1-15.
- Scrivastava, S.K., & Modak, M.J. (1982) Biochemistry 21, 4633-4639.
- Sekimizu, K., Haruhiko, Y. & Natori, S. (1982) J. of Biol. Chem. 257, 2719-2721.
- Sentenac, A., Dezelee, S., Iborra, F., Buhler, J-M., Huet, J., Wyers, F. Ruet, A. & Fromageot, P. (1976) In: RNA Polymerase (Losick, R. & Chamberlin, M., eds.) pp. 763-777. Cold Spring Harbor Laboratory, Cold Spring Harbor.
- Shacter-Noiman, E. & Boon, C.P. (1983) J. of Biol. Chem. 258, 4214-4219.
- Smith, S.S., Kelly, K.H. & Jockusch, B.M. (1979) Biochem. Biophys. Res. Comm. 86, 161-166.
- Sommerville, J. (1984) Nature 310, 189-190.
- Spindler, S.R. (1979) Biochemistry 18, 4042-4048.
- Spoor, T., Persico, F., Evans, J. & Kimball, A.P. (1970) Nature, 227, 57-59.
- Spurr, A.R. (1969) J. Ultra Structural Res. 26, 31-43.
- Staros, J.V., Bayley, H., Standring, D.N. & Knowles, J.R. (1978) Biochem. Biophys. Res. Comm. 80, 568-572.
- Stetler, D.A. & Rose, K.M. (1982) Biochemistry 21, 3721-3728.
- Sugden, B. & Keller, W. (1973) J. of Biol. Chem. 248, 3777-3788.
- Sverdlov, E.D., Tsarev, S.A. & Kuznetsova, N.F. (1980) FEBS Lett. 112, 296-298.
- Sybulski, S. & Tremblay, P.C. (1967) Am. J. Obstet. Gynec. 97, 1111-1118.
- Tavale, S.S. & Sobell, H.M. (1970) J. of Mol. Biol. 48, 109-123.
- Thornburg, W. & Lindell, T.J. (1977) J. of Biol. Chem. 252, 6660-6665.
- Tsai, S.T., Dicker, P., Fang, P., Tsai, M.-J. & O'Malley, B.W. (1984) J. of Biol. Chem. 259, 11587-11593.

- Tsuda, M. & Suzuki, Y. (1982) *J. of Biol. Chem.* 257, 12367-12372.
- Turro, N.J. (1980) In: *Annals of the New York Acad. of Sciences* (Tometsko, A.M. & Richards, F.M., eds.), Volume 346, pp. 1-18. New York Academy of Science, New York.
- Vaisius, A.C & Wieland, T. (1982) *Biochemistry* 27, 3097-3101.
- Valenzuela, P., Bull, P., Zaldivar, J., Venegas, A. & Martial, J. (1978) *Biochem. Biophys. Res. Comm.* 81, 662-666.
- Voigt, H.P., Kaufmann, R. & Matthaei, H. (1970) *FEBS Lett.* 10, 257-260.
- von Hippel, P.H., Bear, D.G., Morgan, W.D. & McSwiggen, J.,A. (1984) *Ann. Rev. Biochem.* volume 53, pp. 389-446.
- Waechter, D.E., Avignolo, C., Freund, E., Riggenbach, C.M., Mercer, W.E., McGuire, P.M. & Baserga, R. (1984) *Molecular and Cellular Biochemistry* 60, 77-82.
- Weil, P.A., Luse, D.S., Segall, J. & Roeder, R.G. (1979) *Cell* 18, 469-484.
- Woody, A.M., Vader, C.R., Woody, R.W. & Haley, B.E. (1984) *Biochemistry* 23, 2843-2848.
- Whipple, G.H., Hill, R.B., Terry, R., Lucas, F.V. & Yuili, C.L. (1955) *J. Exptl. Med.* 101, 617-626.
- Wilkinson, J.K. & Sollner-Webb, B. (1982) *J. of Biol. Chem.* 257, 14375-14383,
- Wray, W., Boulikas, T., Wray, V.P. & Hancock, R. (1981) *Anal. Biochemistry* 118, 197-203.
- Wu, C.-W. & Goldthwait, D.A. (1969a) *Biochemistry* 8, 4450-4458.
- Wu, C.-W. & Goldthwait, D.A. (1969b) *Biochemistry* 8, 4458-4464.
- Wu, C.-W. & Tweedy, N. (1982) *Molecular and Cellular Biochemistry* 47, 129-149.
- Wu, F.-Y.H. & Wu, C-W. (1974) *Biochemistry* 13, 2562-2566.
- Wu, G.J. (1978) *Proc. Natl. Acad. Sci. (USA)* 75, 2175-2179.
- Young, R.A. & Davis, R.W. (1983) *Science* 222, 778-782.
- Yura, T. & Ishihama, A. (1979) *Ann. Rev. Genet.* 13, 59-97.
- Zillig, W., Palm, P., & Heil, A. (1976) In: *RNA Polymerase* (Losick, R. & Chamberlin, M., eds.) pp. 101-125. Cold Spring Harbor Laboratory, Cold Spring Harbor.

## BIOGRAPHICAL SKETCH

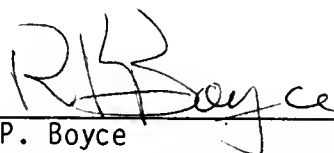
Erwin Freund was born the son of Werner Reinhold Freund and Willy van Donselaar on March 9, 1953, in the town of Bochum, West Falen, West Germany. In 1955 the family settled in the town of de Bilt in the Netherlands. Erwin graduated in 1972 from the F. de Munnik Atheneum at Utrecht. In 1972 he entered the biology program at the State University of Utrecht and moved with his parents to the town of Driebergen. In 1974 he married Simha Mizrahi. Erwin received his Bachelor of Science with honors in the field of biochemistry in 1976. He continued his graduate education in September, 1976, at the State University of Utrecht and participated in the Utrecht-Gainesville student exchange program at the University of Florida. He received his Master of Science degree in 1979 summa cum laude. In the same year Erwin moved to Gainesville, where he entered, in September, 1979, the doctoral program in the Department of Biochemistry and Molecular Biology at the University of Florida. Erwin is the father of Nathaniel who was born in Gainesville. He has accepted a post-doctoral fellowship at the laboratory of Dr. A. Shatkin at the Roche Institute for Molecular Biology.

I certify that I have read this study and that in my opinion it conforms to acceptable standards of scholarly presentation and is fully adequate, in scope and in quality, as a dissertation for the degree of Doctor of Philosophy.



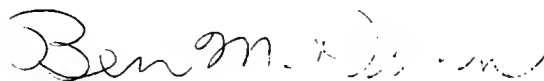
P.M. McGuire, Chairman  
Assistant Professor of  
Biochemistry and Molecular Biology

I certify that I have read this study and that in my opinion it conforms to acceptable standards of scholarly presentation and is fully adequate, in scope and in quality, as a dissertation for the degree of Doctor of Philosophy.



R.P. Boyce  
Professor of Biochemistry and  
Molecular Biology

I certify that I have read this study and that in my opinion it conforms to acceptable standards of scholarly presentation and is fully adequate, in scope and in quality, as a dissertation for the degree of Doctor of Philosophy.



B.M. Dunn  
Associate Professor of  
Biochemistry and Molecular Biology


I certify that I have read this study and that in my opinion it conforms to acceptable standards of scholarly presentation and is fully adequate, in scope and in quality, as a dissertation for the degree of Doctor of Philosophy.



C.M. Allen  
Professor of Biochemistry and  
Molecular Biology

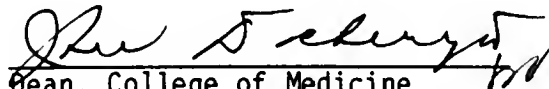


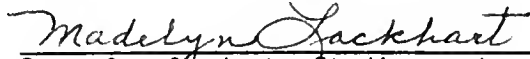
I certify that I have read this study and that in my opinion it conforms to acceptable standards of scholarly presentation and is fully adequate, in scope and in quality, as a dissertation for the degree of Doctor of Philosophy.

  
J.F. Preston  
Professor of Microbiology and  
Cell Science

This dissertation was submitted to the Graduate Faculty of the College of Medicine and to the Graduate School, and was accepted as partial fulfillment of the requirements for the degree of Doctor of Philosophy.

December, 1984

  
Dean, College of Medicine 12/12/84

  
Dean for Graduate Studies and  
Research

UNIVERSITY OF FLORIDA



3 1262 08554 3220